

# Biological activity of macrofungi in South Africa against respiratory and lung disease

J. Didloff

2018

Biological activity of macrofungi in South Africa  
against respiratory and lung disease

by

Jenske Didloff - 212278479

Submitted in fulfilment of the requirements for the degree of  
*Magister Scientiae* in the Department of Biochemistry and  
Microbiology, in the Faculty of Science, at Nelson Mandela  
University

April 2018

Supervisor: Dr S. Govender

Co-supervisor: Dr. G. J. Boukes

DECLARATION BY CANDIDATE

**NAME:** Jenske Didloff

**STUDENT NUMBER:** 212278479

**QUALIFICATION:** *Magister Scientiae* of Microbiology

**TITLE OF PROJECT:** Biological activity of macrofungi in South Africa against respiratory and lung disease

**DECLARATION**

In accordance with rule G5.6.3, I hereby declare that the above-mentioned treatise/ dissertation/ thesis is my own work and that it has not previously been submitted for assessment or completion of any postgraduate qualification to another University or for another qualification.

**SIGNATURE:**

JDidloff

**DATE:**

16/03/2018

## TABLE OF CONTENTS

<b>ACKNOWLEDGEMENTS .....</b>	<b>i</b>
<b>ABSTRACT .....</b>	<b>iii</b>
<b>LIST OF FIGURES .....</b>	<b>v</b>
<b>LIST OF TABLES.....</b>	<b>viii</b>
<b>LIST OF ABBREVIATIONS.....</b>	<b>ix</b>
<b>CHAPTER ONE LITERATURE REVIEW .....</b>	<b>1</b>
1.1. INTRODUCTION .....	1
1.2 RESPIRATORY AND LUNG DISEASE.....	2
1.2.1 TB and HIV .....	3
1.2.2 Respiratory diseases caused by other bacteria .....	4
1.2.3 Lung cancer .....	6
1.3 MACROFUNGI AS A NATURAL SOURCE OF BIOACTIVE COMPOUNDS .....	7
1.4 MEDICINAL POTENTIAL OF MACROFUNGI .....	10
1.4.1 Antimicrobial activity.....	10
1.4.2 Mechanisms of antimicrobial activity.....	12
1.4.3 Cytotoxicity .....	13
1.4.4 Induction of apoptosis as a mechanism of cytotoxicity .....	14
1.4.5 The cell cycle .....	16
1.5 Significance of the study .....	19
1.5.1 Hypotheses to be tested.....	20
1.5.2 Objectives of the study .....	20
<b>CHAPTER TWO ANTIMICROBIAL ACTIVITY OF MACROFUNGAL EXTRACTS .....</b>	<b>21</b>
2.1 INTRODUCTION .....	21
2.2 MATERIALS AND METHODS .....	26
2.2.1 Materials/ chemicals/ reagents .....	26
2.2.2 Macrofungal material and ethanolic and aqueous extract preparation ...	26
2.2.3 Macrofungal extracts.....	27
2.2.4 Antibacterial activity.....	27

2.2.5	Transmission electron microscopy (TEM)	28
2.2.6	Anti-tuberculosis activity	29
2.2.7	Inhibition of HIV-1 enzymes	31
2.3	RESULTS	32
2.3.1	Antimicrobial activity of macrofungal extracts	32
2.3.2	Evaluation of bacterial cellular alterations by TEM	44
2.3.3	MABA assay for activity against <i>M. tuberculosis</i>	46
2.3.4	Inhibition of HIV-1 enzymes	48
2.4	DISCUSSION	51
<b>CHAPTER THREE CYTOTOXICITY OF MACROFUNGAL EXTRACTS AGAINST LUNG CANCER CELLS AND MECHANISM OF ACTION</b>		<b>59</b>
3.2	INTRODUCTION	59
3.2	MATERIALS AND METHODS	64
3.2.1	Materials/ chemicals/ reagents	64
3.2.1	Cell culture conditions and maintenance	64
3.2.2	Cytotoxicity of macrofungal extracts	64
3.2.3	Cell cycle analysis	65
3.2.4	Phosphatidylserine translocation	66
3.2.5	Acridine orange staining	67
3.2.6	Hoechst and Phalloidin-TRITC staining	68
3.2.7	Caspase-8 and -3 staining	68
3.2.8	Statistical analysis	69
3.3	RESULTS	70
3.3.1	Cytotoxicity and IC <sub>50</sub> determination	70
3.2.1	Cell cycle analysis	73
3.3.2	Phosphatidylserine translocation	76
3.3.3	F-actin staining	78
3.3.4	Caspase-8 and caspase-3 activation	80
3.3.5	Acridine orange staining	84
3.4	DISCUSSION	87
<b>CHAPTER FOUR CONCLUSIONS</b>		<b>96</b>
4.1.	THE RESEARCH IN PERSPECTIVE	96
4.2.	POTENTIAL FOR FUTURE DEVELOPMENT OF THE WORK	98

<b>REFERENCES .....</b>	<b>100</b>
<b>APPENDIX .....</b>	<b>118</b>
<b>LIST OF CONFERENCE PRESENTATIONS.....</b>	<b>119</b>

## ACKNOWLEDGEMENTS

The author records her appreciation to:

To Dr. S. Govender and Dr. G.J. Boukes for their continuous support, patience, expertise, and constant encouragement and guidance during the course of this project;

To my parents and sister, I am forever grateful for the unwavering support, love, and encouragement. Thank you for always being there, even sacrificing weekends to spend with me in the Lab;

To all my family and friends, thank you for your love and support;

To my friends and colleagues in the Biochemistry and Microbiology department at NMU for their guidance and support;

To Bresler Swanepoel, for assisting me with cell culture techniques and using the Molecular Devices ImageXpress® Micro XLS widefield microscope. Thank you for your advice and support, with regard to this project;

To Dr. G.J. Boukes, Prof. M. van de Venter and Prof. B. Vijoën for the collection of the mushroom samples and for providing photographs of the mushrooms;

To Prof. M. Lee, Centre for HRTEM, for allowing me to use the transmission electron microscope and his willingness to assist in any way he could;

To Candice Blom, Centre for HRTEM, for the assistance in the sample preparation of the TEM bacterial samples and her colleagues for assistance in viewing of the samples;

To the NHLS, Port Elizabeth, for providing the *S. pneumoniae* and *Mycobacterium tuberculosis* cultures;

To Nelson Mandela University and South African Medical Research Council, for funding of this project;

To Nelson Mandela University and the National Research Foundation, for personal financial support;

To Imtiaz Khan, thank you very much for your continued assistance and guidance with all my bursary applications;

Finally, all glory, honour and thanks go to the Lord Almighty, without whom nothing is possible.



## ABSTRACT

Macrofungi represent an untapped source of natural bioactive compounds for various diseases, which have been targeted as potential therapeutic agents. The medicinal uses of macrofungi discovered to date include anticancer, antidiabetic, antioxidant, antimicrobial, and immunomodulatory properties. The knowledge regarding the medicinal uses of macrofungi in Africa is limited; however, it is believed that Africa may contain a large number of unidentified species of macrofungi. The objectives of this study were to: (i) screen the macrofungal extracts for antimicrobial activity against microorganisms responsible for respiratory diseases (e.g. *Pseudomonas aeruginosa*, *Klebsiella pneumoniae*, *Streptococcus pneumoniae*, *Streptococcus pyogenes*, *Staphylococcus aureus*, *Mycobacterium tuberculosis*, HIV-1), (ii) determine the effect of macrofungal extracts on bacterial morphology, (iii) investigate the cytotoxicity of macrofungal extracts against human lung carcinoma cells, and to elucidate the mechanism/s of action of cytotoxicity/anticancer activity. *In vitro* bioassays for antimicrobial activity included: p-iodonitrotetrazolium chloride assays and microplate alamar blue assay (MABA), while the HIV-1 reverse transcriptase colorimetric ELISA and HIV-1 protease fluorometric assay kits were used for anti-HIV activity. Cytotoxicity of the macrofungal species against A549 lung cancer cell line was measured using the 3-(4,5-dimethylthiazol-2-yl)-2,5-diphenyl tetrazolium bromide (MTT) assay, and the IC<sub>50</sub> values determined for the most cytotoxic macrofungal spp. The mechanism of cytotoxicity was investigated by cell cycle analysis and fluorescent staining to observe morphological and biochemical changes (i.e. acridine orange, caspase activation). Ethanol extracts of *Amanita foetidissima*, *Gymnopilus junonius*, *Pisolithus tinctorius*, *Fomitopsis lilacinogilva*, *Stereum hirsutum* and *Pycnoporus sanguineus* showed higher antimicrobial activity against the Gram-positive bacteria than aqueous extracts, with *S. pneumoniae* being the most susceptible. The ethanol extracts of *Agaricus campestris*, *Chlorophyllum molybdites*, *Gymnopilus penetrans*, *Pseudophaeolus baudonii* and *Laetiporus sulphureus* exhibited anti-TB (tuberculosis) activity with minimum inhibitory concentrations (MICs) ranging between 500-1,000 µg/mL. *C. molybdites* ethanol extract inhibited HIV-1 protease activity (IC<sub>50</sub>: 49.7 µg/mL). The macrofungal extracts did not inhibit HIV-1 reverse transcriptase activity. Ethanol extracts of *F. lilacinogilva*, *G. junonius*, *P. sanguineus* and the aqueous extract

of *P. baudonii* were cytotoxic against A549 lung cancer cells at IC<sub>50</sub> values of 69.2±3.6, 57±5, 7.4±1.1 and 53.6±1.1 µg/mL, respectively. Cell cycle arrest was observed in the G2 phase for both *P. sanguineus* and *P. baudonii*, and G2/M and early M phases for *G. junonius* and *F. lilacinogilva*, respectively. Apoptosis induced by macrofungal extracts was confirmed by fluorescent staining. Morphological and biochemical changes included chromatin condensation, membrane blebbing, loss of cytoskeletal structure, caspase activation and phosphatidylserine translocation. This study demonstrates the biological activities of selected macrofungal extracts and their potential mechanisms of action. Isolation and identification of active compounds require further analysis.

**Keywords:** Macrofungi; antimicrobial; *Mycobacterium tuberculosis*; HIV; protease; reverse transcriptase; cytotoxicity; A549; apoptosis

## LIST OF FIGURES

	<b>Page</b>
<b>Figure 1.1:</b> Top 10 causes of death globally in 2015.	2
<b>Figure 1.2:</b> Twenty-one macrofungal spp. collected for this study in the Eastern and Western Cape provinces of South Africa.	9
<b>Figure 1.3:</b> Schematic representation of extrinsic (1) and intrinsic (2) pathways in apoptosis.	15
<b>Figure 2.1:</b> Visual representation of the colour change produced by <i>S. aureus</i> treated with <i>Pisolithus tinctorius</i> spp. (A) and vancomycin (B) using the INT assay.	32
<b>Figure 2.2:</b> Percentage inhibition of <i>S. pyogenes</i> by active ethanol extracts of macrofungal spp. using INT assay.	37
<b>Figure 2.3:</b> Percentage inhibition of <i>S. pneumoniae</i> using INT assay for active ethanol extracts of macrofungal spp.	38
<b>Figure 2.4:</b> Percentage inhibition of <i>S. aureus</i> by active ethanol extracts of macrofungal spp. using INT assay.	39
<b>Figure 2.5:</b> Percentage inhibition of <i>S. pyogenes</i> by active aqueous extracts of macrofungal spp. using INT assay.	42
<b>Figure 2.6:</b> Percentage inhibition of <i>S. pneumoniae</i> by active aqueous extracts of macrofungal spp. using INT assay.	43
<b>Figure 2.7:</b> Transmission electron micrographs of <i>S. aureus</i> , <i>S. pyogenes</i> and <i>S. pneumoniae</i> treated with <i>Pisolithus tinctorius</i> , <i>Fomitopsis lilacinogilva</i> and <i>F. lilacinogilva</i> , respectively.	45
<b>Figure 2.8:</b> Anti-TB activity of 8 macrofungal spp. (ethanol extracts) and rifampicin and ethambutol dihydrochloride (positive controls) using the MABA assay.	47
<b>Figure 2.9:</b> Percentage inhibition of <i>M. tuberculosis</i> determined for 8 macrofungal spp. using the MABA assay.	48
<b>Figure 2.10:</b> Visual representation of the colour change observed for the ethanol extracts of 8 macrofungal spp. using a non-radioactive colorimetric ELISA assay for HIV-1 reverse transcriptase activity.	49
<b>Figure 2.11:</b> Percentage inhibition of HIV-1 reverse transcriptase following exposure to ethanol extracts of 8 macrofungal spp. and nevirapine (positive control) using the HIV-1 reverse transcriptase assay.	49
<b>Figure 2.12:</b> Percentage inhibition of HIV-1 protease activity following exposure to ethanol extracts of 8 macrofungal spp. and pepstatin A using a fluorescence resonance energy transfer assay.	50

<b>Figure 2.13:</b>	Percentage inhibition of HIV-1 protease activity for the ethanol extract of <i>C. molybdites</i> spp. following 100 min exposure to concentrations ranging between 2.5 – 100 µg/mL.	51
<b>Figure 3.1:</b>	A) Spatial distribution of image sites acquired during cell cycle analysis. B) Excitation/emission wavelengths and filters used to acquire data.	66
<b>Figure 3.2:</b>	A) Spatial distribution of image sites acquired during phosphatidylserine translocation. B) Excitation/emission wavelengths and filters used to acquire data.	67
<b>Figure 3.3:</b>	A) Spatial distribution of image sites acquired during acridine orange staining. B) Excitation/emission wavelengths and filters used to acquire data.	67
<b>Figure 3.4:</b>	A) Spatial distribution of image sites acquired during Hoechst and phalloidin-TRITC staining. B) Excitation/emission wavelengths and filters used to acquire data.	68
<b>Figure 3.5:</b>	A) Spatial distribution of image sites acquired during caspase-3 and -8 activation assays. B) Excitation/emission wavelengths and filters used to acquire data.	69
<b>Figure 3.6:</b>	Dose-response curves of cytotoxicity of <i>Pycnoporus sanguineus</i> (EtOH), <i>Pseudophaeolus baudonii</i> (H <sub>2</sub> O) and cisplatin (positive control) against A549 lung carcinoma cells.	71
<b>Figure 3.7:</b>	Dose-response curve of cytotoxicity of the ethanol extracts of <i>Gymnopilus junonius</i> , <i>Fomitopsis lilacinogilva</i> and <i>P. sanguineus</i> , and the aqueous extract of <i>P. baudonii</i> against MRC5 fibroblast cells.	72
<b>Figure 3.8:</b>	Cell cycle analysis of A549 cells treated with <i>G. junonius</i> , <i>P. sanguineus</i> , <i>P. baudonii</i> and <i>F. lilacinogilva</i> extracts at their IC <sub>25</sub> , IC <sub>50</sub> and IC <sub>75</sub> concentrations for 24 (A) and 48 h (B).	75
<b>Figure 3.9:</b>	PS translocation in A549 cells using Annexin V-FITC/PI dual staining following 24 (A) and 48 h (B) of treatment with <i>G. junonius</i> , <i>P. sanguineus</i> , <i>P. baudonii</i> and <i>F. lilacinogilva</i> extracts and cisplatin (positive control).	77
<b>Figure 3.10:</b>	Visual representation of morphological changes of A549 cells following 48 h exposure to <i>G. junonius</i> , <i>P. sanguineus</i> , <i>P. baudonii</i> , <i>F. lilacinogilva</i> and cisplatin observed by Hoechst and phalloidin-TRITC staining.	79
<b>Figure 3.11:</b>	Activation of cleaved caspase-8 after 24 (A) and 48 h (B) exposure to <i>G. junonius</i> , <i>P. sanguineus</i> , <i>P. baudonii</i> and <i>F. lilacinogilva</i> .	81

- Figure 3.12:** Activation of cleaved caspase-3 after 24 (A) and 48 h (B) exposure to *G. junonius*, *P. sanguineus*, *P. baudonii* and *F. lilacinogilva*. 83
- Figure 3.13:** Morphological changes of A549 cells observed by acridine orange staining following 48 h exposure to *G. junonius*, *P. sanguineus*, *P. baudonii*, *F. lilacinogilva* and cisplatin. 85
- Figure 3.14:** Visual representation of dose-dependent increases in apoptotic A549 cells after treatment with the IC<sub>25</sub>, IC<sub>50</sub> and IC<sub>75</sub> concentrations of *P. sanguineus* 86

**LIST OF TABLES**

	<b>Page</b>
<b>Table 1.1:</b> Upper and lower respiratory tract infections.	5
<b>Table 2.1:</b> MIC values of ethanol extracts of 21 macrofungal species against <i>P. aeruginosa</i> , <i>K. pneumoniae</i> , <i>S. aureus</i> , <i>S. pneumoniae</i> and <i>S. pyogenes</i> determined using the INT assay.	34-35
<b>Table 2.2:</b> MIC values of aqueous extracts of 21 macrofungal species against <i>P. aeruginosa</i> , <i>K. pneumoniae</i> , <i>S. aureus</i> , <i>S. pneumoniae</i> and <i>S. pyogenes</i> determined using the INT assay.	40-41
<b>Table 3.1:</b> IC <sub>50</sub> values (µg/mL) of 11 South African macrofungal spp. against normal lung fibroblast (MRC5) and lung cancer (A549) cell lines.	72
<b>Table 3.2</b> Selectivity indices of the cytotoxicity of <i>G. junonius</i> , <i>P. sanguineus</i> , <i>P. baudonii</i> and <i>F. lilacinogilva</i>	73

## LIST OF ABBREVIATIONS

AO	Acridine orange
AIDS	Acquired immunodeficiency syndrome
ABS	Acute bacterial sinusitis
ADC	Albumin-dextrose-catalase
APC	Anaphase promoting complex
ART	Antiretroviral therapy
Apaf-1	Apoptotic protease activating factor 1
AIF	Apoptosis inducing factor
ATM	Ataxia Telangiectasia Mutated
ATR	Ataxia Telangiectasia and Rad3-related
Bsc	Bachelor of science
BaCl <sub>2</sub>	Barium chloride
Bcl-2	B-cell lymphoma 2
BSA	Bovine serum albumin
Ca <sup>2+</sup>	Calcium ions
CO <sub>2</sub>	Carbon dioxide
CARDs	Caspase activation and recruitment domains
Cdc25a	Cell division cycle 25 homolog A
Cdc25c	Cell division cycle 25 homolog C
Chk1	Checkpoint kinase 1
Chk2	Checkpoint kinase 2
Cu	Copper
CDKs	Cyclin-dependent kinases
DISC	Death signalling complex
°C	Degrees Celsius
DNA	Deoxyribonucleic acid
DMSO	Dimethyl sulfoxide
dUTP	Dioxigenin Uridine Triphosphate
DIABLO	Direct IAP Binding protein with Low pl
ddH <sub>2</sub> O	Double distilled water
DPBS	Dulbecco's phosphate buffered saline
EMEM	Eagle's Minimal Essential medium
E2F	Early gene 2 factor
ELISA	Enzyme Linked Immunosorbent Assay
EtOH	Ethanol
EB	Ethidium bromide
EDTA	Ethylenediaminetetracetic acid

XDR-TB	Extensively drug resistant TB
FBS	Foetal bovine serum
FITC	Fluorescein isothiocyanate
FRET	Fluorescent resonance energy transfer
g	Grams
x g	Gravity
IC <sub>50</sub>	Half maximal inhibitory concentrations
HAART	Highly active antiretroviral therapy
h	Hours
HIV	Human immunodeficiency virus
HIV-1 RT	HIV-1 reverse transcriptase
IC	Inhibitory concentration
IAPs	Inhibitor of apoptosis proteins
IARC	International Agency for Research on Cancer's
JCRB	Japanese Collection of Research Bioresources
kDa	Kilodalton
INT	p-Iodonitrotetrazolium chloride/ 2-(4-Iodophenyl)-3-(4-nitrophenyl)-5-phenyltetrazolium chloride
LRTI	Lower respiratory tract infections
Mg <sup>2+</sup>	Magnesium ions
MABA	Microplate Alamar Blue assay
mg	Milligram
mL	Millilitre
mm	Millimetre
MIC	Minimum inhibitory concentration
min	Minutes
MC	Mitototic catastrophe
M	Molarity
Mdm2	Mouse double minute 2 homolog
MH	Mueller-Hinton
MDR-TB	Multi-drug resistant TB
MTT	3-(4,5-dimethylthiazol-2-yl)-2,5-diphenyl tetrazolium bromide
NHLS	National Health Laboratory Services
nm	Nanometres
NMU	Nelson Mandela University
NEAA	Non-essential amino acids
NNRTI	Non-nucleoside reverse-transcriptase inhibitors
N/A	Not applicable
NRTI	Nucleoside reverse-transcriptase inhibitors



PS	Phosphatidylserine
PARP	Poly (ADP-ribose) polymerase
pH	Potential of hydrogen
PI	Propidium iodide
PIs	protease inhibitors
ROS	Reactive oxygen species
RFU	Relative fluorescence units
Rb	Retinoblastoma protein
RPM	Revolutions per minute
RNA	Ribonucleic acid
RT	Room temperature
Smac	Second mitochondria-derived activator of caspases
NaCl	Sodium chloride
NaOH	Sodium hydroxide
spp	Species
SD	Standard deviation
H <sub>2</sub> SO <sub>4</sub>	Sulphuric acid
TRITC	Tetramethylrhodamine
tRNA	Transfer RNA
TEM	Transmission electron microscopy
TB	Tuberculosis
TNF	Tumour necrosis factor
TRAIL	TNF-related apoptosis inducing ligand
µg	Microgram
µL	Microliter
µm	Micrometre
UT	Untreated
URTI	Upper respiratory tract infections
v/v	Volume/volume
W/V	Weight/ volume
WHO	World Health Organisation

# CHAPTER ONE

## LITERATURE REVIEW

### 1.1. INTRODUCTION

Chronic and infectious diseases remain a serious concern worldwide, even though advances have been made in medicine. A report released by the World Health Organization (WHO) states that cancer is a leading cause of death worldwide, with 8.8 million cancer related deaths in 2015 (WHO, 2017a). Statistics released by the WHO in 2016 have shown a decrease in tuberculosis (TB), and human immunodeficiency virus infection and acquired immune deficiency syndrome (HIV/AIDS) mortality rates. Africa's HIV epidemic remains the largest worldwide and the prevalence of new TB cases ranks second globally (WHO, 2017b). Mortality rates remain high for TB and HIV/AIDS with 1.7 million (WHO, 2017b) and 1.0 million deaths in 2016, respectively (WHO, 2017c).

The incorrect and misuse of antimicrobial drugs have led to an increase in the occurrence of microbial resistance. It is estimated that 70% of bacterial pathogens causing hospital-acquired infections exhibit resistance to at least one commonly used drug. An increase in antimicrobial resistance has also been described in community-acquired infections (Lima et al., 2016) and pathogens such as multidrug- and extensively drug-resistant TB (Krátký et al., 2013). The occurrence of resistance, accompanied with the potential loss of control of serious infectious diseases, signifies a serious health concern. Considerable progress has been made in cancer therapy, however treatment regimens still show disadvantages including numerous side effects (De Silva et al., 2012) and non-specific targeting of available drugs (Patel and Goyal, 2012).

Exploration of biologically active compounds obtained from natural sources may provide an alternative to antibiotics, which could assist in the reduction of antibiotic resistance (Ogidi et al., 2015), and therapeutic agents with anticancer properties that

are less toxic and more effective (Patel and Goyal, 2012). It has been shown that 61% of the anticancer drugs approved in the last 30 years are either natural products or semi-synthesised compounds derived thereof (Luo et al., 2014).

For centuries both micro- and macrofungi have played an important role in human life. It was utilized for cultural purposes, as a source of nutrients, and for the treatment and prevention of diseases. Current advances within the field of Microbiology extended their potential uses to biological control, enzymes, antibiotics and other pharmacological products (Dias et al., 2012). Fungi constitute a group of organisms exhibiting a large diversity of which only a small portion have been explored (De Silva et al., 2013). This relates to a large possibility that the undiscovered fungi may be of nutritional and medicinal value (Bala et al., 2011).

## 1.2 RESPIRATORY AND LUNG DISEASE

Respiratory diseases are a major cause of mortality and morbidity worldwide (Xirogianni et al., 2013). Figure 1.1 illustrates the top ten global causes of death which include lower respiratory disease, TB and lung cancer.

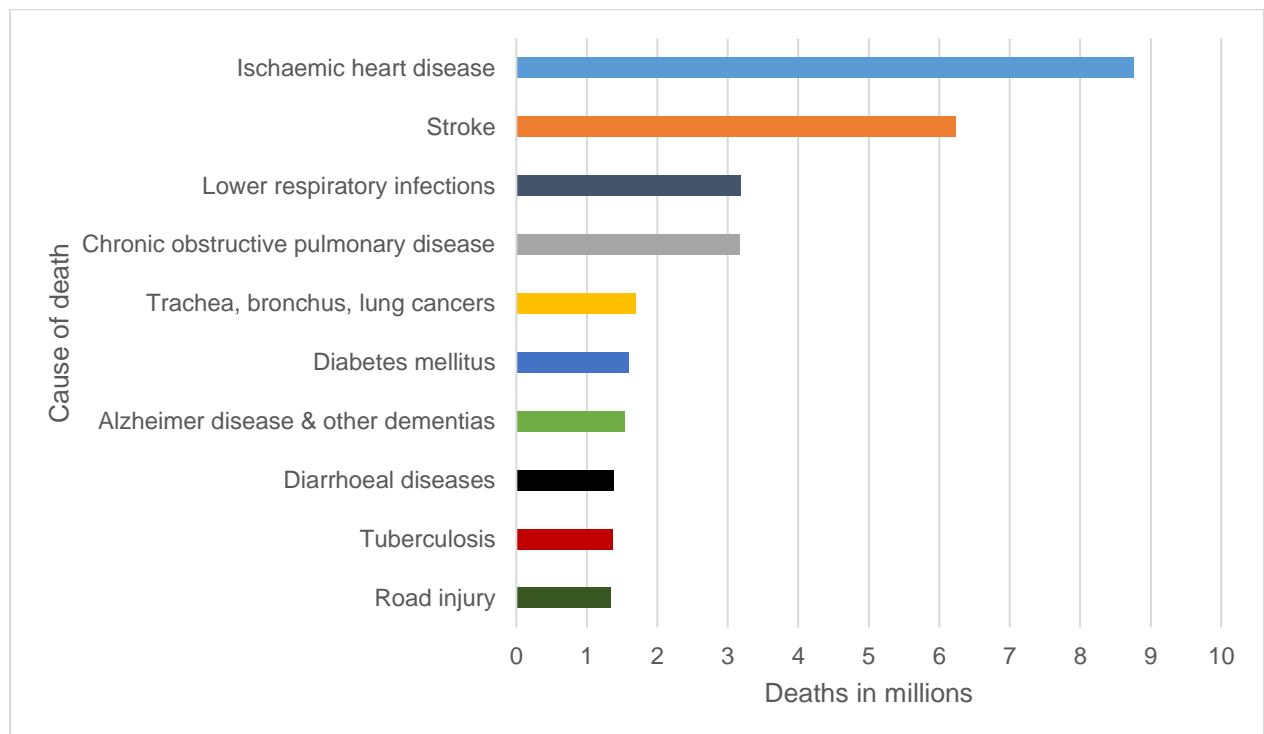


**Figure 1.1:** The top ten causes of death globally in 2015, (WHO, 2017d).

Respiratory disease places a global burden on health and it was estimated that the incidence of upper respiratory tract infections in 2013 was 18.8 billion with approximately 4.4 million deaths worldwide. Upper respiratory tract infection (URTI) is primarily caused by viruses in contrast to lower respiratory tract infections (LRTI) which can be caused by viruses, fungi, mycoplasma and bacteria. The most common bacterial pathogens causing acute respiratory infections include: *Mycobacterium tuberculosis*, *Corynebacterium* spp., *Bordetella pertussis*, *Klebsiella pneumoniae*, *Haemophilus influenzae*, *Streptococcus pyogenes*, *Streptococcus pneumoniae*, and *Staphylococcus aureus* (Yahaya and Fall, 2016).

### **1.2.1 TB and HIV**

TB is an infectious disease caused by *M. tuberculosis* and recognised as one of the leading causes of death (De Silva et al., 2013). This is despite the fact that with early diagnosis and implementation of correct treatment regimens, TB can be cured (WHO, 2017b). Only a small proportion (5-15%) of the population infected with latent TB will become ill with active TB. Individuals with compromised immune systems have a higher risk of infection. In 2016, 10.4 million people were diagnosed with TB with 1.7 million deaths. HIV-associated TB caused 40% death in HIV patients and an estimated 1.4 million new cases of TB were identified in HIV-positive patients in 2016 (74% in Africa) (WHO, 2017b). The treatment of TB requires long-term usage of multiple drugs, which can lead to drug-induced hepatotoxicity. The emergence of multidrug resistant (MDR) strains further complicates the treatment. It is estimated that in 2016, 600 000 new cases were resistant to rifampicin of which 490 000 had MDR-TB. Extreme drug resistant (XDR)-TB comprised about 6.2% of the MDR-TB cases. About 53 million TB patients were successfully diagnosed and treated from 2000 – 2016 (WHO, 2017b).

AIDS remains one of the most life-threatening diseases worldwide, which is caused by HIV. Lung diseases are a significant cause of morbidity and mortality in HIV-infected individuals, and the lung infections and complications associated with HIV infection are broad. The impact of antiretroviral treatment (ART) and chronic infection with HIV on lung health are unknown (Crothers et al., 2011). It was estimated that 36.7 million people globally were living with HIV in 2016 with 1.8 million newly infected individuals. HIV is a major contributor to morbidity globally with 1.0 million HIV-related

deaths recorded in 2016. Sub-Saharan Africa was recognised as the region with the highest prevalence of HIV in 2016 (70%) (WHO, 2017c). Currently there is no cure for HIV/AIDS however ART can assist in controlling the virus and prevent transmission (WHO, 2017c). The compounds used in HIV ART include nucleoside reverse-transcriptase inhibitors (NRTIs), non-nucleoside reverse-transcriptase inhibitors (NNRTIs), or protease inhibitors (PIs). These drugs target two viral enzymes: HIV reverse transcriptase (RT) and HIV protease, which are essential for the viral life cycle. ART drugs can also target the entry of the HIV-1 virus. These can act by interfering with viral attachment to the cell membrane, binding to co-receptors on the cell surface, or fusion of the virus with the cell membrane (Bean, 2005). Several pitfalls still exist, including viral resistance, toxicity, high cost and limited availability (Bessong et al., 2005; Klos et al., 2009). Due to the high cost of treatment approximately 90% of HIV-infected individuals cannot afford treatment. Thus, development of drugs with lower toxicity and reduced cost are required (Wang et al., 2007). The screening of macrofungi for HIV-1 inhibitors show several advantages such as (1) abundant resources, (2) natural compounds generally exhibit lower toxicity and side effects, and (3) affordability due to the availability of medicinal macrofungi enabling compounds to be extracted and produced at a lower cost (Wang et al., 2007).

### **1.2.2 Respiratory diseases caused by other bacteria**

The respiratory tract is a common site of infection due to its continued exposure to environmental and airborne pathogens. It can be divided into upper and lower respiratory tract infections which leads to inflammation of various areas (Table 1.1) (Johnston, 2012). Some of the respiratory diseases caused by bacteria include pharyngitis, sinusitis, bronchitis and tonsillitis. Inflammation of the pharynx or throat (pharyngitis) can be caused by viral or bacterial pathogens. The bacterial pathogens include *Streptococci*, *Chlamydia pneumoniae*, *Mycoplasma pneumoniae*, *Corynebacterium diphtheriae*, and *Neisseria gonorrhoeae* (Rohilla et al., 2013). The causative agent of acute otitis media is often viral with *S. pneumoniae*, *H. influenzae* and *Moraxella catarrhalis* the major bacterial causes (Johnston, 2012).

**Table 1.1:** Upper and lower respiratory tract infections (Johnston, 2012).

Upper respiratory tract infections	Lower respiratory tract infections
Rhinitis - inflammation of the nasal mucosa	Bronchitis - inflammation of the trachea and bronchi
Rhinosinusitis or sinusitis - inflammation of the nares and paranasal sinuses	Bronchiolitis - inflammation of the bronchioles
Nasopharyngitis - inflammation of the nares, pharynx, hypopharynx, uvula and tonsils	Pneumonia - inflammation of the lungs
Pharyngitis - inflammation of the pharynx, hypopharynx, uvula and tonsils	
Epiglottitis - inflammation of superior region of the larynx and subglottic area	
Laryngitis - inflammation of the larynx	
Laryngotracheitis - inflammation of the larynx, trachea and subglottic area	
Tracheitis - inflammation of the trachea and subglottic area	

Sinusitis is inflammation of the mucosal membrane and air-filled cavities, and can be classified into acute and chronic sinusitis. The etiological agents of sinusitis include viral, bacterial or fungal. Acute bacterial sinusitis (ABS) often occurs after a viral URTI or other factors that led to inflammation of the nose and paranasal sinuses (e.g. allergy, dental infection or trauma) (Brink, 2008). The causative agents of ABS are *S. pneumoniae*, *H. influenzae*, *M. catarrhalis* and *S. aureus* (Brink, 2008; Johnston, 2012). Bronchitis is inflammation of the bronchi that can be caused by viruses and bacteria. Smoking, air pollution and seasonal changes have also been found to cause bronchitis. The bacterial agents known to cause bronchitis include *Mycoplasma pneumoniae*, *M. catarrhalis*, *B. pertussis*, *S. pneumoniae* and *H. influenzae* (Rohilla et al., 2013; Johnston, 2012). Tonsillitis is inflammation of the palatine tonsils, pharyngeal tonsils, tubal tonsils, and lingual tonsil. The inflammation of the tonsils causes enlarged size which results in difficulty in swallowing and voice production. The bacterial causative agents are *S. pneumoniae*, *S. aureus*, *M. pneumoniae* and *Chlamydia pneumoniae* (Rohilla et al., 2013). Pneumoniae is inflammation of the lungs and can be viral, bacterial, fungal or parasitic, with bacterial and viral cases the most prevalent. The most common bacterial pathogens include *S. pneumoniae*, *H. influenzae*,

*Legionella* spp., *M. pneumoniae*, *K. pneumoniae*, *S. aureus* and *Pseudomonas aeruginosa* (Carroll, 2002).

### 1.2.3 Lung cancer

Cancer is defined as a disease in which cells grow and divide uncontrollably. The transformation of normal cells to cancer/ tumour cells occur through a series of genome alterations involved in the cell cycle (Sandal, 2002; Hassanpour and Dehghani, 2017). These mutations can contribute to certain growth and survival advantages such as defective apoptotic machinery (Indran et al., 2011) allowing unregulated and excessive proliferation of cells that can lead to tumour development and metastasis (Kasibhatla and Tseng, 2003; Hassan et al., 2014).

Cancer is one of the leading causes of death worldwide. According to the International Agency for Research on Cancer's (IARC) Globocan 2012 Report, 14.1 million new cases were diagnosed in 2012 with 8.2 million cancer related deaths. Lung (1.8 million), breast (1.7 million) and colorectum (1.4 million) cancers were identified as the most prevalent cancers diagnosed in 2012, whereas lung (1.6 million), stomach (0.7 million) and liver (0.8 million) cancers accounted for the most cancer-related deaths worldwide ([www.cansa.org.za](http://www.cansa.org.za)). In South Africa, approximately 77 440 new cancer cases were identified in 2012. Lung cancer was the 4<sup>th</sup> most prevalent with 7 242 new cases (9.4%) and 6 465 (13.7%) deaths ([www.cancerresearchuk.org](http://www.cancerresearchuk.org)). The risk factors for cancer include physical carcinogens (e.g. ultraviolet and ionizing radiation), chemical carcinogens (e.g. tobacco smoke, asbestos, arsenic and aflatoxin) and biological carcinogens (infections caused by bacteria, viruses or parasites). The treatment regimen depends on cancer type, -size -site, and -stage (WHO, 2017a)

The most frequently used cancer treatments are surgery, chemotherapy and radiotherapy (WHO, 2017a), however it is limited as a result of damaging side effects (De Silva et al., 2012) and resistance towards commonly used drugs. Therefore new and effective drugs for the treatment and prevention of cancer are required (Vejselova and Kutlu, 2015).

### 1.3 MACROFUNGI AS A NATURAL SOURCE OF BIOACTIVE COMPOUNDS

Natural sources may contain novel bioactive compounds with therapeutic properties for various diseases. It is known that natural products have been utilised for centuries for the treatment of diseases caused by fungi, bacteria, parasites and viruses. The pure compounds or crude extracts obtained from natural products may provide insight for the discovery of new drugs and for future drug development. Of the available fauna and flora, only a small portion has been explored for their bioactive properties. This relates to a large number of untapped sources that can be utilised and explored to assist current health problems such as drug resistance. Macrofungi have been identified as organisms that produce a vast amount of compounds with biological activities, yet has not been as intensively investigated as other natural sources (Altuner and Akata, 2010; De Silva et al., 2013).

Macrofungi form an important component of the Kingdom Fungi. Macrofungi refer to fungi producing fruiting bodies that are visible with the naked eye (Karaman et al., 2012; Tang et al., 2015), and may be located either above or below the ground. Ecologically, macrofungi may have parasitic, symbiotic and/or saprophytic relationships (Tang et al., 2015). Taxonomically, macrofungi belong to two classes/phylums, *Ascomycetes* and *Basidiomycetes*, with the majority in the latter class (Thaoi and Singdevsachan, 2014). Macrofungi consist of morphological diverse groups, which include mushrooms/toadstools, bracket- , gilled- and cup fungi, truffles and puffballs (Andrew et al., 2013). It is estimated that the number of fungi found on earth is approximately 1.5 million species (Karaman et al., 2012) of which 140 000 species qualify as macrofungi (Enshasy et al., 2013). About 14 000 mushrooms species have been identified and described, and of these 2 000 are edible and 650 species have been used for medicinal and food purposes (Thatoi and Singdevsachan, 2014).

Information regarding the medicinal uses of macrofungi in Africa is limited, however it is believed that Africa may contain a large number of macrofungal species that are currently unknown. Several macrofungal species have been reported in Africa and include *Schizophyllum commune*, *Termitomyces*, *Cantharellus*, *Lentinus*,



*Macrolepiota*, *Coriolopsis*, *Pleurotus*, *Calvatia* and several others (Enshasy et al., 2013).

The kingdom Fungi can be classified into four phyla including Chytridiomycota, Zygomycota, Ascomycota, and Basidiomycota. Ascomycota and Basidiomycota contain fungal species producing visible fruiting bodies (Rahi and Malik 2016). The clade, Agaricomycotina, within Basidiomycota consists of mushrooms, basidiomycetous yeast and jelly fungi. Some of the species are poisonous (e.g. *Amanita phalloides*, *Galerina autumnalis*), edible (e.g. *Agaricus bisporus*, *Lentinula edodes*), while others are hallucinogenic (e.g. *Psilocybe cubensis*). The Basidiomycetes are divided into two subclasses, the Tremellomycetidae (heterobasidiomycetes: species with gelatinous fruiting bodies and septate basidia) and Agaricomycetidae (homobasidiomycetes: mushroom forming fungi with undivided basidia). These two subclasses are further divided into 16 orders. The Agaricomycetidae contains the orders Agaricales, Boletales, Cantharellales, Hymenochaetales, Phallales, Polyporales, Russulales and Thelephorales (Hibbett, 2006; Hibbett and Matheny, 2009).

Boletales is one of the largest orders within Agaricomycetes, and contains species with a variety of morphologies. The majority (77%) of the species have boletoid or gilled fruiting bodies while the remaining species have gasteroid, meruloid or toothed fruiting bodies. The order contains approximately 20 families with 2 000 known species (Hubregtse, 2017). The order Polyporales contains 11 families with about 3 280 described species. They are saprotrophic and the majority are wood-decaying fungi with diverse morphologies that include polypores, corticioid and agarics (Hubregtse, 2017). Russulales is a large order containing about 2 941 spp. with diverse morphologies such as clavarioid, discoid, effuse-reflexed, resupinate, gastroid and pileate. The species within the order are saprotrophic, parasitic and ectomycorrhizal (Hubregtse, 2017). Agaricales is the largest clade of mushroom-forming fungi and contains more than 9 000 species. They are terrestrial, lignicolous, saprobic and mycorrhizal fungi. They have oval or elliptical spores that are dark brown or purple in colour. They grow in a variety of habitats including grasslands, forest, farms, field and several others (Yaling et al., 2014).

Twenty-one macrofungal spp. were screened in this study and classified in the orders Agaricales, Polyporales, Russulales and Boletales (Figure 1.2). *Amanita foetidissima*, *Gymnopilus junonius*, *G. penetrans*, *Hyphaloma fasciculare*, *Pleurotus ostreatus*, *Schizophyllum commune*, *Paneolus papilionaceus*, *Agaricus campestris*, and *Chlorophyllum molybdites* belong to the order Agaricales. *Russula capensis* and *Hericium erinaceus* are macrofungal spp. belonging to the order Russulales. *Fomitopsis lilacinogilva*, *Ganoderma lucidum*, *Pycnoporus sanguineus*, *Stereum hirsutum*, *Lenzites elegans*, *Laetiporus sulphureus*, *Pseudophaeolus baudonii*, and *P. ostreatus* (grey and white) are classified in the order Polyporales. The macrofungal spp. *Pisolithus tinctorius* and *Imlaria badia* included in this study are classified in the order Boletales.

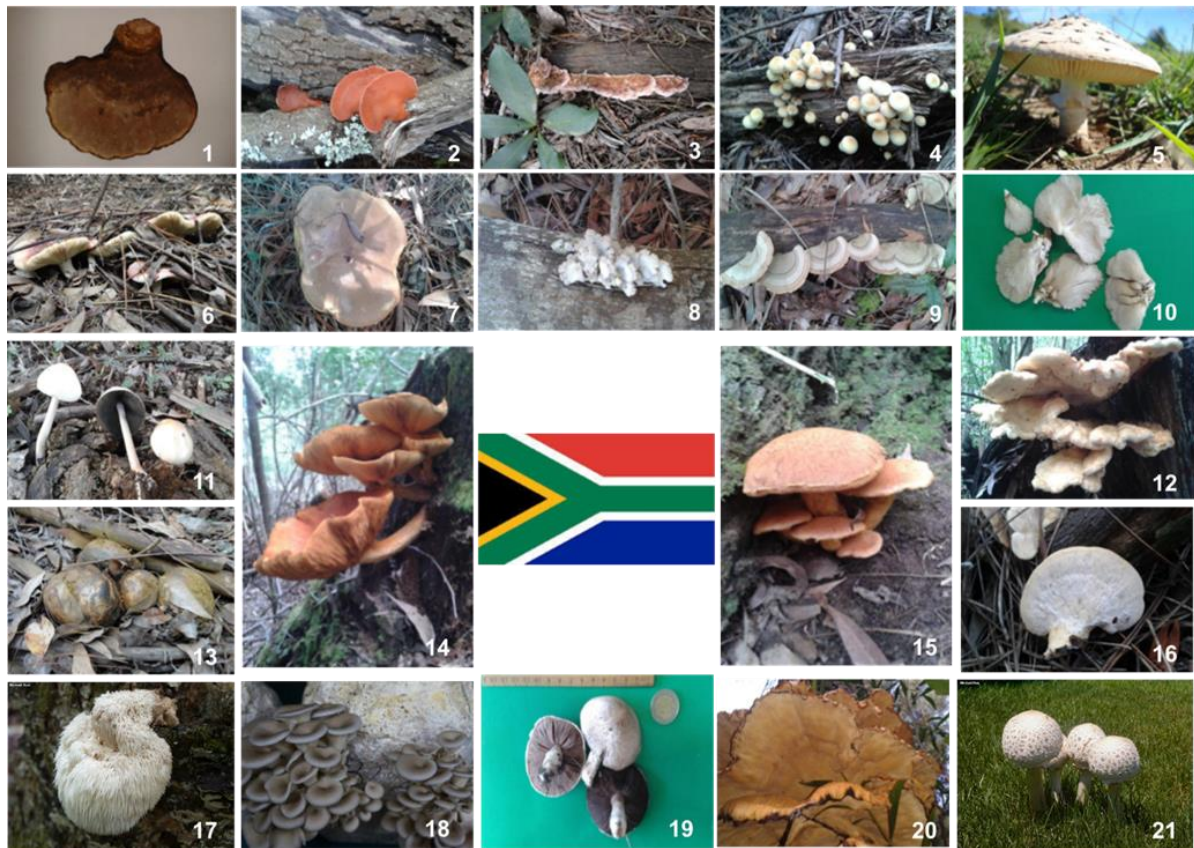


**Figure 1.2:** Twenty-one macrofungal spp. collected in the Eastern and Western Cape provinces of South Africa. 1) *G. lucidum*, 2) *P. sanguineus*, 3) *F. lilacinogilva*, 4) *H. fasciculare*, 5) *A. foetidissima*, 6) *R. capensis*, 7) *I. badia*, 8) *S. commune*, 9) *S. hirsutum*, 10) *P. ostreatus* (white), 11) *P. papilionaceus*, 12) *L. sulphureus*, 13) *P. tinctorius*, 14) *G. penetrans*, 15) *G. junonius*, 16) *L. elegans*, 17) *Hericium erinaceus* (Mushroomexpert.com, 2017a), 18) *Pleurotus ostreatus* (grey) (Team and Team, 2017), 19) *A. campestris*, 20) *P. baudonii*, and 21) *C. molybdites* (Mushroomexpert.com, 2017b) Photographs taken by G.J.Boukes.

## **1.4 MEDICINAL POTENTIAL OF MACROFUNGI**

Mushrooms have been exploited for their medicinal properties since the Neolithic and Paleolithic eras; however the active agents promoting human health were only investigated from the 1960s. It is estimated that medicinal mushrooms possess around 126 therapeutic effects (Badalyan, 2012).

Biological activities and medicinal uses of mushrooms include antioxidant, antidiabetic, anticancer, antiallergic, antiviral, antimicrobial, immunomodulatory, antiparasitic, hepatoprotective effects, among several others. The therapeutic benefits observed by macrofungi are based on their ability to synthesize a wide range of biologically active compounds. These active molecules can be present within the cultured broth, cultured mycelium or fruiting bodies (Thatoi and Singdevsachan, 2014).

The type of active compound and its concentration are affected by several parameters, including the strain, developmental stage, cultivation, age, storage conditions and processing (Valverde et al., 2015). These compounds can be divided into high molecular weight primary metabolites (e.g. proteins, polysaccharides and lipids) and low molecular weight secondary metabolites (e.g. terpenoids, polyphenols, sesquiterpenes, alkaloids, lactones nucleotide analogs and several other) (De Silva et al., 2013; Valverde et al., 2015).

### **1.4.1 Antimicrobial activity**

The search for new antimicrobial agents has increased due to an increase in occurrence of antibiotic resistant pathogenic bacteria. As mushrooms may be a source of natural medicine, they have sparked interest to explore their potential for antimicrobial agents (De Silva et al., 2013). An antimicrobial agent refers to a compound that displays the ability to inhibit the growth of microorganisms (i.e. fungi, bacteria or protozoans) (De Silva et al., 2013; Sathyan et al., 2017).

In order to survive within their natural habitat, mushrooms produce various antimicrobial compounds exhibiting antibacterial-, antiprotozoan- and antifungal activities (Badalyan, 2012). Certain microbial pathogens affect both humans and fungi

and thus the antimicrobial compounds produced by mushrooms against these microorganisms may be of benefit to humans (Karaman et al., 2012). Yamaç and Bilgili (2006) reported that initial studies on the potential of medicinal mushrooms as sources of antibiotics were performed by Anchel, Hervey and Wilkens in 1941, which identified over 2,000 fungal species showing antimicrobial activity. This discovery was followed by the isolation and identification of pleuromutilin, which led to the first commercialised antibiotic obtained from a Basidiomycete (Yamaç and Bilgili, 2006). Research suggests that the degree of antimicrobial activity observed for different mushroom species depends on several factors, including the type of solvent used during extraction, antimicrobial test method employed, microorganisms tested, amount of extract tested and the chemical profile of the specific macrofungi (Poyraz et al., 2015). The antimicrobial properties can also vary with the maturation of the fruiting body (Shen et al., 2017).

Compounds with anti-tuberculosis activity have been isolated from several mushroom species (spp.). Lanostane triterpenes (astraodoric acid A and B), butenolides (ramariolides A-D) and ganorbiformins A-G isolated from *Astraeus* species, *Ramaria cystidiophora* and *Ganoderma orbiforme*, respectively, showed moderate to significant activity against *M. tuberculosis* (De Silva et al., 2013). Several proteinaceous compounds (e.g. proteins, polysaccharides and peptides) have been isolated from macrofungi exhibiting anti-viral activity against the HIV-1 (Roupas et al., 2012). Several bioactive compounds isolated from different species have been documented to show inhibition of the HIV-1 reverse transcriptase and protease activity, which is important in the viral life cycle (Roupas et al., 2012). The antioxidant compounds, dimethylguanosine, iso-senensetin and adenosine, isolated from the macrofungus *Cordyceps militaris* inhibit HIV-1 protease activity. Inhibitory effects in HIV-1 replication have also been documented for proteinaceous compounds such as epococcins E-H isolated from *Cordyceps sinensis*. Besides high molecular proteinaceous compounds several low molecular compounds, such as terpenoids, exhibit inhibitory activity against HIV (e.g. HIV-1 protease inhibition).

The anti-viral bioactive compounds may cause direct anti-viral effects, which include the inhibition of specific viral enzymes, adsorption and uptake into mammalian cells and nucleic acid synthesis (De Silva et al., 2013). These are mainly the result of

smaller compounds produced by macrofungi. Polysaccharides and other complex compounds may also cause indirect effects due to immunomodulating activities (Lindequist et al., 2005).

#### **1.4.2 Mechanisms of antimicrobial activity**

Antimicrobial agents function by interfering with certain processes that are essential for bacterial growth and division. Antimicrobial agents are classified based on whether they inhibit cell growth (bacteriostatic) or induce cell death (bacteriocidal), the cellular component they affect, and their mechanism of action. The primary mechanism of action of antimicrobial agents include: (1) interference with cell wall synthesis, (2) interference with nucleic acid synthesis, (3) interference with protein synthesis, (4) inhibition of metabolic pathways, and (5) disruption of the cytoplasmic membranes (Liwa and Jaka, 2015; Saritha et al., 2015).

Interference with cell wall synthesis has been a key target for the development of antimicrobial agents as it is required for cell shape and protection against osmotic pressure. The absence of cell wall synthesis machinery in humans provide high target selectivity of antimicrobial drugs. Cell wall synthesis can be affected by inhibiting transglycosylase and transpeptidase enzyme reactions required for the synthesis of peptidoglycan. Several classes of antibiotics function to inhibit protein synthesis such as aminoglycosides, macrolides, tetracyclines and several others. Antimicrobial agents can block different stages of protein synthesis by interfering with either the ribosomes or cytoplasmic factors required for protein synthesis. The antimicrobial agents can bind to the 30S ribosomal subunit interfering with the initiation reaction. Inhibition of elongation can also be achieved by interfering with pairing of the mRNA codon with the anticodon of an amino acid-tRNA, binding to the 50S ribosomal subunit or binding to elongation factors. The interference with nucleic acid synthesis can be achieved by inhibiting DNA polymerase and DNA helicase or RNA polymerase, blocking replication or transcription, respectively. The cytoplasmic membrane is composed of lipids, proteins and lipoproteins that functions as a diffusion barrier. Antimicrobial agents may cause an increase in membrane permeability allowing their entry as well as the entry of other compounds that can affect metabolic pathways resulting in bacterial cell death (Liwa and Jaka, 2015). Limited studies have

investigated the mechanism of action of macrofungal extracts on bacterial cells. Matijašević et al. (2016) investigated the effect of a *Coriolus versicolor* methanol extract on *S. aureus* and *Salmonella enteritidis*. *S. aureus* cells were malformed and elongated, whereas *S. enteritidis* cells were aggregated with ruptured cell walls (Matijašević et al., 2016).

### 1.4.3 Cytotoxicity

Cytotoxicity can be defined as having toxic effects at the cellular level, which include cell death, enzymatic inhibition, and alterations in membrane permeability (Ramakrishna et al., 2010). Direct cytotoxicity involves the interference of cytotoxic compounds with cancer phases such as induction, growth and progression. This is due to the inhibition of tumour invasion and metastasis as well as inducing cell cycle arrest and apoptosis (Zong et al., 2012). Medicinal mushrooms and their extracted compounds in several studies performed in China, Korea, Japan and the United States have shown properties that prevent and treat cancer (Poyraz et al., 2015).

Several studies have confirmed the cytotoxic effects of certain mushroom compounds. Compounds exhibiting cytotoxic activities against cancer cells include illudins, acetoxyscirpenediol, triterpenes, sterols and ergosterol peroxide (Fan et al., 2006). The bioactive compounds produced by medicinal mushrooms exerting anti-tumour activity include proteins, polysaccharides, ash, fats, alkaloids, glycosides, volatile oils, tocopherols, phenolics, carotenoids, organic acids, flavonoids and folates. Among these, polysaccharides have been the most extensively studied (Kim et al., 2015). Studies suggest that polysaccharides and polysaccharide peptides function by means of immunomodulation, however *in vitro* studies have shown that certain polysaccharides exert direct cytotoxic effects on multiple cancer cell lines (Smith et al., 2002). There are several other mechanisms in which the bioactive agents exert their anti-cancer activity, including the inhibition of angiogenesis, metastasis and cell proliferation (Valverde et al., 2015).

Acetoxyscirpenediol and triterpenes isolated from *Paecilomyces tenuipes* and *Ganoderma cocinum*, respectively, have shown cytotoxic activity by inducing apoptosis in cell lines in *in vitro* studies (Lindequist et al., 2005). Ganoderic acid T,

produced by *Ganoderma lucidum*, showed cytotoxic activity against metastatic lung tumour cells by inducing apoptosis via the intrinsic pathway (De Silva et al., 2013). Irofulven is an alkylating agent derived from a compound produced by *Omphalotus illudens* and exhibits cytotoxic activity. As an alkylating agent it can induce apoptosis, inhibit DNA synthesis and covalently bind macromolecules. Irofulven also produces a pro-apoptotic signal by interfering with redox homeostasis causing mitochondrial dysfunction and protein oxidation. Studies have also shown that it exerts enhanced activity towards cancer cells rather than normal cells (De Silva et al., 2012).

#### **1.4.4 Induction of apoptosis as a mechanism of cytotoxicity**

Cell death is an essential process to maintain homeostasis, immune regulation and tissue development. Alterations and dysregulation can lead to diseases such as diabetes, neurodegenerative diseases and cancer. Cell death can be classified based on morphological appearances, enzymological criteria, functional aspects or immunological characteristics. Several modes of cell death, i.e. apoptosis, necrosis, autophagy and mitotic catastrophe, exist and can be induced in the same cells (Duprez et al., 2009; Chaabane et al., 2013).

Apoptosis is referred to as programmed cell death that is a key area for cancer research as a means to eliminate cancerous cells. Apoptosis can be characterised by distinct morphological and biochemical features such as cell shrinkage, membrane blebbing, plasma membrane modification, mitochondrial depolarization, chromatin condensation and DNA fragmentation. Apoptosis can be initiated by two pathways, namely the intrinsic (mitochondrial) and extrinsic (receptor-mediated) pathway (Jang et al., 2010; Prateep et al., 2017).

Figure 1.1 summarizes the key events in the extrinsic and intrinsic apoptotic pathways. The extrinsic pathway is mediated by death receptors located on the cell surface and interactions with their respective ligands. The death receptors belong to the TNF-related apoptosis inducing ligand receptors (TRAIL) and tumour necrosis factor (TNF) superfamily. The receptors contain extracellular domains which bind ligands, and intracellular cytoplasmic domains (death domains) which transmit the death signals.

Binding of ligands and activation of the TNF death receptors lead to the recruitment of intracellular proteins forming death signalling complexes (DISCs). This in turn activates procaspase-8, an initiator caspase. Activated caspase-8 continues to activate downstream caspases such as caspase-3, -6 and/or -7 (execution phase of apoptosis). The activated caspases can further reinforce the death signal by inducing mitochondrial damage leading to the release of additional death amplifying proteins (Duprez et al., 2009; Indran et al., 2011).

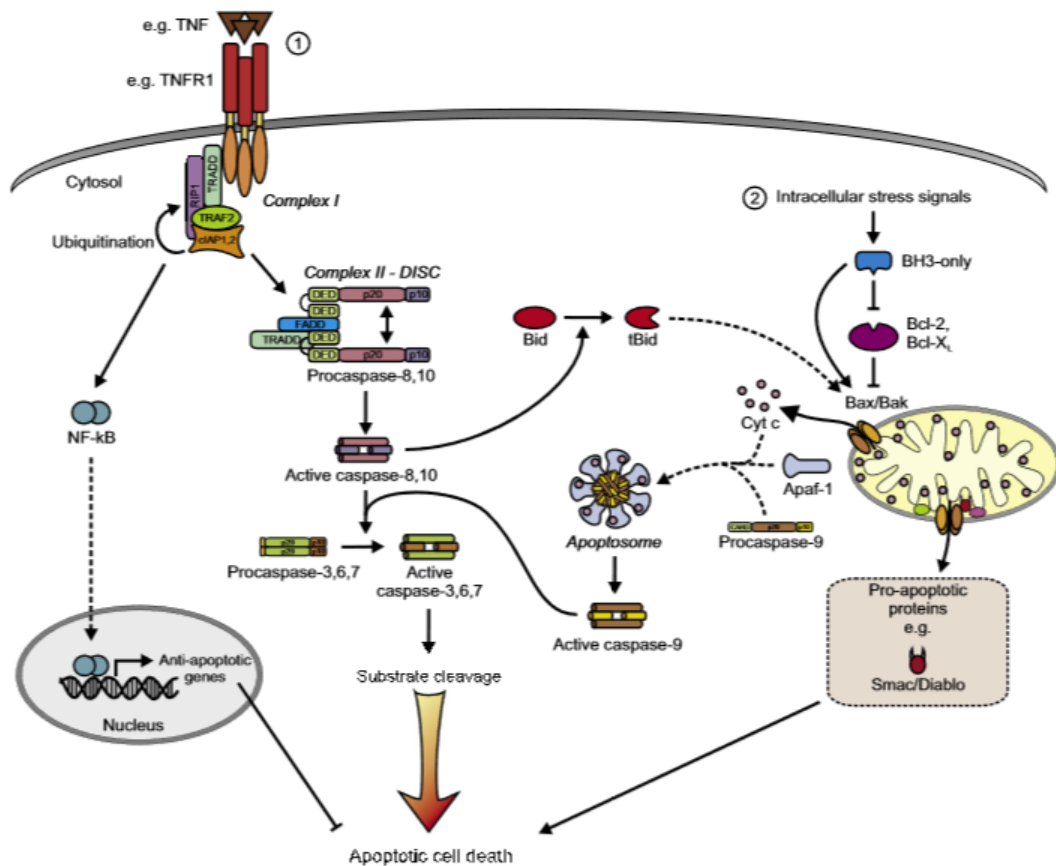


**Figure 1.3:** Schematic representation of the key steps in the extrinsic (1) and intrinsic (2) pathways in apoptosis (Duprez et al., 2009). See text for more detail.

The intrinsic pathway is activated through stimuli such as viral infections, radiation, free radicals and genetic damage. These stimuli cause alterations in the permeability of the mitochondrial membrane, leading to the loss of membrane potential. This in turn causes the release of pro-apoptotic proteins such as cytochrome-c. The pathway is regulated by pro-apoptotic (e.g. Bax, Bad, Bid, Hrk, etc.) and anti-apoptotic (e.g. Bcl-2, Bfl-1, Mcl-1, etc.) proteins belonging to the Bcl-2 family. The initiation of apoptosis is regulated by the balance of pro-apoptotic and anti-apoptotic proteins. Pro-apoptotic



proteins regulate apoptosis by promoting the release of cytochrome-c via pore formation in the mitochondrial membrane causing membrane permeability, whereas anti-apoptotic proteins block the release.

Several other factors are released into the cytoplasm and include apoptosis inducing factor (AIF), direct inhibitor of apoptosis protein binding protein with low pI (DIABLO), second mitochondria-derived activator of caspases (Smac) and Omi/high temperature requirement protein A (HtrA2) (Duprez et al., 2009; Koff et al., 2015). Smac/DIABLO binds and deactivates AIF allowing the apoptotic process to continue (Indran et al., 2011). Cytochrome-c binds to Apaf-1 (a caspase adaptor molecule) causing caspase activation and recruitment domains (CARDs) to be exposed. The binding of pro-caspase-9 leads to the formation of the apoptosome, which dimerizes and auto-activates pro-caspase-9. Activated caspase-9 triggers the executioner pathway leading to the activation of caspase-3 and -7 (Koff et al., 2015). The executioner caspases cleave various substrates such as cytoskeletal proteins, protein kinases and DNA repair proteins. They also effect the cell cycle and signalling pathway which all lead to the characteristic morphological features observed in apoptosis (Wong, 2011). DIABLO/Smac induces the activation of caspase-3/-9 by binding to inhibitor of apoptosis proteins (IAPs) (Wong, 2011).

#### **1.4.5 The cell cycle**

The cell cycle can be defined as a series of events leading to the duplication and division of a cell forming two daughter cells. The cell cycle is composed of four main phases namely the G1-, S-, G2- and M phase. Cells may reversibly exit the cell cycle into G0 phase when there is a lack of appropriate growth-promoting signals. Morphologically the cell cycle can be divided into interphase (G1-, S-, G2 phase) and mitotic phase (prophase, metaphase, anaphase and telophase) (Schafer 1998). The progression of the cell cycle is controlled by protein phosphorylation and cell cycle checkpoints (Collins et al., 1997). Central to the regulation of the cell cycle are cyclin-dependent kinases (CDKs) and cyclin proteins. CDKs are activated due to the formation of a complex when bound to the regulatory cyclin subunit (Gérard and Goldbeter, 2014). Cyclin-CDK complexes have different substrate specificities and are therefore involved in different cell cycle events. They are classified into three

categories, namely (i) complexes involved in the progression of the cell cycle through G1 phase and S-phase commitment, (ii) complexes involved in the initiation and completion of DNA replication, and (iii) complexes involved in mitosis and preventing G1 re-entry (Novák et al., 2002). CDKs are maintained at constant concentrations during the cell cycle and therefore cyclin-CDK complexes activities are regulated based on cyclin availability, cyclin-kinase inhibitors and inactivation by phosphorylation (Novák et al., 2002).

The cell cycle is a highly regulated process and each transition from one phase to the next is regulated by several checkpoints. The term cell cycle checkpoint refers to a mechanism that is in place in order to check whether the required steps have been fulfilled and that the order of events are correct before proceeding to a cell division cycle (Garrett, 2001). The main goal of the checkpoints are to ensure that the genome remains intact. These checkpoints detect problems such as incomplete cell cycle events due to DNA damage or the misalignment of chromosomes. This leads to the generation of inhibitory signals carried by a signal transduction pathway causing cell cycle arrest by an effector. When the cell cycle arrests it allows the cell to resolve and repair the damage (Pucci et al., 2000; Garrett, 2001). If the damage cannot be repaired, the cell will undergo apoptosis (Pucci et al., 2000). The cell cycle events are monitored by checkpoints that occur at the G1/S boundary, S-phase and G2/M phase.

The *G1/S checkpoint* is regulated by two mechanisms. The first pathway to delay the transition into the S-phase involves the activation of checkpoint kinase 2 (Chk2) by ataxia telangiectasia mutation (ATM). This leads to the phosphorylation of Cdc25A causing it to be ubiquitinated and targeted for destruction. The association of CDK2 with cyclin E is required for cells to enter S-phase. The loss of Cdc25A prevents Chk2 activity thereby arresting cells in the G1 phase (Nyberg et al., 2002). The second regulatory pathway involves two tumour suppressor pathways, p53 and retinoblastoma protein (Rb). Activation of p53 occurs due to DNA damage. DNA damage activates ATM which in turn phosphorylates and activates p53 disrupting its interaction with the negative regulator Mdm2, an ubiquitin ligase. This leads to the accumulation of p53 which induces the transcription of several genes including p21<sup>Cip1</sup>, an inhibitor of cyclin-CDK complexes causing cell cycle arrest. Other G1 checkpoints may include an increase in p21, which binds and inactivates cyclin D-CDK4/6 and

cyclin E-CDK2. This causes Rb in its unphosphorylated form to bind the early gene 2 factor (E2F), forming a transcriptional repressing complex causing cell cycle arrest. The p53-dependent pathway maintains G1 cell cycle arrest, initiated by the Cdc25A pathway, until the DNA damage is repaired (Nyberg et al., 2002).

The *S phase checkpoint* is activated by DNA damage that can arise from either double stranded breaks, stalled replication forks or as a result of the repair process. The ataxia telangiectasia and Rad3-related (ATR) kinase detects DNA damage and activates checkpoint kinase 1 (Chk1) that leads to the degradation of Cdc25A and blocking further progression into the S phase (Visconti et al., 2016).

The *G2/M checkpoint* prevents cells with damaged DNA to enter mitosis. This checkpoint targets the mitotic kinase cyclin B-CDK1 which is required for the start of mitosis. ATR inhibits cyclin B/CDK1 by Chk1 that inhibits Cdc25C by phosphorylation, and activating the CDK1 inhibitory kinase (Wee1) thereby preventing cells from entering mitosis (Novák et al, 2002). CDK1 activity is required to enter mitosis as it phosphorylates a variety of substrates that perform specific activities required for mitosis (Molinari, 2000; Kalsbeek and Golsteyn, 2017). Studies also showed that G2 arrest is maintained by p53 and p21 (Pietenpol and Stewart, 2002).

*The spindle (metaphase) checkpoint* ensures proper chromosome segregation and requires the activation of the cdc2/cycB complex. This checkpoint regulates the activity of the anaphase promoting complex (APC), a ubiquitin ligase, that function to degrade cohesin and mitotic cyclins allowing the separation of chromatids and to exit mitosis, respectively (Molinari, 2000). APC degrades securin which inactivates a protease called separase that degrades cohesion proteins leading to the first stage of anaphase (Novák et al., 2002). The association and interaction of APC with p55CDC/cdc20 influence the cleavage of cohesin and its interaction with Chk1 mediates the cleavage of cyclins. Disruptions in spindle formation activate MAD proteins that bind to the cdc20 subunit of APC causing its inactivation. This leads to the arrest of the cell cycle in metaphase. The inactivation of certain kinases (hBub1 and hBub1R) can lead to early mitotic exit with the unequal distribution of genetic material (Molinari, 2000).

*Mitotic catastrophe* is a cell death mechanism that is activated to prevent the proliferation of cells that exhibit a defective mitotic phase or failed to complete mitosis. Mitotic catastrophe can be characterised by the formation of multinucleated cells by abnormal chromosome separation, or micronucleated cells by chromosome fragments that are excluded during telophase when the daughter cells are formed (McGee, 2015).

### **1.5 Significance of the study**

Antimicrobial resistance is a serious therapeutic concern that limits the treatment options for life-threatening diseases such as TB and HIV. Due to the high cost and adverse side effects of TB and HIV treatments, the regimens are frequently not completed. Cancer therapy also has several disadvantages that include non-specific drug targeting and damaging side effects (De Silva et al., 2012; Patel and Goyal, 2012). This emphasises the need for therapeutic compounds that are less-toxic and more effective, while exhibiting their intended biological activities (Patel and Goyal, 2012).

It is well documented that mushrooms produce bioactive compounds with numerous biological activities, which include antimicrobial and anticancer activities (Yamac and Bilgili, 2006). This suggests that mushrooms could be useful in the search for safe and effective alternative therapeutic agents. Of the available mushrooms species only a small number have been explored for their pharmaceutical potential (De Silva et al., 2013). Scientific information regarding the medicinal and therapeutic uses of macrofungi in Africa is limited; hence this study investigated the medicinal properties of endemic and exotic macrofungal species found in South Africa, which will expand the knowledge in this field. This study could identify macrofungal species with medicinal properties within South Africa, which can be further investigated for their potential use as therapeutic agents to alleviate some of the problems associated with current treatment options.

### 1.5.1 Hypotheses to be tested

It was hypothesised that:

- I Macrofungal species exhibit antimicrobial activity against selected respiratory pathogens.
- II Macrofungal extracts are cytotoxic and inhibit the proliferation of human lung carcinoma cells.
- III Cytotoxic properties of macrofungal extracts are due to the induction of apoptosis.

### 1.5.2 Objectives of the study

The following objectives were established to test the above hypotheses:

- I To screen the macrofungal extracts for antimicrobial activity against microorganisms responsible for respiratory diseases (e.g. *Pseudomonas aeruginosa*, *Klebsiella pneumoniae*, *Streptococcus pneumoniae*, *S. pyogenes*, *S. aureus*, *M. tuberculosis*, and HIV-1),
- II To determine the effect of macrofungal extracts on bacterial morphology,
- III To investigate the cytotoxicity of macrofungal extracts against human lung carcinoma cells, and
- IV To elucidate the mechanism/s of action of cytotoxicity/anticancer activity.

## CHAPTER TWO

### ANTIMICROBIAL ACTIVITY OF MACROFUNGAL EXTRACTS

#### 2.1 INTRODUCTION

The upper respiratory tract contains several bacterial species such as *Streptococcus pneumoniae*, *Haemophilus influenza*, *Staphylococcus aureus* and several other species which form part of the normal microbiota. These species, although serving a beneficial role within the body, are potential pathogens. Imbalances within the normal microbiota as well as failure of the defences of the respiratory system may lead to disease (Bosch et al., 2013). The most common causative agents of respiratory infections are viral. However, the respiratory tract remains susceptible to infectious organisms such as bacteria, fungi and parasites (Johnston, 2012). Lower respiratory tract infections were identified as the second highest cause of death in the sub-Saharan Africa region in 2012, causing over 1 million deaths (Africa Check, 2016).

The most common bacteria identified as causative agents of respiratory tract infections include *Pseudomonas* spp., *Klebsiella* spp., *Streptococcus* spp., *Staphylococcus* spp., *Enterobacter* spp., *Acinetobacter* spp., *Proteus* spp., and *H. influenzae* (Siddalingappa et al., 2013). The inappropriate use of antibiotics for the treatment of infectious diseases has led to the spread of resistance (Ramya et al., 2013). Antibiotic resistant bacteria may survive due to innate resistance or the acquisition of resistance to a particular antibiotic. The latter occurs by either acquiring genes conferring resistance from another microorganism by means of gene transfer or through genetic mutation (Johnston, 2012).

TB is a serious chronic infectious disease caused by *Mycobacterium tuberculosis* with high mortality rates. Multidrug treatment regimens are used for the treatment of TB and include at least two of the following first-line antibiotics: rifampicin, isoniazid, ethambutol and pyrazinamide. Although treatment is available, TB continues to spread worldwide and remains a global problem. There are several drawbacks to multidrug treatment, including long-term (~ 6 months) usage, which can lead to drug-induced hepatotoxicity. The prolonged treatment increases the possibility to develop MDR-TB.

The increasing number of MDR-TB and XDR-TB strains have increased the search for antitubercular agents from natural products with fewer side effects (Nguta et al., 2015). Several studies have confirmed that natural products show antitubercular activity and may be useful leads for the discovery of TB drugs. Antitubercular compounds have been found in a variety of natural sources such as plants, marine organisms and fungi (Nguta et al., 2015). Several of the natural products that showed antitubercular activity have not progressed to clinical trials. This is due to several factors that include, (1) low yields of isolated compounds; (2) structural complexity; (3) low activity [minimum inhibitory concentration (MIC)  $\geq 1 \mu\text{g/mL}$ ]; (4) difficulty in the isolation of compounds with novel targets; and (5) difficulties in the identification of isolated compounds (Nguta et al., 2015).

Literature has shown that numerous fungal species produce different classes of compounds with inhibitory activity of pathogenic viruses. This enables the development of antiviral drugs that affect different stages of the viral lifecycle (Teplyakova and Kosogova, 2016). Bioactive compounds produced by macrofungi have shown to affect and inhibit several human pathogenic viruses that include, herpesvirus, West Nile virus, influenza virus, human immunodeficiency virus, orthopoxviruses, poliovirus and hepatitis viruses (Teplyakova and Kosogova, 2016). Human immunodeficiency virus (HIV) is the causative agent of Acquired Immunodeficiency Syndrome (AIDS). There are two types of HIV: HIV-1 and HIV-2, both causing AIDS (Rege et al., 2015). HIV-1 is the most pathogenic strain and causes the most HIV infections, whereas HIV-2 is less prevalent and found in specific geographic locations such as Western Africa (Klos et al., 2009). It was estimated that 36.7 million people globally were living with HIV at the end of 2016 with 1.8 million newly infected individuals. In 2016, 1.0 million HIV-related deaths were recorded. Sub-Saharan Africa was recognised as the region with the highest prevalence of HIV in 2016 (70%) (WHO, 2017b).

Thirty antiretroviral drugs are approved for the treatment of HIV, which are defined based on their target sites in the HIV lifecycle. Highly active antiretroviral therapy (HAART), in which combinations of three antiretroviral drugs are used, have shown a reduction in AIDS-related deaths. Several challenges exist with HAART and include the potential development of drug resistance, hepatotoxicity and several other detrimental

side effects. As a result of the limitations of antiretroviral therapy there is a need to discover safe, cheap and effective therapeutic agents. The viral lifecycle consists of several targets such as HIV-1 reverse transcriptase (RT), HIV-1 protease and HIV-1 integrase that can be exploited for drug development (Rege et al., 2015). Other sites that are targeted for the development of anti-HIV drugs, include: (1) receptor inhibitors to prevent entry into cells, (2) inhibitors of viral accessorial proteins, (3) viral nucleoside inhibitors, (4) glycosidase inhibitors and (5) virus assembly inhibitors (Wang et al., 2007). HIV-1 reverse transcriptase, HIV-1 protease and HIV-1 integrase are vital for the viral lifecycle. HIV-1 RT transcribes the viral RNA into functional double stranded DNA. HIV integrase functions to incorporate the viral DNA into the genome of the infected cells. The protease enzyme is required for the assembly of the infectious virus, and inhibition of the enzyme activity will lead to the formation of immature non-infectious virions (Rege et al., 2015).

The emergence and spread of antibiotic resistance poses health problems and can lead to treatment failure, increased costs, prolonged illness and potentially death. Prolonged illness results in individuals remaining infectious which could possibly lead to an outbreak (Johnston, 2012). Antibiotic resistant strains of *S. aureus*, *S. pneumoniae* and *H. influenza* have been isolated from individuals with lower respiratory tract infections (Craig et al., 2009), and an increase in MDR-TB and XDR-TB have been observed (Nguta et al., 2015). Therefore the search for new compounds with antimicrobial properties is a priority in order to combat diseases with high morbidity and mortality rates as well as those resistant to current treatment options (Alves et al., 2012a), either for the development of new therapeutic agents or to be used to assist current treatment options (Nowacka et al., 2015).

Natural sources, such as fungi, have been explored in the search for bioactive compounds exhibiting therapeutic properties (e.g. antimicrobial activity) since the discovery of penicillin in microfungi. It is assumed that fungi produce antifungal and antibacterial compounds in order to survive in their natural habitat and to compete with other organisms (Kalyoncu et al., 2010; Bala et al., 2012). Certain bacterial species (e.g. *Pseudomonas aeruginosa*, *Escherichia coli*, *S. aureus*, etc.) can infect both humans and fungi, and the compounds produced by macrofungi (mushrooms) against these microorganisms may be of benefit to humans (Beattie et al., 2010; Ranadive et



al., 2013). The antimicrobial activity of macrofungi has been documented since the 1900s (Robbins et al., 1947; Hirata and Nakanishi, 1950). Several antimicrobial agents (e.g. grifolin, pleuromutilin, scorodonin, etc.) have been isolated from macrofungi of which retapamulin has been approved and is commercially produced for the treatment of skin infections caused by *S. aureus* and *Streptococcus pyogenes* (Bala et al., 2012). Studies (Smânia et al., 1995; Rosa et al., 2003; Ren et al., 2014) have confirmed the antimicrobial activity of macrofungi against several human pathogens. Therefore macrofungi represents a promising source of potential alternative agents exhibiting antimicrobial activity. The current knowledge regarding the antimicrobial potential of macrofungi is limited to studies investigating the crude mushroom extracts for antimicrobial activity, while information regarding the compounds that confer these activities are limited (Rezaeian and Pourianfar, 2016). A few low molecular weight compounds (e.g. terpenes, organic acids, steroids, etc.), proteins and some peptides have been described to produce antimicrobial activity (Alves et al., 2012a). Several macrofungal species have been investigated for their antibacterial activity, which include *Agaricus*, *Boletus*, *Ganoderma*, *Pycnoporus*, *Hyphaloma*, *Lentinus* and several others (Rezaeian and Pourianfar, 2016).

Scientific literature regarding the antitubercular activity of macrofungal species is limited. The first century Greek physician, Dioscorides, included in his encyclopaedia on herbal medicine (De Materia medica) two macrofungal spp. (i.e. *Laricifomes officinalis* and *Fomitopsis officinalis*) for the treatment of tuberculosis (Wani et al., 2010). *Fomes fomentarius* and *Lentinus edodes* have shown to inhibit *M. smegmatis* and *M. tuberculosis*, respectively (Robles-Hernández et al., 2008). *Ganoderma* is a medicinal mushroom used in traditional medicine for more than 2 millennia and has been intensively investigated worldwide. Lanostanoids isolated from *Ganoderma* spp. have shown antituberculosis activity (Isaka et al., 2017). Several studies have confirmed the anti-HIV activity of macrofungi. *Trametes versicolor*, *Flammulina velutipes*, *Grifola frondosa*, *Fuscoporia obliqua* and *Inonotus obliquus* are some macrofungal spp. inhibiting HIV (Teplyakova and Kosogova, 2015). Therefore, macrofungi could be considered as natural sources for drug development.

Various approaches can be employed to evaluate the antibacterial activity of mushrooms, which include micro-broth dilution (with or without a chromogenic

reagent) and agar diffusion methods (Rezaeian and Pourianfar, 2016). Agar diffusion methods, although cost-efficient, may produce false positive and negative results when examining the activity of extracts. Several factors influence the antimicrobial results obtained when employing the agar diffusion method such as the molecular size of the bioactive compounds, agar type, incubation temperature and salt concentration. This method also does not allow the determination of the MIC value. An alternative technique employed to determine antimicrobial activity is macrodilution/ microdilution method in which the MIC value can be quantified (Eloff, 1998). Microplate Alamar Blue assay (MABA), is a colorimetric assay that can be utilised for antimycobacterial drug screening. The assay uses alamar blue, an oxidation/reduction indicator dye, that changes colour from blue to pink, indicating bacterial growth. The colour change can be visually monitored or the reduced form of the dye can be quantified spectrophotometrically or fluorimetrically (Collins and Franzblau, 1997).

The mechanisms of action of antimicrobial agents involve the modification of cell wall synthesis, alteration in membrane permeability, DNA and protein synthesis, osmoregulation and/or respiration processes. Maintaining membrane integrity is essential for performing vital cellular functions, and disruption in membrane integrity can lead to metabolic dysfunction and eventually cell death. The cell wall is required for bacterial shape and serves as an osmotic barrier. Electron microscopy (EM) can be employed in order to observe alteration in bacterial cell structure (morphological and ultrastructure) and assist to elucidate the mode of action of antibacterial agents such as mushroom extracts (Matijašević et al., 2016).

The objective of this chapter was to screen ethanol and aqueous extracts of twenty-one South African macrofungal spp. (based on seasonal availability) for their potential antimicrobial activity against respiratory bacterial pathogens and inhibition of HIV-1 enzymes.

## 2.2 MATERIALS AND METHODS

### 2.2.1 Materials/ chemicals/ reagents

Rifampicin, ethambutol dihydrochloride, gentamicin sulfate and vancomycin hydrochloride were purchased from Sigma (St. Louis, MO, USA). SensoLyte® 490 HIV-1 protease assay- and HIV-1 reverse transcriptase assay kits were purchased from AnaSpec (AnaSpec, Inc., Fremont, CA, USA) and Roche (Roche Diagnostics GmbH, Mannheim, Germany), respectively.

### 2.2.2 Macrofungal material and ethanolic and aqueous extract preparation

The fruiting bodies of various macrofungal species were collected. *Amanita foetidissima* and *Chlorophyllum molybdites* were collected in Despatch, Eastern Cape, South Africa. *Imlaria badia*, *Fomitopsis lilacinogilva*, *Ganoderma lucidum*, *Gymnopilus junonius*, *Gymnopilus penetrans*, *Hypholoma fasciculare*, *Lenzites elegans*, *Pisolithus tinctorius*, *Pycnoporus sanguineus*, *Russula capensis*, *Schizophyllum commune*, *Stereum hirsutum*, *Agaricus campestris*, *Paneolus papilionaceus*, *Laetiporus sulphureus* and *Pseudophaeolus baudonii* were collected in Plettenberg Bay/Knysna, Western Cape, South Africa. *Pleurotus ostreatus* (white; W) was bought at a local supermarket. *Pleurotus ostreatus* (grey; G) and *Hericium erinaceus* were obtained from Professor B. Viljoen (University of the Free State). Macrofungal species were identified using South African mushroom guides (van der Westhuizen and Elcker, 1994; Levin et al., 1987; Branch, 2001; Gryzenhout, 2010) and identification confirmed by the Mushroom Guru (Pty) Ltd (Somerset West, South Africa).

Macrofungal fruiting bodies were cleaned and dried in an oven at 25-30°C, for 2-3 days. The fruiting bodies were submerged in liquid nitrogen and crushed using a mortar and pestle. Ethanolic (80%) extracts were prepared using a material: solvent ratio of 1:15 (w/v). Aqueous extracts (double distilled water; ddH<sub>2</sub>O) were prepared using a material: solvent ratio of 1:10 (w/v). Macrofungal material was extracted at room temperature (25±2 °C) for 24 h on a magnetic stirrer. Extracts were centrifuged at 1 800 × g for 5 min. The supernatant was filtered twice through Whatman No. 4 filter paper under vacuum. Ethanol was evaporated at 50 °C using a BUCHI Rotavapor R-210 rotary evaporator (Switzerland). The extracts were freeze dried using a VirTis SP

Scientific sentry 2.0 freeze dryer (Gardiner, NY, USA) and stored at 4 °C in a desiccator in the dark, until further use.

### **2.2.3 Macrofungal extracts**

Macrofungal extracts were dissolved in dimethyl sulfoxide (DMSO) or double distilled water for ethanol and aqueous extracts, respectively, at stock concentrations of 100 mg/mL. Aqueous extracts were filter sterilized (0.2 µm filter). Working concentrations of 4 mg/mL were prepared in Mueller-Hinton (MH) broth.

### **2.2.4 Antibacterial activity**

#### **2.2.4.1 Microorganisms, growth conditions and media**

Test microorganisms used in this study included Gram positive bacteria (i.e. *Streptococcus pneumoniae*, *Staphylococcus aureus* and *Streptococcus pyogenes*) and Gram negative bacteria (i.e. *Pseudomonas aeruginosa* and *Klebsiella pneumoniae*). Bacterial cultures were grown on MH agar or Blood agar (for *Streptococcus* spp.) plates at 37 °C. An overnight streak plate was used to inoculate MH broth (Merck, USA) or Brain Heart Infusion broth (for *Streptococcus* spp.; Merck, USA) and allowed to grow for 16 h (log growth phase) at 37 °C.

#### **2.2.4.2 Control antibiotics**

Gentamicin sulfate and vancomycin hydrochloride (Sigma, USA) were used as positive controls against Gram-negative and Gram-positive bacteria, respectively. Antibiotics were dissolved in double distilled water at stock concentrations of 2 mg/mL and filter sterilized (0.2 µM filter). Working concentrations of the antibiotics were prepared in MH broth, depending on the antibiotics' MIC values.

#### **2.2.4.3 Microplate p-Iodonitrotetrazolium chloride (INT) assay**

This assay was carried out as described by Eloff (1998), using p-Iodonitrotetrazolium chloride (INT) dye. Briefly, 50 µL of MH or Brain Heart Infusion Broth (*Streptococcus* spp.) was added to the wells of a sterile 96-well plate from columns 2 to 8. Macrofungal extracts (50 µL) were added to columns 1 and 2. This was followed by the transfer of 50 µL from column 2 to 3 and serially diluted (two-fold dilutions) until column 8. The cultures were assessed and adjusted to a 0.5 McFarland standard [1.175% BaCl<sub>2</sub>

(0.1175 g in 10 mL ddH<sub>2</sub>O) and 1% H<sub>2</sub>SO<sub>4</sub> (0.5 mL H<sub>2</sub>SO<sub>4</sub> in 50 mL ddH<sub>2</sub>O)] (absorbance at 600 nm = 0.08-0.1; equivalent to  $\sim 1.5 \times 10^8$  cells/mL) and 50  $\mu$ L added to each test well to give a final volume of 100  $\mu$ L. The concentration of extracts ranged from 15.6 – 2,000  $\mu$ g/mL. Additional dilutions were prepared if MICs showed to be lower than above mentioned concentration range. The following controls were prepared: (i) antibiotic/medium control (50  $\mu$ L MH broth + 50  $\mu$ L of highest antibiotic concentration); (ii) macrofungal extract colour control (50  $\mu$ L MH broth + 50  $\mu$ L of highest macrofungal extract concentration); (iii) 4% DMSO control (50  $\mu$ L MH broth + 50  $\mu$ L 8% DMSO); and (iv) microorganism control (50  $\mu$ L MH broth + 50  $\mu$ L microorganism). Plates were sealed with microplate sealing tape and incubated at 37°C for 24 h.

INT was prepared at a working concentration of 0.2 mg/mL in ddH<sub>2</sub>O and filtered (0.2  $\mu$ M filter). INT (50  $\mu$ L) was added to each well, and the plates were further incubated for 30-60 min at 37 °C until there was a colour change. A colour change from yellow (dye) to a pink/purple colour showed the reduction of the dye by viable bacteria. No colour change indicated the inhibition of bacterial growth (non-viable bacteria). The MIC was determined as the lowest concentration (highest dilution) of the macrofungal extract that does not show visible growth when compared to the control. The absorbance was measured at 600 nm using a BioTek® PowerWave XS spectrophotometer (Winooski, VT, USA).

Percent inhibition was defined as: Percent inhibition =  $1 - (\text{test well absorbance} / \text{mean absorbance triplicate bacteria only well}) \times 100$

### **2.2.5 Transmission electron microscopy (TEM)**

Ultrastructural damage to the bacterial cells was investigated using TEM. *S. aureus*, *S. pyogenes* and *S. pneumoniae* in the log growth phase (16 h at 37 °C in MH/Brain-Heart Infusion broth) were treated with the macrofungal extracts at the MIC concentration or left untreated. The bacteria exposed to the crude extracts were incubated for 8 h at 37 °C. The cells were harvested by centrifugation (8 000 rpm for 5 min) and prefixed with 2.5% glutaraldehyde overnight at 4 °C. After fixation overnight, the cells were centrifuged and the fixative removed. The obtained pellets were washed two times for 5 min each with 0.1 M sodium phosphate buffer (pH 7.2). Thereafter, cell

pellets were post fixed with 1% osmium tetroxide for 1 h at room temperature and washed twice for 5 min each with 0.1 M sodium phosphate buffer. The samples were subsequently dehydrated with a graded ethanol series (30, 50, 75 and 100%; 15 min each). This was followed by acetone dehydration starting with 1:2 acetone: ethanol for 10 min, followed by 2:1 acetone: ethanol for 15 min, and finally 100% acetone for 10 min. The samples were infiltrated with 1:2 resin: acetone for 45 min, followed by 1:1 resin: acetone for 2.5 h. This was replaced with 3:1 resin: acetone and left overnight at room temperature. The samples were polymerized at 60 °C for 16-20 h. Ultra-thin sections (70 nm) were processed with an ultramicrotome and placed on 300 mesh Cu grids. The samples were stained with 2% uranyl acetate/drops of UranylLess for 2 min and lead citrate (0.1 mL 10 N NaOH and 0.04 g lead citrate in 10 mL ddH<sub>2</sub>O; Venable and Coggeshall, 1965) for 1 min. The prepared samples were examined with a transmission electron microscope (JEOL JEM 2100, USA).

## **2.2.6 Anti-tuberculosis activity**

### **2.2.6.1 Microorganism, growth conditions and media**

The *Mycobacterium tuberculosis* strain, H37, was obtained from the National Health Laboratory Services (NHLS), Port Elizabeth, South Africa. *M. tuberculosis* was grown in Difco™ Middlebrook 7H9 broth (BD) [88.98 mL ddH<sub>2</sub>O; 0.470 g Difco™ Middlebrook 7H9 broth base; 0.8 mL glycerol (Merck); 0.005 mL Tween®80 (Sigma-Aldrich); 1 mL Middlebrook albumin-dextrose-catalase (ADC) growth supplement (Sigma) added after autoclaving]. Cultures were incubated at 37 °C for 10 days.

### **2.2.6.2 Control drugs**

Rifampicin and ethambutol dihydrochloride were used as antibiotic positive controls against *M. tuberculosis*. Rifampicin and ethambutol dihydrochloride were dissolved in sterile water at stock concentrations of 1 and 2 mg/mL, respectively. Working concentrations of 16 µg/mL and 1 mg/mL were prepared for rifampicin and ethambutol dihydrochloride, respectively, in culture broth (without Tween®80) and filter sterilized (0.2 µm filter).

### **2.2.6.3 Microplate Alamar blue assay (MABA)**

The assay was performed as described by Franzblau *et al.* (1998) with modifications. The outer perimeter wells of sterile, clear 96-well plates were filled with sterile water

to minimize evaporation of medium in experimental wells during incubation. In brief, culture broth (50  $\mu$ L) was added to all experimental wells (i.e. macrofungal extracts and antibiotics); except to the highest macrofungal extract and antibiotic concentration wells to which 50  $\mu$ L of the working concentrations were added. Serial dilutions (1:2) were prepared for the ethanol macrofungal extracts (15.6-2,000  $\mu$ g/mL), rifampicin (0.0625-8  $\mu$ g/mL) and ethambutol dihydrochloride (3.906-500  $\mu$ g/mL). The *M. tuberculosis* culture was assessed and adjusted to a 0.5 McFarland standard (absorbance at 600 nm = 0.08-0.1; equivalent to  $\sim 1.5 \times 10^8$  cells/mL) and 50  $\mu$ L added to each test well. The following controls were prepared: (i) antibiotic/medium control (50  $\mu$ L medium + 50  $\mu$ L of highest antibiotic concentration); (ii) macrofungal extract/medium control (50  $\mu$ L medium + 50  $\mu$ L of highest macrofungal extract concentration); (iii) 4% DMSO control (50  $\mu$ L medium + 50  $\mu$ L 8% DMSO); and (iv) microorganism growth control (50  $\mu$ L medium + 50  $\mu$ L *M. tuberculosis* inoculum). Plates were sealed with microplate sealing tape and incubated at 37 °C for seven days.

After treatment, 20  $\mu$ L of CellTiter-Blue<sup>®</sup> Reagent (Promega) and 12.5  $\mu$ L 20% Tween<sup>®</sup> 80 were added to each well. Wells were observed for colour change, where a blue colour represented no growth (non-viable cells) and a pink colour represented growth (viable cells). After 6 h, *M. tuberculosis* was killed by adding 35% formaldehyde to reach a final concentration of 10% in each well. This was done to eliminate the biosafety hazard of *M. tuberculosis* aerosols. The fluorescence was read at excitation and emission wavelengths of 560 and 590 nm, respectively, using a BioTek<sup>®</sup> SYNERGY Mx fluorometer (Winooski, VT, USA). The absorbance was read at 570 nm and at a reference wavelength of 600 nm using a BioTek<sup>®</sup> PowerWave XS spectrophotometer (Winooski, VT, USA).

Percent inhibition was defined as:

Percent inhibition =  $1 - (\text{test well RFU} / \text{mean RFU triplicate bacteria only well}) \times 100$

## 2.2.7 Inhibition of HIV-1 enzymes

### 2.2.7.1 HIV-1 reverse transcriptase (RT)

Ethanol extracts (5 and 50 µg/mL) of the 8 macrofungal species were screened for HIV-1 RT inhibition using the colorimetric HIV-1 reverse transcriptase assay kit. The protocol, as described in the kit's insert, was followed. Controls included nevirapine (1 and 10 µg/mL; positive control), DMSO (0.015%, v/v; vehicle control) and no HIV-1 reverse transcriptase (negative control).

### 2.2.7.2 HIV-1 protease

Ethanol extracts (50 µg/mL) of the 8 macrofungal species were screened for HIV-1 protease inhibition using the fluorometric SensoLyte<sup>®</sup> 490 HIV-1 protease assay kit. The protocol, as described in the kit's insert, was followed. HIV-1 protease at 75 ng/well was tested. Controls included Pepstatin A (100 nM; positive control), DMSO (0.01%, v/v; vehicle control) and no HIV-1 protease (negative control). The macrofungal extracts were tested for autofluorescence by measuring the fluorescence of the macrofungal extracts together with assay buffer and substrate. None of the macrofungal extracts showed autofluorescence. Kinetic fluorescence readings were taken every 5 min for 100 min. To determine the IC<sub>50</sub> value of *C. molybdites*, concentrations ranging between 2.5 and 100 µg/mL, were tested. HIV-1 protease inhibition was measured by calculating the slope between 15 and 75 min.



## 2.3 RESULTS

### 2.3.1 Antimicrobial activity of macrofungal extracts

The *in vitro* antimicrobial activities of twenty-one macrofungal species, collected in South Africa, were tested against selected bacterial respiratory pathogens. The  $\rho$ -iodonitrotetrazolium chloride assay was used and both ethanol- and aqueous macrofungal extracts were screened. The antimicrobial activity in terms of MIC was visually determined by a colour change from yellow to a pink/purple colour, which indicated reduction of the dye by viable bacteria (Figure 2.1) and summarised in Table 2.1 (ethanol extracts) and Table 2.2 (aqueous extracts). The MIC values obtained for the crude ethanolic and aqueous extracts showed the selective/differential antimicrobial activity of the various macrofungal species against the bacterial pathogens. The data (Tables 2.1 and 2.2) obtained indicate that extracts prepared in organic solvents (e.g. ethanol) showed improved/enhanced antimicrobial activities when compared to the aqueous extracts.

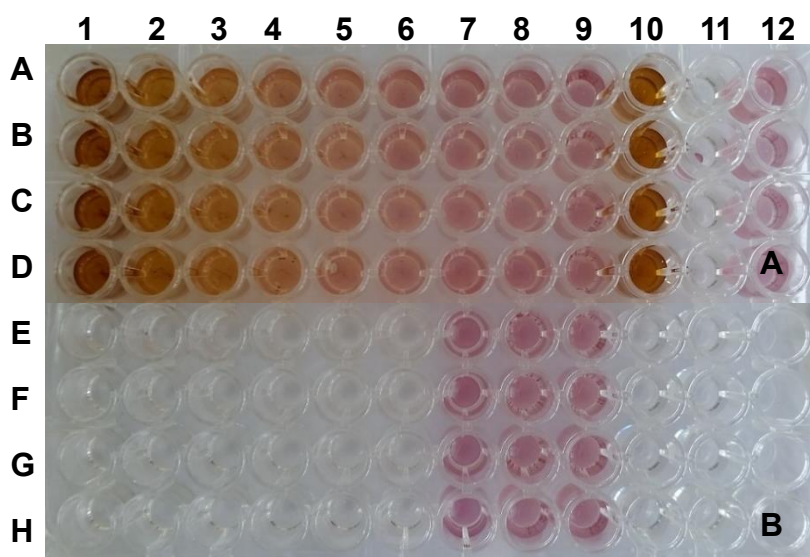


**Figure 2.1:** Antimicrobial activity of crude *Pisolithus tinctorius* spp. (ethanol extract) (A) and vancomycin (positive control; B) against *S. aureus* using the INT assay. Well 9 (all rows): bacterial growth control (0.5 McFarland Standard). Well 10 (all rows): macrofungal extract/antibiotic control. Well 11 (all rows): media control. Well 12 (A): DMSO control. Rows A-D: replicates of *Pisolithus tinctorius* and E-H: replicates of vancomycin. Concentration ranges of *Pisolithus tinctorius*: wells 1 – 8: 2,000 - 15.6  $\mu\text{g/mL}$  and vancomycin: wells 1 – 8: 64 – 0.25  $\mu\text{g/mL}$ .

### **2.3.1.1 Ethanolic macrofungal extracts**

The crude ethanol macrofungal extracts of all the species tested (Table 2.1) showed no inhibition of *P. aeruginosa* and *K. pneumoniae* at the selected concentration range (15.6 - 2,000 µg/mL). Inhibition of growth by the twenty-one ethanol extracts (Table 2.1) was observed for *S. aureus* (2/21), *S. pyogenes* (13/21) and *S. pneumoniae* (20/21). *A. foetidissima*, *C. molybdites*, *G. junonius*, *G. penetrans*, *H. fasciculare*, *F. lilacinogilva*, *L. sulphurous*, *P. sanguineus* and *P. tinctorius* were some of the most active macrofungal species screened against the Gram-positive bacteria. The standard antibiotics (i.e. gentamicin and vancomycin) showed lower MIC values than the active macrofungal extracts as seen in Table 2.1. The antimicrobial activities for ethanol extracts ranged between 31.3 – 2,000 µg/mL. DMSO did not have any inhibitory effect on the tested organisms.

**Table 2.1:** Minimum inhibitory concentration (MIC) of ethanol extracts of 21 macrofungal species tested against *P. aeruginosa*, *K. pneumoniae*, *S. pyogenes*, *S. pneumoniae* and *S. aureus* between a concentration range of 15.6 - 2,000 µg/mL (lower concentrations used if required). Control antibiotics included vancomycin and gentamicin with a concentration range of 0.5 - 64 µg/mL. Semi-quantitative analysis: visually.

	Gram-negative bacteria			Gram-positive	
	<i>P. aeruginosa</i>	<i>K. pneumoniae</i>	<i>S. pyogenes</i>	<i>S. pneumoniae</i>	<i>S. aureus</i>
<b>Agaricales</b>					
<i>Agaricus campestris</i>	> 2,000 µg/mL	> 2,000 µg/mL	1,000 µg/mL	1,000 µg/mL	> 2,000 µg/mL
<i>Amanita foetidissima</i>	> 2,000 µg/mL	> 2,000 µg/mL	> 2,000 µg/mL	125 µg/mL	> 2,000 µg/mL
<i>Chlorophyllum molybdites</i>	> 2,000 µg/mL	> 2,000 µg/mL	125 µg/mL	500 µg/mL	> 2,000 µg/mL
<i>Gymnopilus junonius</i>	> 2,000 µg/mL	> 2,000 µg/mL	> 2,000 µg/mL	125 µg/mL	> 2,000 µg/mL
<i>Gymnopilus penetrans</i>	> 2,000 µg/mL	> 2,000 µg/mL	250 µg/mL	250 µg/mL	2,000 µg/mL
<i>Hypholoma fasciculare</i>	> 2,000 µg/mL	> 2,000 µg/mL	250 µg/mL	500 µg/mL	> 2,000 µg/mL
<i>Paneolus papilionaceus</i>	> 2,000 µg/mL	> 2,000 µg/mL	1,000 µg/mL	1,000 µg/mL	> 2,000 µg/mL
<i>Pleurotus ostreatus</i> (White)	> 2,000 µg/mL	> 2,000 µg/mL	> 2,000 µg/mL	250 µg/mL	> 2,000 µg/mL
<i>Pleurotus ostreatus</i> (Grey)	> 2,000 µg/mL	> 2,000 µg/mL	2,000 µg/mL	1,000 µg/mL	> 2,000 µg/mL
<i>Schizophyllum commune</i>	> 2,000 µg/mL	> 2,000 µg/mL	> 2,000 µg/mL	250 µg/mL	> 2,000 µg/mL
<b>Polyporales</b>					
<i>Fomitopsis lilacinogilva</i>	> 2,000 µg/mL	> 2,000 µg/mL	62.5 µg/mL	31.3 µg/mL	> 2,000 µg/mL
<i>Ganoderma lucidum</i>	> 2,000 µg/mL	> 2,000 µg/mL	1,000 µg/mL	> 2,000 µg/mL	> 2,000 µg/mL
<i>Laetiporus sulphurous</i>	> 2,000 µg/mL	> 2,000 µg/mL	500 µg/mL	250 µg/mL	> 2,000 µg/mL

**Table 2.1:** *Continued...* Minimum inhibitory concentration (MIC) of ethanol extracts of 21 macrofungal species

	Gram-negative bacteria			Gram-positive bacteria	
	<i>P. aeruginosa</i>	<i>K. pneumoniae</i>	<i>S. pyogenes</i>	<i>S. pneumoniae</i>	<i>S. aureus</i>
<b>Polyporales</b>					
<i>Lenzites elegans</i>	> 2,000 µg/mL	> 2,000 µg/mL	> 2,000 µg/mL	2,000 µg/mL	> 2,000 µg/mL
<i>Pseudophaeolus baudonii</i>	> 2,000 µg/mL	> 2,000 µg/mL	2,000 µg/mL	2,000 µg/mL	> 2,000 µg/mL
<i>Pycnoporus sanguineus</i>	> 2,000 µg/mL	> 2,000 µg/mL	250 µg/mL	125 µg/mL	> 2,000 µg/mL
<i>Stereum hirsutum</i>	> 2,000 µg/mL	> 2,000 µg/mL	> 2,000 µg/mL	125 µg/mL	> 2,000 µg/mL
<b>Boletales</b>					
<i>Imleria badia</i>	> 2,000 µg/mL	> 2,000 µg/mL	> 2,000 µg/mL	250 µg/mL	> 2,000 µg/mL
<i>Pisolithus tinctorius</i>	> 2,000 µg/mL	> 2,000 µg/mL	500 µg/mL	62.5 µg/mL	1,000 µg/mL
<b>Russulales</b>					
<i>Russula capensis</i>	> 2,000 µg/mL	> 2,000 µg/mL	> 2,000 µg/mL	250 µg/mL	> 2,000 µg/mL
<i>Hericium erinaceus</i>	> 2,000 µg/mL	> 2,000 µg/mL	2,000 µg/mL	1,000 µg/mL	> 2,000 µg/mL
<b>Positive controls</b>					
Vancomycin	N/A	N/A	1 µg/mL	2 µg/mL	2 µg/mL
Gentamicin	1 µg/mL	2 µg/mL	N/A	N/A	N/A

Percentage inhibition induced by macrofungal treatment was also assessed by measuring the absorbance at 600 nm. The percentage growth of *S. pyogenes* after exposure to the ethanolic extracts of macrofungi is summarized in Figure 2.2. The macrofungal extracts produced statistically significant ( $p \leq 0.05$ ) growth inhibitory effects at their respective MIC concentrations. The percentage inhibition ranged between 83.9 - 100%, 90.1 - 96.7% and 74.6 - 100% for macrofungal species classified in the orders Agaricales, Boletales/Russulales and Polyporales, respectively. Vancomycin (positive control) showed 100% growth inhibition at a concentration of 1  $\mu\text{g/mL}$ .

*S. pneumoniae* was the most susceptible bacterial species to the macrofungal extracts, with 20 macrofungal spp. (ethanol extracts) causing growth inhibition (Figure 2.3). The percentage inhibition ranged between 60.6 - 100%, 81.6 - 91.6% and 60.4 - 100% for Agaricales, Boletales/Russulales and Polyporales, respectively. Twelve of the extracts inhibited >80% of *S. pneumoniae* growth. The inhibition of *S. pneumoniae* growth by macrofungal extracts were significant [ $p \leq 0.05$ , except for *P. ostreatus* (grey)].

Only the ethanol extracts of *P. tinctorius* (MIC: 1,000  $\mu\text{g/mL}$ ) and *G. penetrans* (MIC: 2,000  $\mu\text{g/mL}$ ) showed activity against *S. aureus*, inhibiting growth by 55.4% and 60.1%, respectively (Figure 2.4). Vancomycin (positive control) caused complete inhibition of growth at a MIC value of 2  $\mu\text{g/mL}$ .

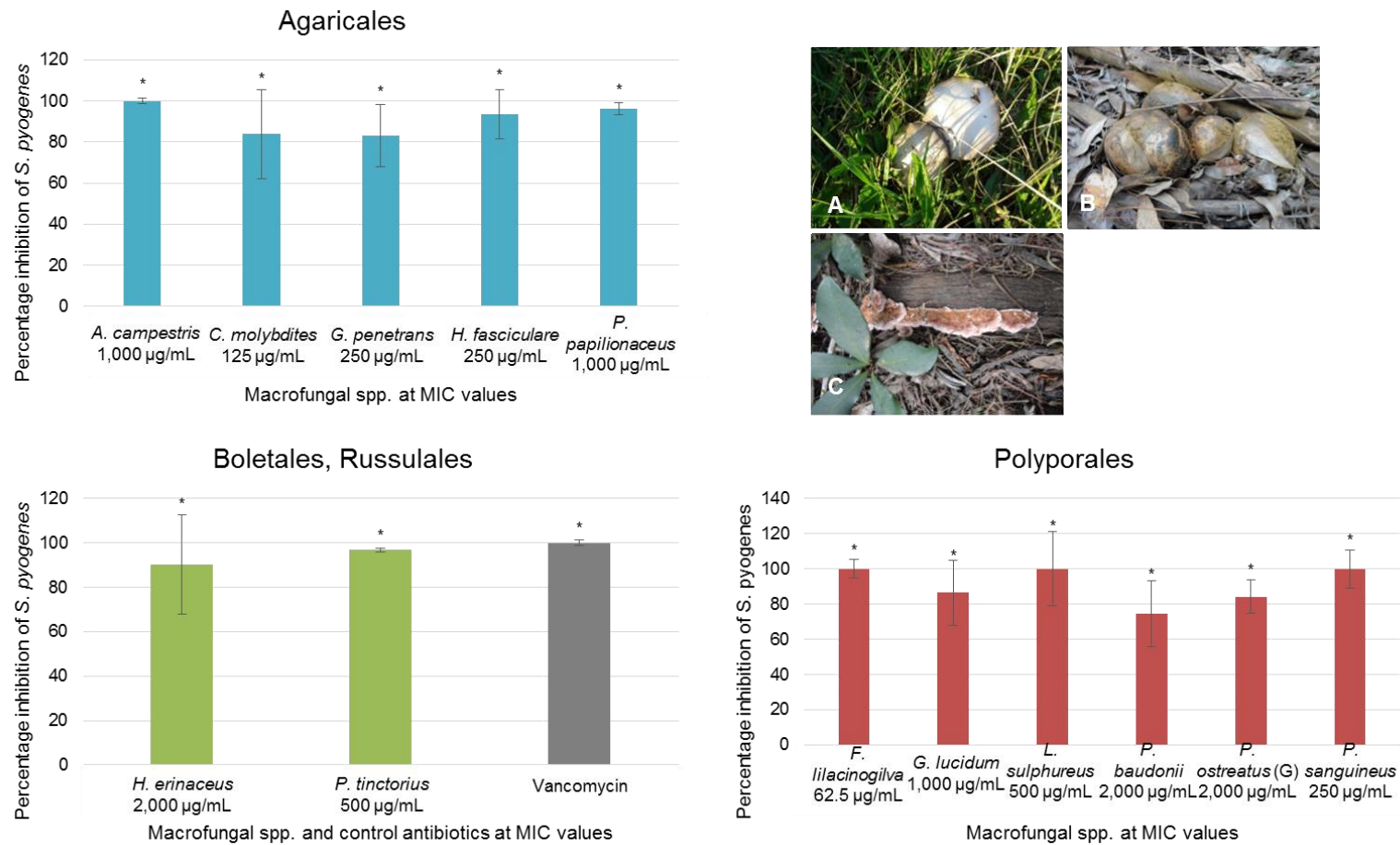


**Figure 2.2:** Percentage inhibition of *S. pyogenes* determined using INT assay for active ethanol extracts of macrofungal spp. classified in the orders Agaricales (blue), Boletales/Russulales (green) and Polyporales (red). Bar graphs represent the average of three independent experiments each performed in triplicate. SD is represented by error bars. Quantitative analyses: OD 600 nm. Significance was determined using the two-tailed Student t-test: \* $p \leq 0.05$  compared to the untreated (UT) control. Photographs of one of the most active macrofungal spp. in each order: (A) *A. campestris*; (B) *P. tinctorius*; (C) *F. lilacinogilva* (Dr. G. J. Boukes).

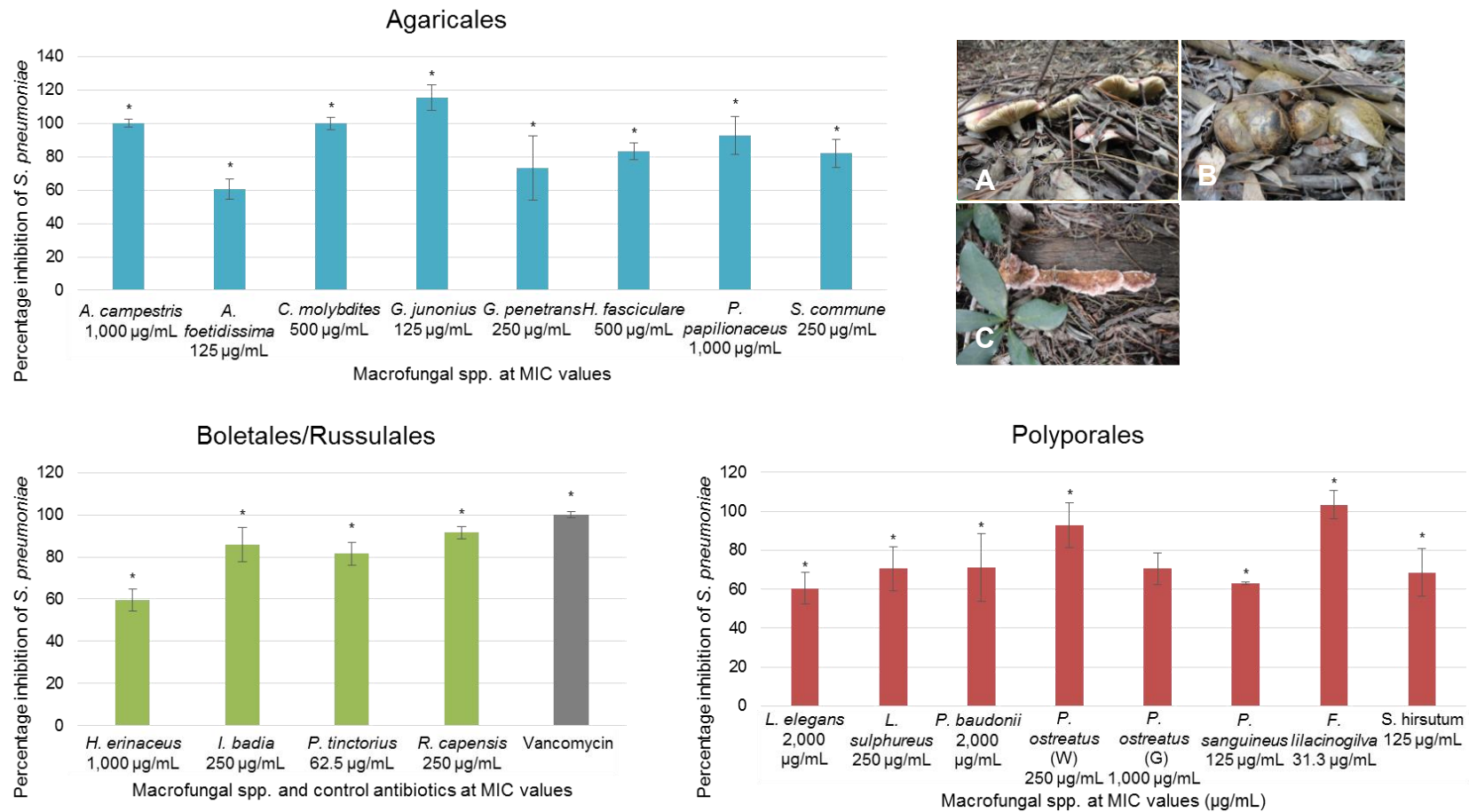


**Figure 2.3:** Percentage inhibition of *S. pneumoniae* determined using INT assay for active ethanol extracts of macrofungal spp. classified in the orders Agaricales (blue), Boletales/Russulales (green) and Polyporales (red). Bar graphs represent the average of three independent experiments each performed in triplicate. SD is represented as error bars. Quantitative analyses: OD 600 nm. Significance was determined using the two-tailed Student t-test: \* $p \leq 0.05$  compared to the untreated (UT) control. Photographs of one of the most active macrofungal spp. in each order: (A) *G. junonius*; (B) *R. capensis*; (C) *F. lilacinogilva* (Dr. G. J. Boukes).

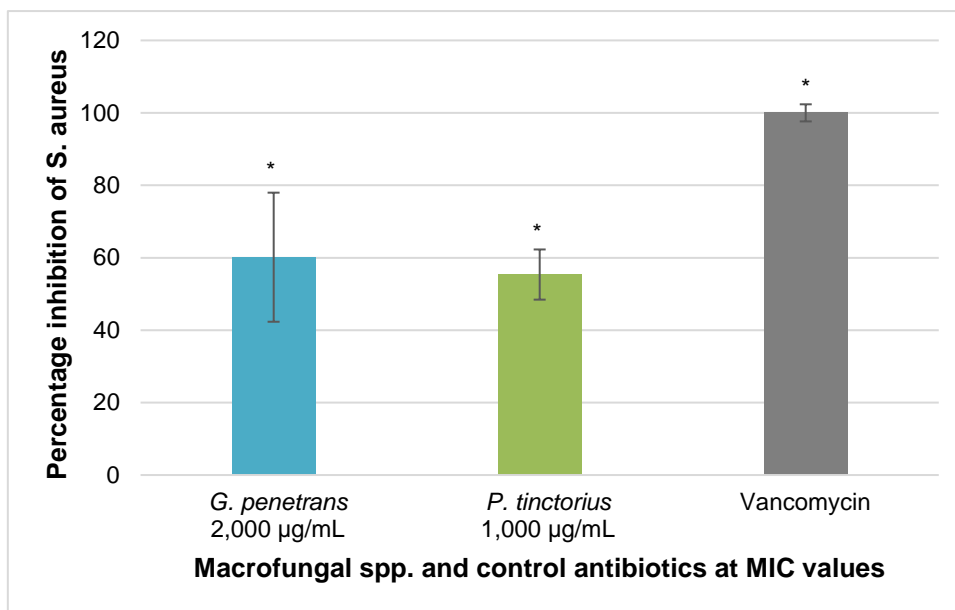


**Figure 2.4:** Percentage inhibition of *S. aureus* determined using INT assay for active ethanol extracts of macrofungal spp. classified in the orders Agaricales (blue) and Boletales (green). Bar graph represents the average of three independent experiments each performed in triplicate. SD is represented by error bars. Quantitative analyses: OD 600 nm. Significance was determined using the two-tailed Student t-test: \* $p \leq 0.05$  compared to the untreated (UT) control.

### 2.3.1.2 Aqueous macrofungal extracts

The crude aqueous macrofungal extracts (Table 2.2) showed no inhibition of *P. aeruginosa*, *K. pneumoniae* and *S. aureus* at the concentration range tested (15.6 - 2,000 µg/mL). The aqueous extracts of *G. junonius*, *P. sanguineus*, *P. tinctorius*, *P. baudonii* and *L. elegans* were active against *S. pyogenes*, and showed MIC values of 1,000 µg/mL for *G. junonius* and 2,000 µg/mL for the other macrofungal spp. Five of the macrofungal spp. showed to be active against *S. pneumoniae* at a MIC value of 2,000 µg/mL. The macrofungal species include *A. foetidissima*, *G. junonius*, *H. fasciculare*, *R. capensis* and *I. badia*. The standard antibiotics (gentamicin and vancomycin) showed lower MIC values than the active macrofungal extracts as seen in Table 2.2. The effect of DMSO (negative control) did not cause inhibition of the test organisms.



**Table 2.2:** Minimum inhibitory concentration (MIC) of aqueous extracts of 21 macrofungal species tested against *P. aeruginosa*, *K. pneumoniae*, *S. pyogenes*, *S. pneumoniae* and *S. aureus* between a concentration range of 15.6 - 2,000 µg/mL (lower concentrations used if required). Control antibiotics included vancomycin and gentamicin with a concentration range of 0.5 - 64 µg/mL. Semi-quantitative analyses: visually.

	Gram-negative bacteria			Gram-positive bacteria	
	<i>P. aeruginosa</i>	<i>K. pneumoniae</i>	<i>S. pyogenes</i>	<i>S. pneumoniae</i>	<i>S. aureus</i>
<b>Agaricales</b>					
<i>Agaricus campestris</i>	> 2,000 µg/mL	> 2,000 µg/mL	> 2,000 µg/mL	> 2,000 µg/mL	> 2,000 µg/mL
<i>Amanita foetidissima</i>	> 2,000 µg/mL	> 2,000 µg/mL	> 2,000 µg/mL	2,000 µg/mL	> 2,000 µg/mL
<i>Chlorophyllum molybdites</i>	> 2,000 µg/mL	> 2,000 µg/mL	> 2,000 µg/mL	> 2,000 µg/mL	> 2,000 µg/mL
<i>Gymnopilus junonius</i>	> 2,000 µg/mL	> 2,000 µg/mL	1,000 µg/mL	2,000 µg/mL	> 2,000 µg/mL
<i>Gymnopilus penetrans</i>	> 2,000 µg/mL	> 2,000 µg/mL	> 2,000 µg/mL	> 2,000 µg/mL	2,000 µg/mL
<i>Hypholoma fasciculare</i>	> 2,000 µg/mL	> 2,000 µg/mL	> 2,000 µg/mL	2,000 µg/mL	> 2,000 µg/mL
<i>Paneolus papilionaceus</i>	> 2,000 µg/mL	> 2,000 µg/mL	> 2,000 µg/mL	> 2,000 µg/mL	> 2,000 µg/mL
<i>Pleurotus ostreatus</i> (White)	> 2,000 µg/mL	> 2,000 µg/mL	> 2,000 µg/mL	> 2,000 µg/mL	> 2,000 µg/mL
<i>Pleurotus ostreatus</i> (Grey)	> 2,000 µg/mL	> 2,000 µg/mL	> 2,000 µg/mL	> 2,000 µg/mL	> 2,000 µg/mL
<i>Schizophyllum commune</i>	> 2,000 µg/mL	> 2,000 µg/mL	> 2,000 µg/mL	> 2,000 µg/mL	> 2,000 µg/mL
<b>Polyporales</b>					
<i>Fomitopsis lilacinogilva</i>	> 2,000 µg/mL	> 2,000 µg/mL	> 2,000 µg/mL	> 2,000 µg/mL	> 2,000 µg/mL
<i>Ganoderma lucidum</i>	> 2,000 µg/mL	> 2,000 µg/mL	> 2,000 µg/mL	> 2,000 µg/mL	> 2,000 µg/mL
<i>Laetiporus sulphurous</i>	> 2,000 µg/mL	> 2,000 µg/mL	> 2,000 µg/mL	> 2,000 µg/mL	> 2,000 µg/mL

**Table 2.2:** *Continued...* Minimum inhibitory concentration (MIC) of aqueous extracts of 21 macrofungi species

	Gram-negative bacteria			Gram-positive bacteria	
	<i>P. aeruginosa</i>	<i>K. pneumoniae</i>	<i>S. pyogenes</i>	<i>S. pneumoniae</i>	<i>S. aureus</i>
<b>Polyporales</b>					
<i>Lenzites elegans</i>	> 2,000 µg/mL	> 2,000 µg/mL	2,000 µg/mL	> 2,000 µg/mL	> 2,000 µg/mL
<i>Pseudophaeolus baudonii</i>	> 2,000 µg/mL	> 2,000 µg/mL	2,000 µg/mL	> 2,000 µg/mL	> 2,000 µg/mL
<i>Pycnoporus sanguineus</i>	> 2,000 µg/mL	> 2,000 µg/mL	2,000 µg/mL	> 2,000 µg/mL	> 2,000 µg/mL
<i>Stereum hirsutum</i>	> 2,000 µg/mL	> 2,000 µg/mL	> 2,000 µg/mL	> 2,000 µg/mL	> 2,000 µg/mL
<b>Boletales</b>					
<i>Imleria badia</i>	> 2,000 µg/mL	> 2,000 µg/mL	> 2,000 µg/mL	2,000 µg/mL	> 2,000 µg/mL
<i>Pisolithus tinctorius</i>	> 2,000 µg/mL	> 2,000 µg/mL	2,000 µg/mL	> 2,000 µg/mL	> 2,000 µg/mL
<b>Russulales</b>					
<i>Russula capensis</i>	> 2,000 µg/mL	> 2,000 µg/mL	> 2,000 µg/mL	2,000 µg/mL	> 2,000 µg/mL
<i>Hericium erinaceus</i>	> 2,000 µg/mL	> 2,000 µg/mL	> 2,000 µg/mL	> 2,000 µg/mL	> 2,000 µg/mL
<b>Positive controls</b>					
Vancomycin (Positive control)	N/A	N/A	1 µg/mL	2 µg/mL	2 µg/mL
Gentamicin(Positive control)	1 µg/mL	2 µg/mL	N/A	N/A	N/A

The absorbance at 600 nm was measured for the aqueous extracts exhibiting antimicrobial activity to determine the percentage of inhibition for each bacterial species at the MIC concentration. The percentage inhibition of *S. pyogenes* calculated at the MIC value was 74%, 54%, 75%, and 100% for *P. sanguineus*, *L. elegans*, *G. junonius* and *P. tinctorius*, respectively (Figure 2.5). Vancomycin (positive control) showed complete inhibition of growth at a concentration of 1 µg/mL. The inhibition of growth observed by the aqueous extracts were significant when compared to the untreated control ( $p \leq 0.05$ ).

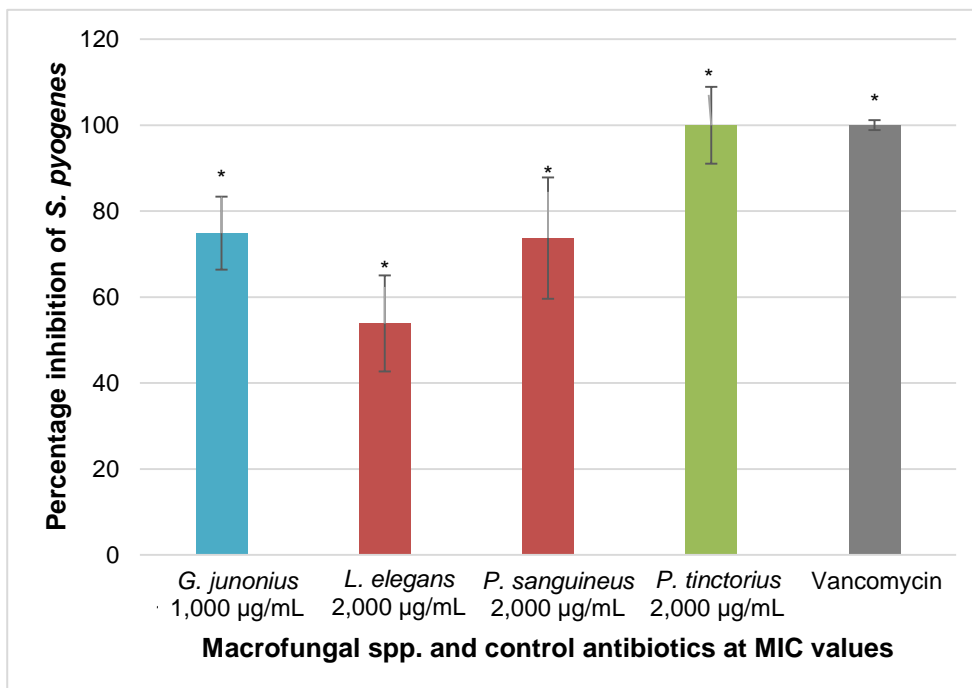


**Figure 2.5:** Percentage inhibition of *S. pyogenes* determined using INT assay for active aqueous extracts of macrofungal spp. classified in the orders Agaricales (blue), Polyporales (red) and Boletales (green). Bar graph represents the average of three independent experiments each performed in triplicate. SD is represented by error bars. Quantitative analyses: OD 600 nm. Significance was determined using the two-tailed Student t-test: \* $p \leq 0.05$  compared to the untreated (UT) control.

Five of the 21 macrofungal species inhibited the growth of *S. pneumoniae* (Figure 2.6). The percentage inhibition for *A. foetidissima*, *G. junonius*, *H. fasciculare*, *R. capensis* and *I. badia* were 55%, 71%, 61%, 74% and 75%, respectively. Vancomycin inhibited the growth of *S. pneumoniae* at 2 µg/mL.

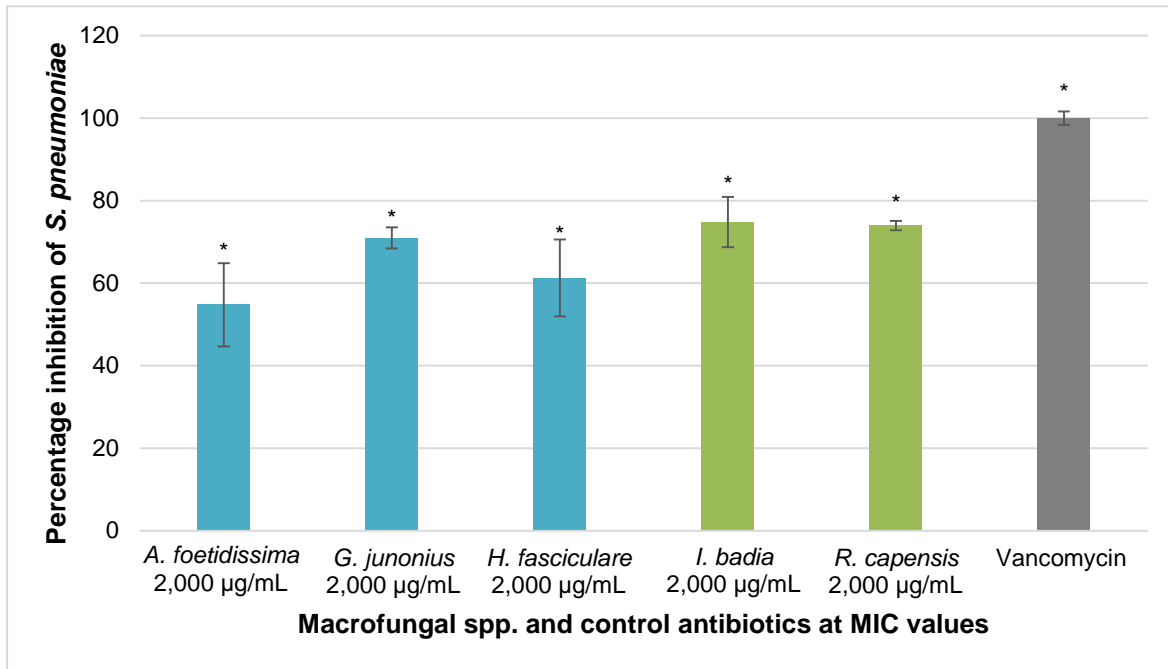


**Figure 2.6:** Percentage inhibition of *S. pneumoniae* determined using INT assay for active aqueous extracts for macrofungal spp. classified in the orders Agaricales (blue) and Boletales (green). Bar graph represents the average of three independent experiments each performed in triplicate. SD is represented by error bars. Quantitative analyses: OD 600 nm. Significance was determined using the two-tailed Student t-test: \* $p \leq 0.05$  compared to the untreated (UT) control.

### 2.3.2 Evaluation of bacterial cellular alterations by TEM

Some antimicrobial agents cause cell lysis by damaging the membranes. The morphological alterations of *S. pneumoniae*, *S. pyogenes* and *S. aureus* were analysed by TEM after treatment with macrofungal extracts at their respective MIC concentrations (Figure 2.7). Changes in the ultrastructure of bacterial cells, exposed to the ethanolic extracts of macrofungal spp. for 8 h, were confirmed.

The TEM micrographs of the untreated bacterial cells showed round cells with undamaged cell walls (Figure 2.7A, D and G). Cells at different stages in the division process were evident with the start of septation (long white arrow) in *S. aureus* untreated cells (Figure 2.7A) during which growth of wall material into the cytoplasm occurs (Matijašević et al., 2016). Cross-wall formation (long black arrows) was observed for *S. pyogenes* (Figure 2.7D) and *S. pneumoniae* (Figure 2.7G) separating into two daughter cells. The untreated bacterial cells showed a clearly defined cytoplasmic membrane.

*S. pneumoniae* and *S. pyogenes* were treated with *F. lilacinogilva* ethanolic extract and *S. aureus* was treated with the ethanolic extract of *P. tinctorius*. The TEM micrographs, following 8 h of treatment, exhibited damaged and ruptured cell walls (Figure 2.7B-C; short white arrows). A few cells with lysed and depleted cellular content (short black arrows) were also noted after treatment with *P. tinctorius* (Figure 2.7C). The leakage is due to the rupture of the cell membrane. Cytoplasmic membrane damage was also visible for *S. pyogenes* (Figure 2.7E-F) and *S. pneumoniae* (Figure 2.7H-I) treated cells.

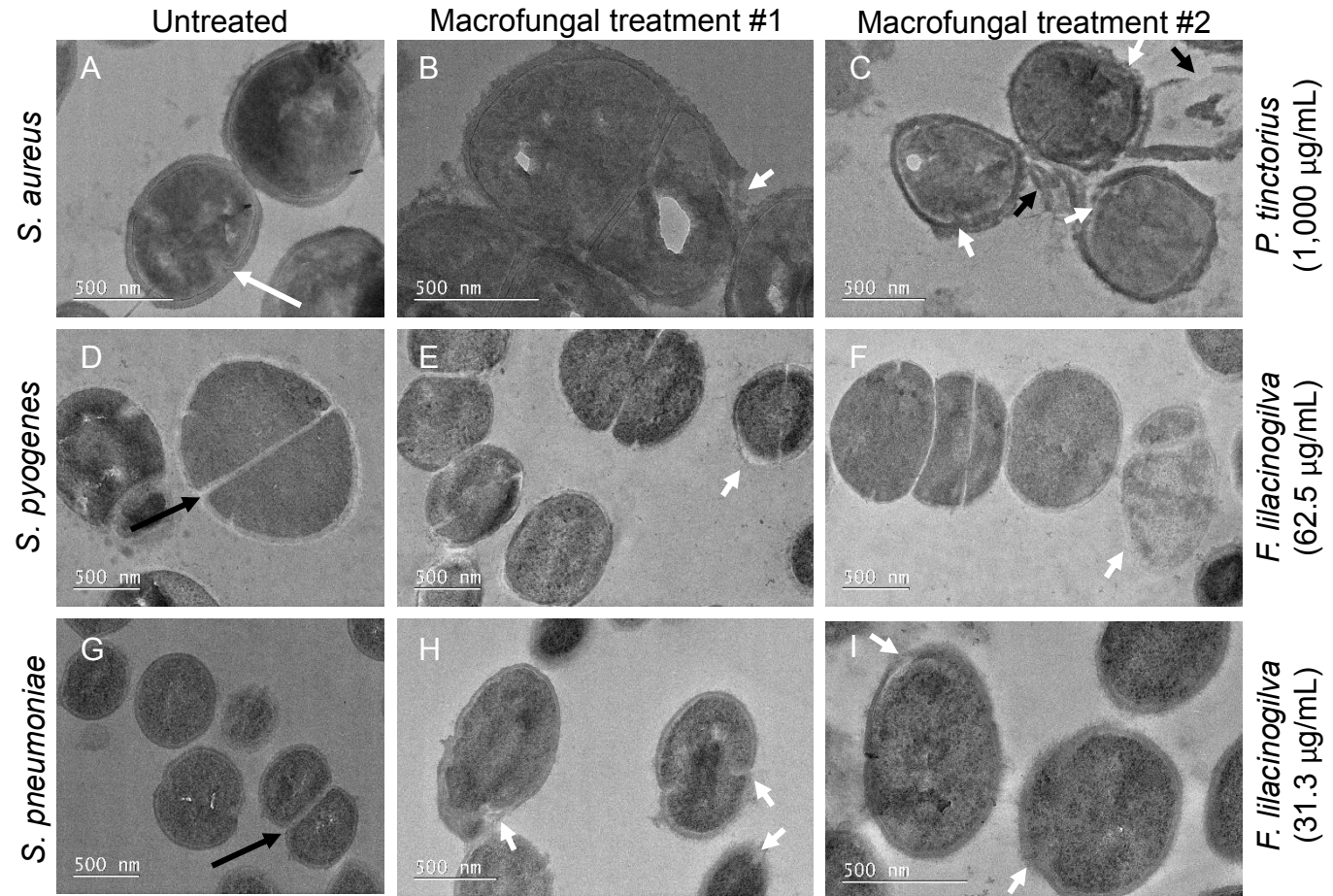


**Figure 2.7:** Transmission electron micrographs of untreated and treated *S. aureus*, *S. pyogenes* and *S. pneumoniae* bacterial cells. *S. aureus*, *S. pyogenes* and *S. pneumoniae* were treated with the MIC concentration of ethanol extracts of *P. tinctorius* (1,000 µg/mL), *F. lilacinogilva* (62.5 µg/mL) and *F. lilacinogilva* (31.3 µg/mL), respectively. B-C, E-F and H-I are duplicates of each treatment. Long white arrow- septa formation; long black arrows- cross-wall formation; short white arrows- damaged cell wall; short black arrows- lysed cells.

### 2.3.3 MABA assay for activity against *M. tuberculosis*

The antitubercular activity of the macrofungal species were screened against *M. tuberculosis* H37Rv (ATCC 27294) using the MABA assay. A blue colour in the well was interpreted as no growth and a pink colour was scored as growth (Figure 2.8).

The ethanol extracts of *A. foetidissima*, *G. lucidum*, *H. fasciculare*, *P. ostreatus* (white), *R. capensis*, *S. commune*, *P. tinctorius*, *S. hirsutum*, *I. badia*, *P. sanguineus*, *G. junonius*, *F. lilacinogilva* and *L. elegans* were screened during a previous study by Dr. G. J. Boukes. The ethanol extracts of *F. lilacinogilva* and *G. junonius* inhibited the growth of the *M. tuberculosis* H37 strain at IC<sub>50</sub> values of 49.9±4.2 and 60.8±9.3 µg/mL, respectively (unpublished data).

The ethanol and aqueous extracts of *A. campestris*, *C. molybdites*, *G. penetrans*, *P. papilionaceus*, *P. ostreatus* (grey), *L. sulphurous*, *P. baudonii* and *H. erinaceus* were screened for antitubercular activity in this study. The aqueous extracts of the macrofungal spp. did not show any inhibitory effect on *M. tuberculosis*. From visual observation (semi-quantitative analyses), the MICs of the control drugs, ethambutol dihydrochloride and rifampicin were >500 µg/mL and <0.0625 µg/mL, respectively (Figure 2.8). The high MIC of ethambutol dihydrochloride might be due to resistance of the *M. tuberculosis* H37 strain to this specific antibiotic. Five of the eight extracts inhibited the growth of *M. tuberculosis*. *G. junonius* and *C. molybdites* showed visual MICs of 500 µg/mL, whereas *L. sulphurous*, *P. baudonii* and *A. campestris* showed MICs of 1,000 µg/mL (Figure 2.8).

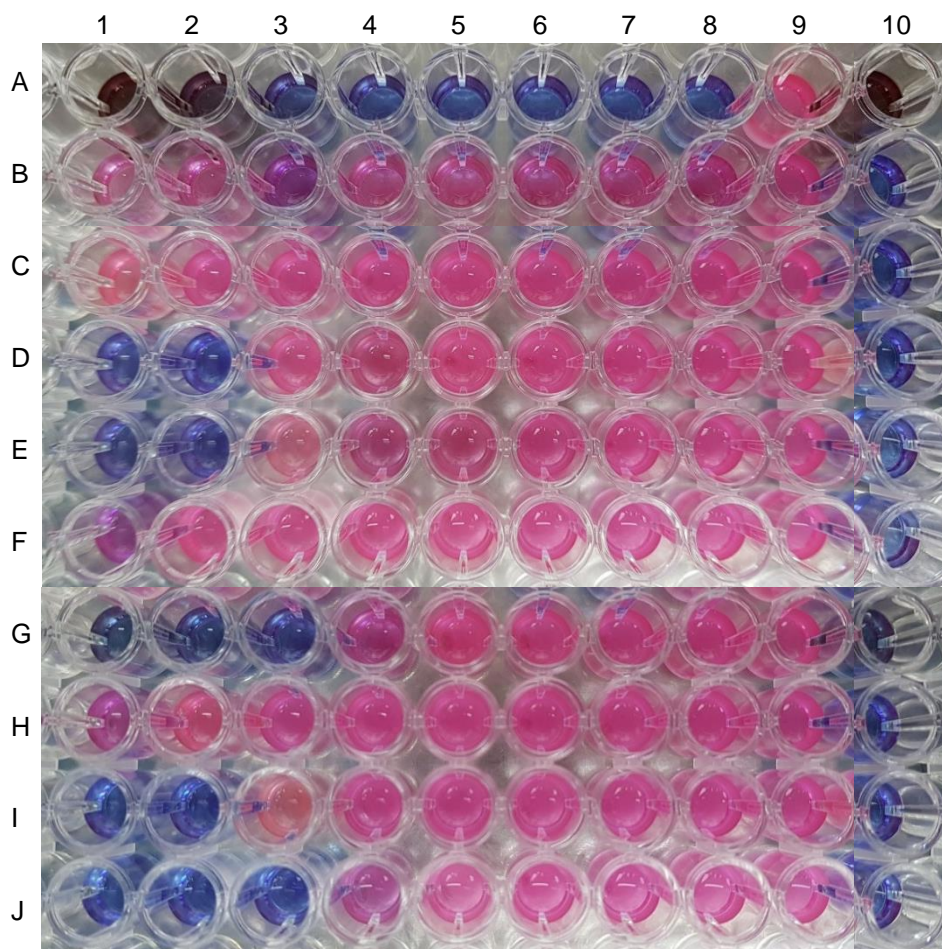


**Figure 2.8:** Anti-TB activity of the ethanol extracts of eight macrofungal spp. using MABA. Well 9 (all rows): Bacterial growth control. Well 10 (all rows): Antibiotic/macrofungal extract control. Concentrations of antibiotics: Rifampicin row A (8 - 0.0625  $\mu\text{g/mL}$ ) and ethambutol dihydrochloride row B (500 - 3.906  $\mu\text{g/mL}$ ). Concentrations of macrofungal extracts ranged between 2,000 – 15.6  $\mu\text{g/mL}$ . Rows: C, *H. erinaceus*; D, *L. sulphureus*; E, *P. baudonii*; F, *P. ostreatus* (grey); G, *G. penetrans*; H, *P. papilionaceus*; I, *A. campestris*; J, *C. molybdites*.

The percentage inhibition of *M. tuberculosis*, calculated from the MABA fluorescence values (quantitative analyses) for the active macrofungal spp were: 90.2%, 93.3%, 71.7%, 88.5% and 91.9% for *L. sulphureus*, *P. baudonii*, *G. penetrans*, *A. campestris* and *C. molybdites*, respectively (Figure 2.9). The macrofungal extracts inhibited 50% of growth at concentrations ranging between 74.6 - 480.8  $\mu\text{g/mL}$  (Appendix Table A1).



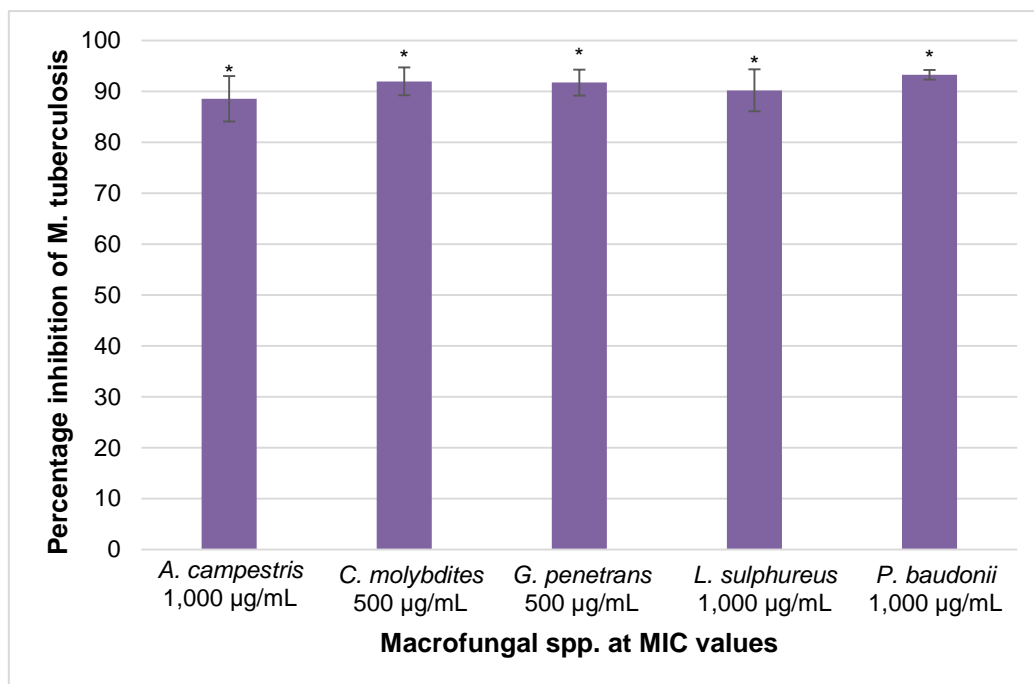


**Figure 2.9:** Percentage inhibition of *M. tuberculosis* determined using MABA assay for active ethanol extracts of macrofungal spp. Bar graph represents the average of three independent experiments each performed in triplicate. SD is represented by error bars. Quantitative analyses: Fluorescence Ex/Em= 560/590. Significance was determined using the two-tailed Student t-test: \* $p \leq 0.05$  compared to the untreated (UT) control.

## 2.3.4 Inhibition of HIV-1 enzymes

### 2.3.4.1 HIV-1 reverse transcriptase (RT) Assay

The inhibition of RT was determined using the non-radioactive colorimetric ELISA assay. Retroviral RT activity is measured by the incorporation of digoxigenin- and biotin-labelled dUTP into DNA. The ethanol extracts of *A. campestris*, *C. molybdites*, *G. penetrans*, *P. papilionaceus*, *P. ostreatus* (grey), *L. sulphureus*, *P. baudonii* and *H. erinaceus* were screened in this study for HIV-1 RT inhibition. The ethanolic extracts were selected as they would contain both polar and non-polar compounds which could inhibit the enzyme's activity.

A visual representation of the colour change is depicted in Figure 2.10 while Figure 2.11 summarizes the HIV-1 RT activity following treatment with the eight macrofungal spp. and nevirapine (positive control). Of the eight macrofungal spp., *P. baudonii* showed the greatest inhibition of HIV-1 RT activity, with slight inhibition by *P.*

*papilionaceus* (5 and 50  $\mu\text{g/mL}$ ) and *H. erinaceus* (5  $\mu\text{g/mL}$ ). *P. baudonii*, at 5 and 50  $\mu\text{g/mL}$ , inhibited HIV-1 RT activity by 12.97% and 30.05%, respectively. Nevirapine, 1 and 10  $\mu\text{g/mL}$ , was used as the positive control and exhibited 84.8% and 89.2% inhibition of HIV-1 RT activity, respectively (Figure 2.11).

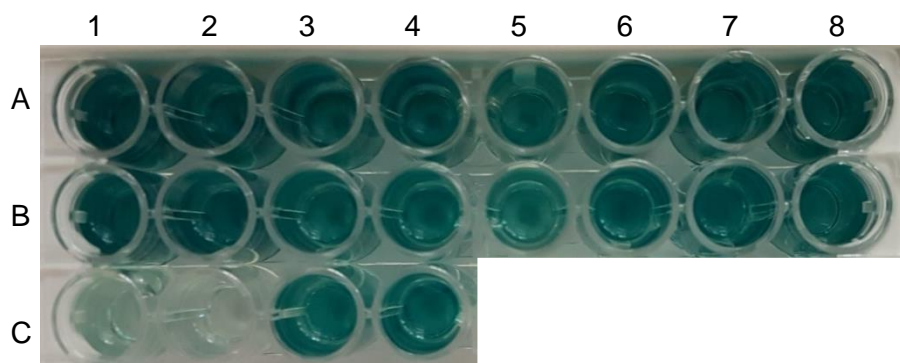


**Figure 2.10:** Visual representation of colour change observed for the ethanol extracts of macrofungal spp. A1-8: 5  $\mu\text{g/mL}$ ; B1-8: 50  $\mu\text{g/mL}$ ; C1: 1  $\mu\text{g/mL}$  Nevirapine; C2: 10  $\mu\text{g/mL}$  Nevirapine; C3: DMSO control; C4: No inhibitor control. A/B1: *A. campestris*; A/B2: *L. sulphureus*; A/B3: *P. papilionaceus*; A/B4: *H. erinaceus*; A/B5: *P. baudonii*; A/B6: *P. ostreatus* (grey); A/B7: *G. penetrans*; A/B8, *C. molybdites*.

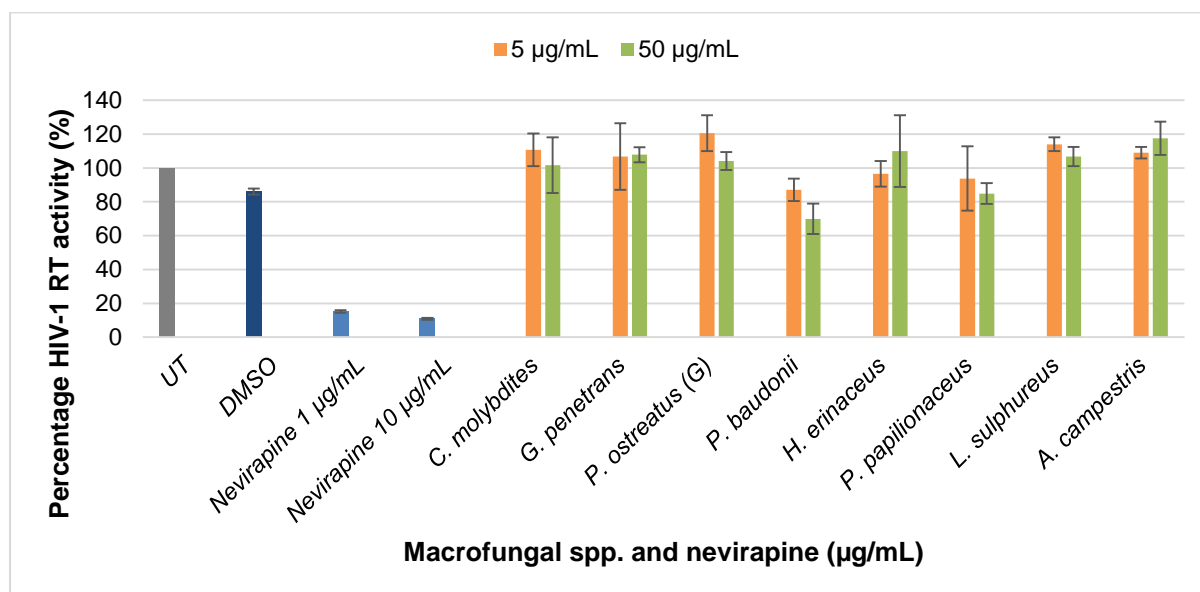


**Figure 2.11:** Percentage inhibition of HIV-1 reverse transcriptase following 1 h exposure to the ethanol extracts of eight South African macrofungal spp. HIV-1 RT was exposed to the ethanol extracts of eight macrofungal spp. (5 and 50  $\mu\text{g/mL}$ ), nevirapine (1 and 10  $\mu\text{g/mL}$ ; positive control) and DMSO (0.1%, vehicle control). Error bars represent the mean  $\pm$  SD performed in duplicate.

### 2.3.4.2 HIV-1 Protease Assay

The HIV-1 protease inhibitory activity of eight macrofungal spp. (ethanol extracts) was assessed using a fluorescence resonance energy transfer (FRET) assay. Figure 2.12 summarizes the HIV-1 protease activity following treatment with the 8 macrofungal spp. and pepstatin A (positive control). Initial screening of the macrofungal spp. showed that *G. penetrans*, *P. ostreatus* (grey), *H. erinaceus*, *P. papilionaceus*, *L. sulphureus* and *A. campestris* did not have any inhibitory activity. *P. baudonii* inhibited HIV-1 protease activity by 8.4%. *C. molybdites* significantly inhibited HIV-1 protease activity by 61% at 50 µg/mL. Pepstatin A (200 nM) inhibited HIV-1 protease activity by 86.9% (Figure 2.12)

The ethanol extract of *C. molybdites* inhibited HIV-1 protease activity in a concentration dependent manner (Figure 2.12). The IC<sub>50</sub> value of *C. molybdites* was 49.7 µg/mL.

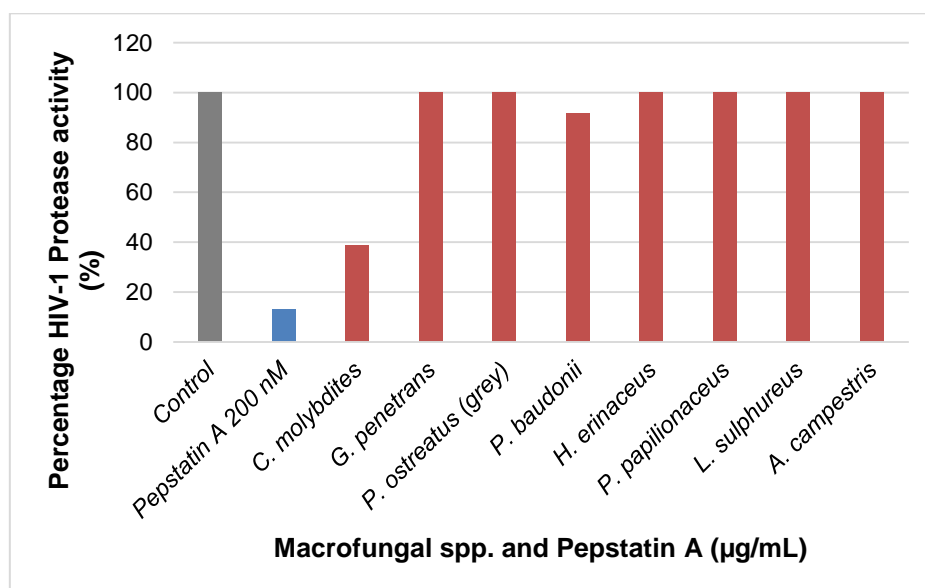


**Figure 2.12:** HIV-1 protease inhibition, following 100 min exposure to the ethanol extracts of eight South African macrofungal spp. HIV-1 protease was exposed to the ethanol extracts of eight macrofungal extracts (50 µg/mL), pepstatin A (100 nM) and DMSO (0.1%, vehicle control).

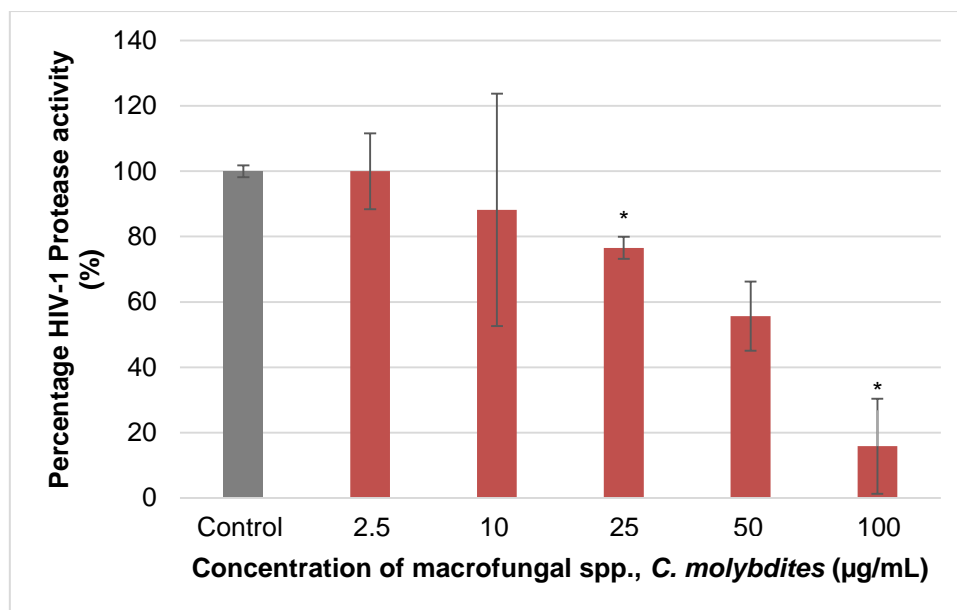


**Figure 2.13:** HIV-1 protease inhibition, following 100 min exposure to the ethanol extract of *C. molybdites*. HIV-1 protease was exposed to *C. molybdites* (concentrations ranging between 2.5 - 100 µg/mL) to determine the IC<sub>50</sub> value. Error bars represent the mean ± SD performed in triplicate. Statistical analysis: \*p≤0.05

## 2.4 DISCUSSION

The increase in occurrence of multidrug-resistant pathogenic bacteria highlights the importance for the search of alternative antimicrobial agents. The present study investigated South African macrofungal species for their potential antimicrobial activity, which could lead to the identification and isolation of novel antimicrobial compounds. Knowledge regarding the medicinal properties of macrofungi in Africa is scarce and mainly limited to studies performed in Nigeria (Udu-Ibiam et al., 2014), Tanzania (Mwita et al., 2010) and Zimbabwe (Reid et al., 2016). Therefore, this study expands the antimicrobial activity knowledge of macrofungi found in South Africa and Africa. Twenty-one macrofungal species from 4 orders and 13 families were screened using the INT microbroth dilution assay against selected respiratory bacterial pathogens.

Differences in the antimicrobial activity were observed for the ethanol- and aqueous extracts of the 21 macrofungi screened against three Gram-positive (i.e. *S. aureus*, *S. pyogenes* and *S. pneumoniae*) and two Gram-negative (i.e. *P. aeruginosa* and *K. pneumoniae*) bacterial species. Twenty-one ethanol extracts and eight aqueous

extracts exhibited antibacterial activity against at least one microorganism screened. The concentration ranged between 31.3 – 2,000 µg/mL and 1,000 – 2,000 µg/mL for ethanol and aqueous extracts, respectively. The difference in activity may be attributed to differences in the constituents found in the macrofungi, concentration of bioactive compounds and their respective mechanisms of action (Nwachukwu and Uzoeto, 2010; Reid et al., 2016). As the extracts are composed of a mixture of compounds, the antimicrobial activity may be due to individual compounds or several compounds (Kosanic et al., 2016), which may have additive or synergistic effects.

The extraction solvent may also influence the antimicrobial activity as it determines which compounds are extracted. Solvents are classified based on their dielectric constants into non-polar, semi-polar and polar solvents. Therefore based on their dielectric constants one can select for the compounds to be extracted. Solvents with a high dielectric constant (polar) extract more bioactive compounds (polar and non-polar compounds) compared to non-polar solvents (Doğan et al., 2013). The lowest MIC values were observed for the ethanol extracts (Table 2.1) compared to the aqueous extracts (Table 2.2) and therefore represent the more effective solvent for antimicrobial substances, which agrees with the latter statement. These results are consistent with other reports where organic solvents, such as ethanol, generally extracted greater amounts of compounds with antimicrobial properties compared to water extracts (Bala et al., 2012; Reid et al., 2016).

The results obtained in this study showed that the macrofungal extracts did not exhibit any antimicrobial activity towards the Gram-negative bacteria tested (i.e. *K. pneumoniae* and *P. aeruginosa*; Table 2.1 and 2.2). This may be due to the structural complexity of bacterial cell walls. Gram-negative bacteria are surrounded by an outer membrane which restricts the diffusion of various compounds. Their periplasmic space also contains enzymes that can inactivate harmful compounds introduced into the cell. This therefore serves as an effective barrier against antibiotics and other compounds. In contrast, Gram-positive bacteria lack an outer membrane which makes them more permeable and vulnerable to the effects of mushroom compounds (Ren et al., 2014; Matijašević et al., 2016).

*P. aeruginosa*'s low susceptibility to currently used antibiotics can be explained by several factors such as the bacteria's ability to acquire resistance, intrinsic resistance and decreased permeability of the cellular envelope (Mesaros, 2007). Other studies have also shown the low susceptibility of Gram-negative bacteria (e.g. *P. aeruginosa* and *K. pneumoniae*) to macrofungal species, even when the extracts' concentrations were increased (Beattie et al., 2010; Chowdhury et al., 2015). *Amanita caesarea* and *Russula virescens* screened against *K. pneumoniae* and *P. aeruginosa* have shown weak antimicrobial activity at MIC ranging between 25 – 50 mg/mL (Dimitrijevic et al., 2015).

The three Gram-positive bacterial species were inhibited by at least one of the macrofungal extracts (Tables 2.1 and 2.2). The sensitivity of Gram-positive bacterial spp. in decreasing order was *S. pneumoniae* > *S. pyogenes* > *S. aureus*. *P. tinctorius* and *G. penetrans* were the only macrofungal species that inhibited the growth of *S. aureus* (Table 2.1). Antimicrobial activity of another species of *Pisolithus*, *Pisolithus albus*, has been reported and shown moderate activity towards *S. aureus* producing inhibition zone diameters between 15.25 - 18.33 mm (Ameri et al., 2011). A study performed by Nowacka et al. (2015) tested several ethanol extracts, which included different species of *Amanita*, *Fomitopsis*, *Gymnopilus*, *Russula*, *Trametes* and *Stereum hirsutum* against *S. aureus*. The study has found that the ethanol extracts of *Amanita*, *Fomitopsis*, *Gymnopilus*, *Russula*, *Trametes* and *Stereum hirsutum* gave MIC values ranging between 2.5 – 5 mg/mL (Nowacka et al., 2015). Therefore an increase in the concentration of the macrofungal extracts that did not exhibit antimicrobial activity in this study may possibly exhibit antimicrobial activity against *S. aureus*. However an increase in the concentration may not be feasible for therapeutic applications as this could result in toxic effects.

*S. pneumoniae* was the most sensitive bacterial pathogen and was inhibited by 20 ethanol and five aqueous macrofungal extracts. The MIC values ranged between 31.3 – 2,000 µg/mL for the ethanol extracts, and 2,000 µg/mL for the aqueous extracts. Reid et al. (2016) investigated the effect of several macrofungal species, including *Ganoderma lucidum*, *Boletus edulis* and *Amanita* species. The study observed the formation of inhibition zones for all the ethanol macrofungal extracts tested against *S. pneumoniae*, but no inhibition zone for the aqueous extracts (Reid et al., 2016).

*S. pyogenes* growth was suppressed by 13 ethanol and five aqueous macrofungal extracts. The MIC values ranged between 62.5 – 2,000 µg/mL for ethanol extracts, and 1,000 – 2,000 µg/mL for aqueous extracts. A recent study screened 13 different macrofungal species for their antimicrobial activity and observed the extracts to yield MIC values ranging between 5 – 20 mg/mL against *S. pyogenes* (Alves et al., 2012b). However, Dogan et al. (2013) investigated the antimicrobial activity of three mushroom species (*Terfezia boudieri*, *Lactarius vellereus* and *Agaricus brunnescens*) with MIC values ranging between 2.4 – 625 µg/mL against *S. pyogenes*. The study employed a similar microbroth dilution method however a different extraction method was used. The study investigated the chloroform, acetone and methanol extracts of the three macrofungal spp. This implies that factors such as the bioassay employed and the mushroom extract preparation methods may influence the variability in the results among the different research groups.

Algiannis et al. (2001) proposed the classification of macrofungal extracts into weak-, moderate- and strong inhibitors based on their respective MIC values. Extracts with MIC values above 1.6 mg/mL are considered as weak inhibitors, MIC values between 0.6 – 1.5 mg/mL as moderate inhibitors and MIC values up to 0.5 mg/mL as strong inhibitors. The current study shows the selective antimicrobial activity of macrofungal extracts as some exhibited strong activity whereas others moderate to no activity. Thirteen of the 21 ethanol extracts that exhibited activity against at least one microorganism were categorised as strong inhibitors based on the classification system by Algiannis et al. (2001), as the MIC values ranged between 31.3 – 500 µg/mL. Ethanol extracts of *G. lucidum*, *L. elegans*, *P. tinctorius*, *A. campestris*, *P. papilionaceus* and *P. ostreatus* (grey) were classified as moderate inhibitors (1,000 µg/mL). The aqueous extract of *G. junonius* against *S. pyogenes* could be classified as a moderate inhibitor (1,000 µg/mL). The other active aqueous extracts were considered as weak inhibitors as activity was observed at a concentration of 2,000 µg/mL.

The metabolite profile of a specific macrofungal species could also be influenced by its growth conditions. This relates to a high diversity of metabolites as macrofungi thrive in a wide range of ecological niches, which may have different environmental

and nutritional conditions. During growth, primary and secondary metabolites are accumulated including compounds with antimicrobial properties such as: terpenoids, steroids, phenolics, proteins, peptides, volatile fatty acids sesquiterpenes, flavonoids terpenes, steroids, quinolines, proteins, peptides and benzoic acid derivatives (Matijašević et al., 2016). It is proposed that quinones function by means of binding irreversibly with nucleophilic amino acids, leading to the inactivation and loss of protein function. Flavonoids are secondary compounds that may inhibit energy metabolism and nucleic cell membrane, cell wall and nucleic acid synthesis (Matijašević et al., 2016). Terpenes mode of action involves disruption of microbial membranes, while antimicrobial peptides form ion channels, disrupt cell membranes and inhibit DNA and protein synthesis (Matijašević et al., 2016).

The screening of extracts to determine susceptible bacteria is useful, however investigating the mechanism of action is important for the development of drugs. To explore the possible mechanism of antibacterial activity of macrofungal extracts, the effect of extracts on morphological changes of *S. aureus*, *S. pyogenes* and *S. pneumoniae* cells were investigated by TEM. TEM illustrates the morphological changes that are induced by active antibacterial agents and thereby giving insight into their mechanism of action. The mechanism of action of antimicrobial compounds can be due to damage to the bacterial cell wall and cytoplasmic membrane leading to the lysis of cells and leakage of cellular content (Lee et al., 2015). The untreated control cells showed round morphology and intact membranes with a distinct septum and cross-wall formation (Figure 2.7). As shown by the TEM micrographs, treatment with extracts caused cell membrane damage. *S. aureus* treated with *P. tinctorius* also showed the presence of leakage of cellular content and lysed cells (Figure 2.7C). Limited studies have investigated the mechanism of antibacterial activities of macrofungal extracts. This is the first study investigating the effects of *F. lilacinogilva* and *P. tinctorius* ethanolic extracts on Gram-positive bacterial cells. Matijašević et al. (2016) investigated the effect of a *Coriolus versicolor* methanol extract on *S. aureus*. Treated *S. aureus* cells were elongated and malformed with membrane enclosed vesicles and lysed cells (Matijašević et al., 2016).

The long duration of TB treatment, and several adverse side effects, highlight the importance to discover new drugs to expand the treatment options. Research has



confirmed the promise of natural sources for antitubercular activity such as plants, microbes, and marine organisms (Zhou et al., 2015). Research on the antitubercular activity of macrofungi is limited to a few studies. Two naturally occurring chlorinated coumarins, 6-chloro-4-phenyl-2H-chromen-2-one and ethyl 6-chloro-2-oxo-4-phenyl-2H-chromen-3-carboxylate, were isolated from a *Fomitopsis officinalis* ethanol extract. The former has shown no antitubercular activity ( $MIC_{90} > 100 \mu\text{g/mL}$ ), whereas the latter has shown antitubercular activity ( $MIC_{90} < 50 \mu\text{g/mL}$ ) against wild-type *M. tuberculosis* and rifampicin-, isoniazid- and streptomycin resistant *M. tuberculosis*. Analogues of the two coumarins have also shown activity against wild-type *M. tuberculosis* and rifampicin-, isoniazid-, streptomycin-, kanamycin- and cycloserine resistant *M. tuberculosis* (Hwang et al., 2013). Stanikunaite et al. (2008) isolated three lanostane triterpenes from the ethanol extract of *Astraeus pteridis* that showed moderate antitubercular activity with MIC values ranging between 34.0 - 64.0  $\mu\text{g/mL}$ . The isolated compounds did not show cytotoxicity against African green monkey kidney fibroblasts at concentrations  $\leq 100 \mu\text{g/mL}$  (Stanikunaite et al., 2008).

This study has shown that crude ethanol extracts of *L. sulphurous*, *P. baudonii*, *G. penetrans*, *A. campestris* and *C. molybdites* inhibited the *M. tuberculosis* H37 strain. *G. penetrans* and *C. molybdites* inhibited *M. tuberculosis* at MICs of 500  $\mu\text{g/mL}$ , whereas the other macrofungal spp. had MICs of 1,000  $\mu\text{g/mL}$ . To the best of our knowledge we have shown for the first time that crude ethanol extracts of *P. baudonii*, *G. penetrans*, *A. campestris* and *C. molybdites* inhibited *M. tuberculosis*. The MIC only serves as an indication of active macrofungal spp., and the potential to isolate a bioactive compound with antitubercular activity might not only depend on the MIC. An extract exhibiting high activity (i.e. low MIC) may have a large quantity of the bioactive compound/s with moderate activity, whereas a crude extract exhibiting moderate activity might have small amount of compound/s with high activity (Nguta et al., 2015). Although the MICs obtained for the active macrofungal spp. are relatively high, their active compound/s could still serve as scaffolds for new drugs.

There is also a lack in literature on the safety of isolated compounds with antitubercular activity, and therefore there is a need to investigate not only their antimicrobial activity but also the cytotoxicity on mammalian cells in order to determine their use as new leads for antitubercular drugs (Nguta et al., 2015). The lack of new anti-TB compounds

are also due to their inability to produce effective *in vivo* effects as seen during *in vitro* studies. This is likely due to their inability to reach the target site or to maintain activity for a prolonged time (Amaral et al., 2007). Additional studies are therefore required to determine the cytotoxicity of active macrofungal extracts against mammalian cells.

Anti-retroviral therapy has improved and prolonged the life of HIV/AIDS infected patients. However, the treatment is limited by several disadvantages incl. high cost, limited availability, toxicity and the emergence of drug resistant HIV strains (Bessong et al., 2005; Klos et al., 2009). It is therefore important to search for alternative antiretroviral agents. HIV reverse transcriptase, integrase and protease are enzymes required for the lifecycle of HIV and are ideal targets for anti-HIV therapy (Wang et al., 2014a).

Several studies have investigated the anti-HIV activity of macrofungal spp. specifically concerning their inhibitory activity against the RT enzyme. RT catalyzes the synthesis of double stranded DNA from the HIV RNA genome. The screening of eight South African macrofungal spp. did not show any inhibitory effects on HIV-1 RT activity (Figure 2.11). Macrofungi and their purified compounds and isolated fractions with HIV-1 RT inhibitory activity include *Pholiota adiposa* (methyl gallate, IC<sub>50</sub>: 80.1 µM; Wang et al., 2014a), *Russula paludosa* (fraction SU2, IC<sub>50</sub>: 11 µM; Wang et al., 2007), *Tricholoma giganteum* (laccase, IC<sub>50</sub>: 2.2 µM, Wang and Ng, 2004), *Lentinus edodes* (lentin, IC<sub>50</sub>: 1.5 µM; Ngai and Ng, 2003), *Pleurotus citrinopileatus* (homodimeric lectin, IC<sub>50</sub>: 0.93 µM; Li et al., 2008), *Pleurotus eryngii* (protease, IC<sub>50</sub>: 30 µM; Wang and Ng, 2001) and several other compounds. *Hericium erinaceum* agglutinin (HEA), a lectin, was isolated from *Hericium erinaceum*/*H. erinaceus* fruiting bodies extracted in 0.15 M NaCl. The lectin exhibited HIV-1 RT inhibitory activity with an IC<sub>50</sub> of 31.7 µM (Li et al., 2010). Laccases, lectins, peptides, ribonucleases and ribosome inactivating proteins of mushrooms have shown inhibitory activities against HIV-1 RT (Wang et al., 2012). The lack of any inhibitory activity of the eight mushroom spp. screened might be due to the extraction solvent (ethanol) used during this study. Other extraction solvents (e.g. 0.15 M NaCl) might extract larger quantities of compounds that confer antiviral activity.

The inhibitory effect on HIV-1 protease was also investigated that is required for the processing of viral polyproteins leading to the formation of structural and functional proteins (Wang et al., 2014a). *C. molybdites* significantly inhibited HIV-1 protease activity by 61.6% at a concentration of 50 µg/mL. The ethanol extract of *C. molybdites* has an IC<sub>50</sub> value of 49.7 µg/mL. Pepstatin A is a standard inhibitor of aspartic acid proteinases and known inhibitor of HIV-1 protease (Wang et al., 2014a). Pepstatin A (200 nM) inhibited HIV-1 protease activity by 86.9%. A polysaccharide fraction (50 µg/mL) isolated from *Fomitiporia punctata* inhibited HIV-1 protease activity by 19.6% (Liu et al., 2017). HIV-1 protease was inhibited by 17% by a methyl gallate (10 mM) isolated from *Pholiota adipose* (Wang et al., 2014a). Four triterpenes, colossolactone E, schisanlactone A, colossolactone V and colossolactone VII, inhibited HIV-1 protease activity with IC<sub>50</sub> values of 8.0, 5.0, 9.0 and 13.8 µg/mL, respectively (El Dine et al., 2008). Ganoderic acid B, ganoderiol B, ganoderic acid C1, 3b-5a-dihydroxy-6b-methoxyergosta-7,22-diene, ganoderic acid a, ganoderic acid H and ganoderiol A isolated from *Ganoderma lucidum* showed moderate inhibitory activity of HIV-1 protease with IC<sub>50</sub> values between 0.17-0.23 mM (El-Mekkawy et al., 1998).

In conclusion, these findings provide evidence that natural sources, such as macrofungi, produce compounds that exhibit antibacterial activity against human pathogens as well as antiviral activity. The study identified macrofungal species within South Africa that showed promising activity against *S. pneumoniae*, *S. pyogenes* and *S. aureus*. According to the results obtained from TEM, it can be deduced that the macrofungal extracts acted on the cytoplasmic membrane causing cell lysis. Further work is required to understand the mechanism/s of action involved in antibacterial activity of the macrofungal extracts, and whether other components are also affected that can lead to cell death. The complete understanding of the mechanism of action is required in order to find new natural antimicrobial agents. Macrofungal spp. also inhibited *M. tuberculosis* and could serve as a source for new compounds that can be used as scaffolds for drug development. Additional research is required in order to observe whether the extracts are toxic to mammalian cells in order to determine their *in vivo* potential. The antiviral activity of mushrooms is encouraging and the active extracts might show activity towards other viral infections.

## CHAPTER THREE

### CYTOTOXICITY OF MACROFUNGAL EXTRACTS AGAINST LUNG CANCER CELLS AND MECHANISM OF ACTION

#### 3.2 INTRODUCTION

Cancer is one of the leading causes of death worldwide, and it is estimated that 14.1 million new cases were diagnosed in 2012 ([www.cansa.org.za](http://www.cansa.org.za)). Tumour cells are characterised by uncontrolled cell division due to mutations of genes involved in the cell cycle. The genes involved are oncogenes that arise by mutation of proto-oncogenes (a gain of function mutation) and/or mutation of tumour suppressor genes causing gene loss or inactivation. Tumour suppressor genes function to inhibit cell proliferation; hence the lack thereof leads towards unregulated cell division (Sandal, 2002; Hassanpour and Dehghani, 2017). These mutations can contribute to certain growth and survival advantages, such as defective apoptotic machinery (Indran et al., 2011) allowing unregulated and excessive proliferation of cells that can lead to tumour development and metastasis (Kasibhatla and Tseng, 2003; Hassan et al., 2014). The unregulated proliferation of cells allows the preservation of these mutations (Simstein et al., 2003). Cancer cells possess certain abilities that enable their survival, which include 1) sustaining proliferative signal, 2) evading growth suppressors, 3) resisting cell death, 4) enabling replicative immortality, 5) inducing angiogenesis, 6) activating invasion and metastasis, 7) genome instability, and 8) tumour-promoting inflammation (Hanahan and Weinberg, 2011).

The treatment options of cancer include surgery, chemotherapy and radiation therapy. The treatment option selected depends on several factors, including cancer type, -grade and -location, and the overall health of the patient. The advances made in the treatment of cancer still suffer from several pitfalls. For example, chemotherapy has harmful toxic side-effects and resistance occurs (Younis et al., 2014; Badmus et al., 2015). This has driven the search for alternative anticancer agents from natural sources in order to develop safe and effective drugs for the treatment of cancer (Younis et al., 2014).

Mushrooms have been utilized since ancient times for the treatment of ailments, including cancer. They produce a variety of secondary metabolites of which a number of them exhibit antitumour activities (Choi et al., 2007). Calvacin is an example of a compound isolated from the puffball, *Calvatia gigantea*, which has been used for cancer treatment. Other compounds derived from mushrooms, and approved for use in Japan, include lentinan, schizophyllan and krestin (Fernando et al., 2016). Mushrooms have shown to counteract the side effects (e.g. lowered resistance anaemia and nausea) associated with chemo- and radiation therapy. Studies also suggest that some mushrooms, in combination with currently used drugs, can exhibit synergistic effects and may be useful in the treatment of drug-resistant cancers (Patel and Goyal, 2012).

A characteristic feature of cancer cells is uncontrolled proliferation. The evasion of apoptosis and deregulation of the cell cycle are key pathways exploited by cancer cells assisting in metastases. Cell cycle regulation constitutes a key target for the treatment of cancer. Therefore, compounds that exhibit apoptotic and cell cycle controlling properties with limited cytotoxicity are crucial (Arora and Tandon, 2014). Cytotoxicity is defined as the ability of a compound to produce toxic effects on cells. Cytotoxicity assays are employed to screen substances to determine their cytotoxic nature on cancer cells. MTT [3-(4,5-dimethylthiazol-2-yl)-2,5-diphenyl tetrazolium bromide] has been identified as a simple, reproducible assay in order to screen anti-cancer drugs (Sreejaya and Santhy, 2013).

Cells progress through the phases of the cell cycle in order to duplicate and divide, producing daughter cells. Checkpoints exist to ensure that the cell progress through the cycle following a specific sequence of events. In the case of DNA damage or DNA stress, the checkpoints will induce cell cycle arrest (Garrett, 2001; Senese et al., 2014). Cell cycle arrest can be defined as a large quantity of cells in a cell cycle phase at a specific time (Nojima, 2004). DNA content analysis of the cells enables the determination of the cell cycle position, and can also reveal apoptotic cells (Darzynkiewicz, 2010). A growing population of cells contains cells with different DNA content. Cells have 2N DNA content in the G<sub>0</sub>/G<sub>1</sub> phase (growth), 4N DNA content in the G<sub>2</sub>/M phase (growth and mitosis) and between 2-4N DNA content in the S phase (synthesis). Based on fluorescence intensity, cells are distributed into their respective

cell cycle phases. Cells with the same DNA content can be differentiated due to variations in the binding of the nuclear dye or nuclear condensation (Jayat and Ratinaud, 1993).

Natural product research, and its use in cancer therapy, is primarily focused on the induction of apoptosis. Apoptosis is defined as programmed cell death that occurs in order to maintain cell populations and homeostasis by eliminating damaged and harmful cells (Prateep et al., 2017). The disruption of apoptosis causes abnormal cell populations which can lead to tumour initiation and diseases such as cancer. The morphological changes associated with apoptosis, include chromatin condensation, cell shrinkage, membrane blebbing and cytoskeletal disruption (Ferreira et al., 2002; Erođlu et al., 2016). Biochemical changes include caspase activation, protein and DNA degradation, and membrane surface modification [phosphatidylserine (PS) translocation] (Wong, 2011; Koff et al., 2015). Several studies have proved that chemotherapeutic drugs induce apoptosis causing cell death in cancer cells (Alshatwi et al., 2012).

The plasma membranes of healthy, living cells are highly organised with an asymmetric distribution of phospholipids between the inner and outer leaflets of the cell membrane. The anionic lipid PS is primarily located on the inner leaflet. The distribution of phospholipids is maintained by lipid-translocating proteins. An early feature of apoptosis is loss of phospholipid asymmetry. The exposure of PS on the outer leaflet functions as signal for the engulfment of apoptotic cells by macrophages. The translocation of PS also occurs during necrosis in response to loss in membrane integrity (Demchenko, 2013). Annexin V is a calcium-dependent phospholipid binding protein (35-36 kDa) with high affinity for negatively charged phospholipids. Annexin V can be labelled with fluorochromes, such as fluorescein isothiocyanate (FITC), for the detection of PS translocation during early apoptosis (Mourdjeva et al., 2005). Propidium iodide (PI) is used in conjunction with FITC-labelled Annexin V in order to distinguish between viable, early apoptotic and late apoptotic/dead cells. PI is a cell-impermeable dye that can only enter cells with disintegrated membranes. PI will therefore be unable to stain early apoptotic cells with intact membranes. The Annexin V-FITC/PI apoptosis assay allows for the differentiation of three cell population stages.

This include healthy cells that are negative for both Annexin V and PI; early apoptotic cells that are Annexin V positive and PI negative; and late apoptotic/dead cells that are positive for both Annexin V and PI (Demchenko, 2013).

The activation of caspases is central to the mechanism of apoptosis, and can be initiated by the intrinsic and/or extrinsic pathway/s. The intrinsic pathway is triggered as a result of physical or chemical stress signals, whereas the extrinsic pathway is activated by the binding of extracellular molecules to death receptors on the cell surface (Wong, 2011). Caspases are endoproteases that function in cell death and inflammation. Caspases contain a cysteine residue in their active site which enables the catalytic hydrolyses of peptide bonds of various substrates. They are synthesised as inactive procaspases that have been classified as either initiator or effector caspases based on their mode of action. Initiator caspases are activated by an upstream signal that causes dimerization of the inactive procaspase. This enables autocatalysis between the small and large subunits, which stabilizes the dimer. Executioner caspases are activated through cleavage by initiator caspases. The cleavage of inactive executioner caspases causes conformational changes that expose the active sites and forms a functional protease (McIlwain et al., 2013). Caspase-8 is an initiator caspase that is activated by the extrinsic pathway involving the binding of ligands to Fas/tumour necrosis factor (TNF) receptors. The activated caspase-8 triggers the execution phase of apoptosis leading to the activation of effector caspases (i.e. caspase-3/-6/-7). The executioner caspases are responsible for the morphological changes of apoptotic cells as they cleave various substrates, such as poly (ADP-ribose) polymerase (PARP), nuclear protein NuMA, cytokeratins and several others. Caspase-3 causes chromatin condensation, disruption of the cytoskeletal structure and cell division (Elmore, 2007; Wong, 2011). Activation of the apoptotic extrinsic- and intrinsic pathways are associated with increased caspase-3 and caspase-8 and caspase-3 levels, respectively.

Apoptosis can be determined using several methods, which include morphology-, immunohistochemistry-, biochemistry-, immunology- and array based methods. Due to the overlapping features of the different types of cell death, more than one method is required to confirm apoptosis (Ulukaya et al., 2011).

Morphological changes induced by apoptosis can be visually detected by fluorescent staining such as acridine orange -, Hoechst - and phalloidin staining. Acridine orange is a cell permeable dye, which penetrates both viable and dead cells. The dye has a high affinity for double- and single stranded DNA. When intercalated with double stranded DNA, it emits green fluorescence upon excitation (480-490 nm). Ethidium bromide (EB) can be included in order to stain the DNA of dead cells orange. Acridine orange staining can be used to differentiate between viable cells with uniformly green stained nuclei, and early apoptotic cells with bright green condensed or fragmented nuclei (Ribble et al., 2005; Kocyigit et al., 2016).

The cytoskeleton of cells is composed of three main molecules: microfilaments, intermediate filaments and microtubules. These molecules together form and maintain the shape and structure of cells. Microfilaments function in certain cellular events such as cellular movement, cell division and intracellular transport. Microfilaments are composed of actin filaments and actin binding proteins. Actin is divided into G-actin (monomeric form) or F-actin (polymeric form). The length of microfilaments is regulated through actin regulatory proteins by varying the ratio of G-actin and F-actin (Francis and Antonipillai, 2017). The organisation and structure of the cytoskeleton can be investigated using immunofluorescent staining. Phalloidin is a phallotoxin that is produced by the *Amanita phalloides* mushroom. It is a cyclic peptide that can be modified with fluorescent labels. Phalloidin binds to the polymeric form of F-actin, enabling the study of the organisation and structure of the cytoskeleton. Phalloidin can be labelled with different fluorophores, depending on the experiment and if dual-staining is required (Chazotte, 2010).

The aim of this chapter was to determine the cytotoxicity of macrofungal extracts against lung cancer cell line, A549, and to determine the mechanism of cell death. This was achieved by analysing the morphological and biochemical characteristics of apoptosis, namely PS translocation, loss of plasma membrane asymmetry, nuclear condensation and DNA fragmentation, caspase activation and cell cycle arrest.



## **3.2 MATERIALS AND METHODS**

### **3.2.1 Materials/ chemicals/ reagents**

A549 (human lung carcinoma) cancer cell line and MRC5 (human fibroblast) normal cell line were purchased from the Japanese Collection of Research Bioresources (JCRB) Cell Bank (Osaka, Japan). 3-(4,5-dimethyl-2-thiazolul)-2,5-diphenyl-2H-tetrazolium bromide (MTT), cisplatin, bisBenzimide H33342 trihydrochloride (Hoechst), acridine orange, trypan blue, penicillin/streptomycin and Bovine Serum Albumin Fraction V were purchased from Sigma (St. Louis, MO, USA). Dimethyl sulfoxide (DMSO) and formaldehyde were purchased from Merck Millipore (Germany). Annexin V-FITC/PI kit was purchased from MACS Miltenyi Biotec (Germany). NucRed™ Live 647 was purchased from Molecular Probes®, Invitrogen (Logan, Utah, USA). HyClone™ EMEM with EBSS and L-glutamine, and HyClone™ non-essential amino acid solution (100x) were purchased from GE Healthcare Life Sciences (Logan, Utah, USA). Trypsin-EDTA (100x), BioWhittaker® Dulbecco's phosphate buffered saline (DPBS) with/without Ca and Mg, were purchased from Lonza (Wakersville, MD, USA). Cleaved caspase 3 (Asp 174) (D3E9) rabbit monoclonal antibody, cleaved caspase 8 (Asp 391) (18C8) rabbit monoclonal antibody and anti-rabbit IgG (H+L), F(ab')<sub>2</sub> fragment (Alexa fluor® conjugate) were purchased from Cell Signalling Technology (Massachusetts, USA). Phalloidin tetramethylrhodamine B isothiocyanate (TRITC) was purchased from Sigma (St. Louis, MO, USA).

### **3.2.1 Cell culture conditions and maintenance**

A549 and MRC5 cell lines were routinely maintained in Eagle's Minimal Essential medium (EMEM) supplemented with 10% foetal bovine serum (FBS), 1% (v/v) non-essential amino acids and 1% (v/v) penicillin/streptomycin in a humidified 5% CO<sub>2</sub> incubator at 37 °C. The cells were monitored daily for contamination using an Axiovert 40C inverted microscope (Carl Zeiss, Germany). Cells were sub-cultured when they reached 80% confluence.

### **3.2.2 Cytotoxicity of macrofungal extracts**

Cytotoxicity of macrofungal extracts on MRC5 (normal) and A549 (cancerous) cell lines was evaluated using the colourimetric MTT assay. Briefly, A549 and MRC5 cells

were seeded in 96-well plates at cell densities of 5,000 cells/100  $\mu\text{L}$ /well. Cells were incubated overnight at 37 °C in a humidified 5%  $\text{CO}_2$  incubator to allow attachment. Stock concentrations of macrofungal extracts were prepared in DMSO at 100 mg/mL. Working concentrations were prepared in complete medium (i.e. EMEM, 10% FBS, penicillin-streptomycin and non-essential amino acids) and concentrations ranging between 0.1 – 200  $\mu\text{g}/\text{mL}$  tested. Cisplatin was used as a positive control, and tested at a concentration range of 0.1 – 80  $\mu\text{g}/\text{mL}$ . Both cell lines were treated for 48 hours at 37 °C in a humidified 5%  $\text{CO}_2$  incubator. Cell viability was determined using the MTT assay as described by Holst-Hansen and Br nner (1998). Briefly, the medium containing extract was removed prior to the addition of 100  $\mu\text{L}$  MTT (0.5 mg/mL) and incubated for 3 hours. Thereafter, the culture medium was aspirated and the formazan product solubilized in DMSO. Absorbance was measured at 540 nm using a BioTek<sup>®</sup> PowerWave XS Spectrophotometer (Winooski, VT, USA). Each treatment was performed in quadruplicate and the experiment carried out at three independent times.  $\text{IC}_{50}$  values of macrofungal extracts were determined using GraphPad Prism Version 5.0 (GraphPad Software, San Diego, USA).

Any compound/crude extract with anticancer activity *in vitro* must be tested on viable, non-cancerous cells in order to determine the effect of the treatment in question. This is important in order to determine if the compound/crude extract will target the cancerous cells only or have mild effects on non-cancerous cells. The human lung fibroblast cell line (MRC5) was selected and the effect of macrofungal species exhibiting cytotoxicity against A549 cancer cells screened.

Growth inhibition =  $[1 - \text{A540 nm of treated cells} / \text{A540 nm of control cells}] \times 100\%$

Selectivity index =  $\text{IC}_{50}$  value of MRC5 /  $\text{IC}_{50}$  value of A549

### 3.2.3 Cell cycle analysis

Cell cycle arrest was determined by using the fluorescent stain, NucRed<sup>™</sup> Live 647 with modifications. NucRed is a red fluorescent nuclear stain, which stain both live and dead cells. When NucRed<sup>™</sup> is bound to DNA it is excited at 638 nm and emits at a maximum wavelength of 686 nm (ThermoScientific). A549 cells were seeded at cell densities as described in section 3.2.2. Cells were treated with the  $\text{IC}_{25}$ ,  $\text{IC}_{50}$  and  $\text{IC}_{75}$  values (Table 3.1; Appendix Table A2) of the macrofungi for 24 and 48 hours. After

treatment, NucRed and Annexin V-FITC staining were performed. Briefly, the culture medium was aspirated and cells washed with PBS (containing  $\text{Ca}^{2+}$  and  $\text{Mg}^{2+}$ ). Cells were stained with Annexin V (50  $\mu\text{L}$  in 5 mL Binding Buffer) and incubated for 15 min at room temperature (RT). Annexin V-FITC staining was done as a marker for apoptotic cells. The medium was aspirated and washed with PBS (containing  $\text{Ca}^{2+}$  and  $\text{Mg}^{2+}$ ). Cells were fixed by adding 50  $\mu\text{L}$  of 4% formaldehyde to each well, and incubated at room temperature for 15 min. The fixative was aspirated and cells washed with PBS (containing  $\text{Ca}^{2+}$  and  $\text{Mg}^{2+}$ ). Thereafter, the cells were stained with NucRed (50  $\mu\text{L}$  in 10 mL). Fluorescent micrographs were captured using Molecular Devices ImageXpress<sup>®</sup> Micro XLS widefield microscope (CA, USA) for high content analysis. Nine image sites were acquired per well (Figure 3.1) using a 10 X magnification. Micrographs were analysed using the MetaXpress<sup>®</sup> High-Content Image Acquisition and Analysis software, and the cell cycle module based on DNA average intensity and positive staining for Annexin V-FITC.

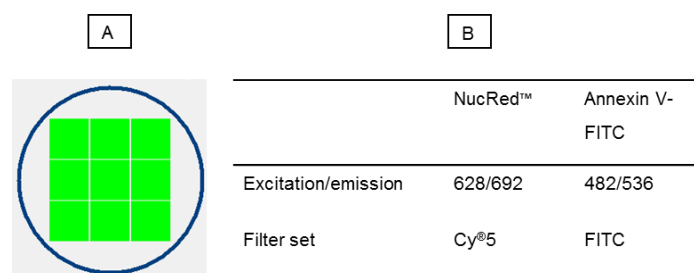


**Figure 3.1:** A – Spatial distribution of image sites acquired during cell cycle analysis. In green is the area that is covered by each image site of a single well (total nine sites). B – Excitation/emission wavelengths and filters used to acquire data.

### 3.2.4 Phosphatidylserine translocation

Phosphatidylserine translocation was determined using the Annexin V-FITC/PI kit with modifications. Briefly, A549 cells were seeded and treated as explained in section 3.2.2. Cells were treated for 24 and 48 hours after which the culture medium was aspirated. In brief, 50  $\mu\text{L}$  of a Hoechst/Annexin mixture (5  $\mu\text{L}$  Hoechst and 50  $\mu\text{L}$  Annexin V in 5 mL binding buffer) was added to each well. The cells were incubated for 15 min in the dark at RT. Thereafter, 50  $\mu\text{L}$  PI (2  $\mu\text{g}/\text{mL}$ ; 100  $\mu\text{L}$  in 5 mL binding buffer) was added to the Annexin/Hoechst stain prior to acquiring the fluorescent micrographs using an ImageXpress<sup>®</sup> Micro XLS widefield microscope for high content analysis. Nine image sites were acquired per well (Figure 3.2) using a 10 X

magnification. Micrographs were analysed using the MetaXpress® High-Content Image Acquisition and Analysis software, and the multi-wave cell scoring module based on DNA average intensity and positive staining for Annexin V-FITC and PI.

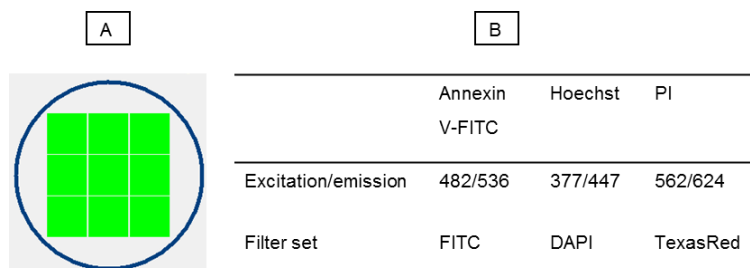


**Figure 3.2:** A – Spatial distribution of image sites acquired during PS translocation analysis. In green is the area that is covered by each image site of a single well (total nine sites). B – Excitation/emission wavelengths and filters used to acquire data.

### 3.2.5 Acridine orange staining

A549 cells were seeded and treated as explained in section 3.2.2 for 48 hours. After treatment, the culture medium was aspirated. Cells were stained by adding 100  $\mu$ L of acridine orange (20  $\mu$ L in 10 mL; 1  $\mu$ g/mL) to each well. The cells were incubated at 37 °C for 15 min in the dark. Fluorescent micrographs were captured using ImageXpress® Micro XLS widefield microscope for high content analysis. Four image sites were acquired per well (Figure 3.3) using a 20 X magnification. Micrographs were visually analysed for apoptotic features.

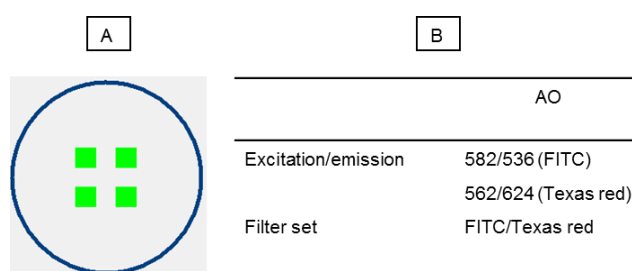


**Figure 3.3:** A – Spatial distribution of image sites acquired during acridine orange staining analysis. In green is the area that is covered by each image site of a single well (total four sites). B –Excitation/emission wavelengths and filters used to acquire data.

### 3.2.6 Hoechst and Phalloidin-TRITC staining

A549 cells were seeded and treated as explained in section 3.2.2 for 48 h. Thereafter, the culture medium was aspirated, cells fixed by adding 100  $\mu\text{L}$  of 4% formaldehyde, incubated for 15 min at room temperature in the dark, and washed with DPBS. The cells were stained with phalloidin-TRITC (1  $\mu\text{M}$ ; 100  $\mu\text{L}$ ) for 15 min at 37  $^{\circ}\text{C}$  in the dark. Subsequently, the nuclei of cells were stained with Hoechst 33342 (5  $\mu\text{g}/\text{mL}$ , 100  $\mu\text{L}$ ). Fluorescent micrographs were captured using ImageXpress<sup>®</sup> Micro XLS widefield microscope for high content analysis. Nine image sites were acquired per well (Figure 3.4) using a 40 X magnification. Micrographs were visually analysed for changes in cytoskeletal structure.

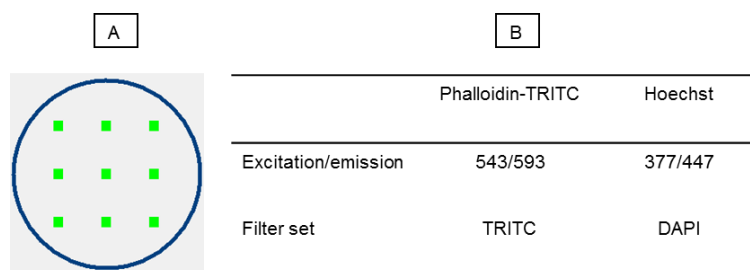


**Figure 3.4:** A – Spatial distribution of image sites acquired during Hoechst and phalloidin-TRITC staining analysis. In green is the area that is covered by each image site of a single well (total nine sites). B –Excitation/emission wavelengths and filters used to acquire data.

### 3.2.7 Caspase-8 and -3 staining

A549 cells were seeded and treated as explained in section 3.2.2 for 24 and 48 hours. After treatment, cells were fixed with 4% formaldehyde at room temperature. The fixative was aspirated and the cells washed with PBS (containing  $\text{Ca}^{2+}$  and  $\text{Mg}^{2+}$ ). The cells were permeabilized by adding cold 80% methanol and incubated at -20  $^{\circ}\text{C}$  for 10 min. The medium was aspirated and antibody staining was performed. Cleaved caspase 3 (Asp 175) and cleaved caspase 8 (Asp 391) rabbit monoclonal antibodies were used to determine the presence of activated caspase-3 and -8, respectively. After permeabilization, the cells were washed with PBS (containing  $\text{Ca}^{2+}$  and  $\text{Mg}^{2+}$ ) and blocked using PBS containing 0.5% bovine serum albumin (BSA). Thereafter, the cells were incubated separately with the respective antibodies (1:200 for caspase-3 and 1:100 for caspase-8) for 1 h at 37  $^{\circ}\text{C}$  in the dark. Cells were washed once with blocking

solution (PBS containing 0.5% BSA) and incubated with the conjugated secondary antibody, anti-rabbit IgG (H + L), F(ab')<sub>2</sub> Fragment (Alexa Fluor® 647 Conjugate; 1:500) for 30 min at 37 °C in the dark. The medium was aspirated and cells washed once with blocking solution before Hoechst (5 µg/mL) counterstaining was performed. Fluorescent micrographs were acquired using an ImageXpress® Micro XLS widefield microscope for high content analysis. Nine image sites were acquired per well (Figure 3.5) using a 40 X magnification. Micrographs were analysed using the MetaXpress® High-Content Image Acquisition and Analysis software, and the multi-wave cell scoring module based on fluorescence intensity and positive staining for caspase -3/-8.

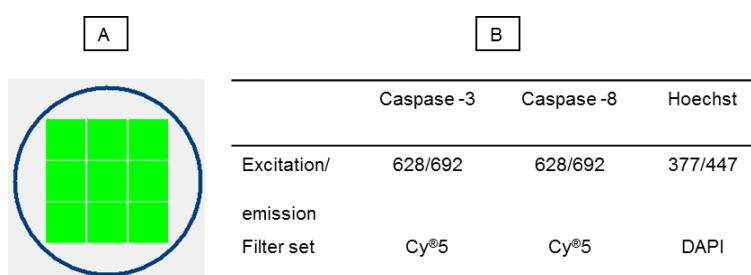


**Figure 3.5:** A – Spatial distribution of image sites acquired during caspase-3 and -8 activation analysis. In green is the area that is covered by each image site of a single well (total nine sites). B –Excitation/emission wavelengths and filters used to acquire data.

### 3.2.8 Statistical analysis

All treatments of the A549 and MRC5 cell lines were performed in triplicate, and three independent experiments carried out. Standard deviation (SD) of the mean of three independent experiments was calculated. For each assay, the Student two-tailed t-test was performed in order to determine statistical significance.  $p < 0.05$  was considered significant and indicated by \*,  $p < 0.005$  was indicated by \*\*.

### 3.3 RESULTS

#### 3.3.1 Cytotoxicity and IC<sub>50</sub> determination

Aqueous and ethanolic macrofungal extracts were screened against human lung carcinoma (A549) and fibroblast (MRC5) cell lines for cytotoxicity. The half maximal inhibitory concentration (IC<sub>50</sub>) was determined from dose-response curves (Figs. 3.6 and 3.7), where inhibition of proliferation was observed. Levels of cytotoxicity against Hela, HT-29, MCF-7, MIA PaCa-2 and PC-3 were assessed according to Boukes et al. (2017), where crude macrofungal extracts with IC<sub>50</sub> values of <100 µg/mL were considered significantly cytotoxic and IC<sub>50</sub> values between 100 – 200 µg/mL were considered moderately cytotoxic.

The IC<sub>50</sub> values of *F. lilacinogilva* and *G. junonius* were determined in a previous study performed by Dr. G.J. Boukes (unpublished data). IC<sub>50</sub> values of 69.2±3.6 and 57±5 µg/mL were obtained for *F. lilacinogilva* and *G. junonius*, respectively. The crude ethanol extracts of *A. foetidissima*, *G. lucidum*, *H. fasciculare*, *P. ostreatus* (white), *R. capensis*, *S. commune*, *P. tinctorius*, *S. hirsutum*, *I. badia* and *L. elegans* were also screened, but did not show any cytotoxic activity.

The crude macrofungal extracts screened during this study included *H. erinaceus*, *P. papilionaceus*, *L. sulphurous*, *P. ostreatus* (grey), *A. campestris*, *P. baudonii*, *C. molybdites*, *G. penetrans* and *P. sanguineus* (aqueous and ethanolic). The aqueous extract of *P. baudonii* (IC<sub>50</sub>: 53.6±1.1 µg/mL) and ethanolic extract of *P. sanguineus* (IC<sub>50</sub>: 7.4±1.1 µg/mL) were cytotoxic to A549 cells. The macrofungal species showing no cytotoxicity were excluded from further experiments.

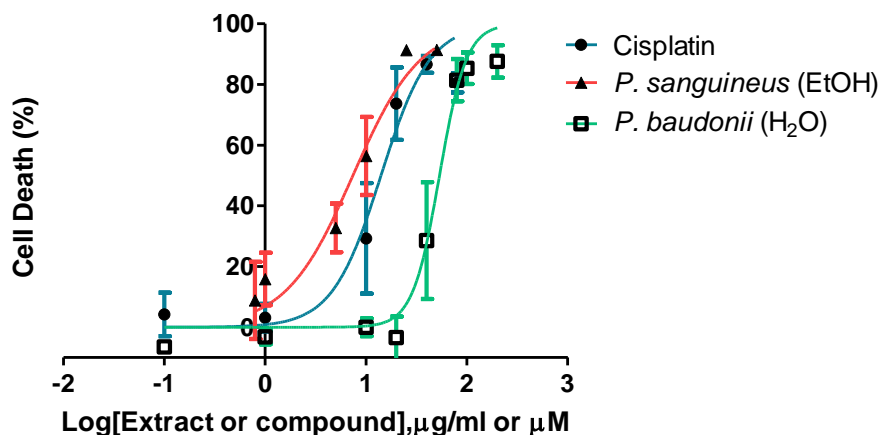


**Figure 3.6:** Dose-response curves of cytotoxicity of *P. sanguineus*, *P. baudonii* and cisplatin (positive control) against A549 cells. Cells were treated with varying concentrations of crude macrofungal extracts (0.1 – 200  $\mu\text{g/mL}$ ) for 48 h and MTT assay was performed to determine cell viability. Data presented as mean  $\pm$  S.D of triplicate values of three independent experiments (n=3).

The MRC5 cell line showed a decrease in viability when increasing the concentration above 110.4, 141.2 and 158.3  $\mu\text{g/mL}$  for *F. lilacinogilva*, *P. sanguineus* and *G. junonius*, respectively (Figure 3.7). The *P. baudonii* spp. was cytotoxic to MRC5 cells at concentrations  $\geq 100$   $\mu\text{g/mL}$ . Table 3.1 summarizes the  $\text{IC}_{50}$  values of 11 macrofungal species following 48 h exposure to the A549 and MRC5 cell lines. The concentrations used in all further experiments are summarised in Table 3.1. The  $\text{IC}_{25}$  and  $\text{IC}_{75}$  values were determined using GraphPad Prism online software (Appendix Table A2). Cisplatin was used as a positive control and the  $\text{IC}_{50}$  was  $14.1 \pm 1.1$   $\mu\text{g/mL}$ . The ethanol extracts of *F. lilacinogilva*, *G. junonius* and *P. sanguineus* and the aqueous extract of *P. baudonii* were selected for further investigation. Table 3.2 shows the selectivity indices for the treated A549 and MRC5 cell lines. The selectivity indices were calculated to determine the discrimination ability of the macrofungal extracts and cisplatin between treated non-cancerous (MRC5) and cancerous cells (A549). Treatments with *G. junonius* and *P. sanguineus* afforded the highest selectivity indices of 2.8 and 19.1, respectively. *P. baudonii* and *F. lilacinogilva* showed lower selectivity of 1.9 and 1.6, respectively. The results obtained for *G. junonius* and *P. sanguineus* is encouraging as the higher selectivity indexes show their preferential activity against A549 cells in *in vitro* experiments.



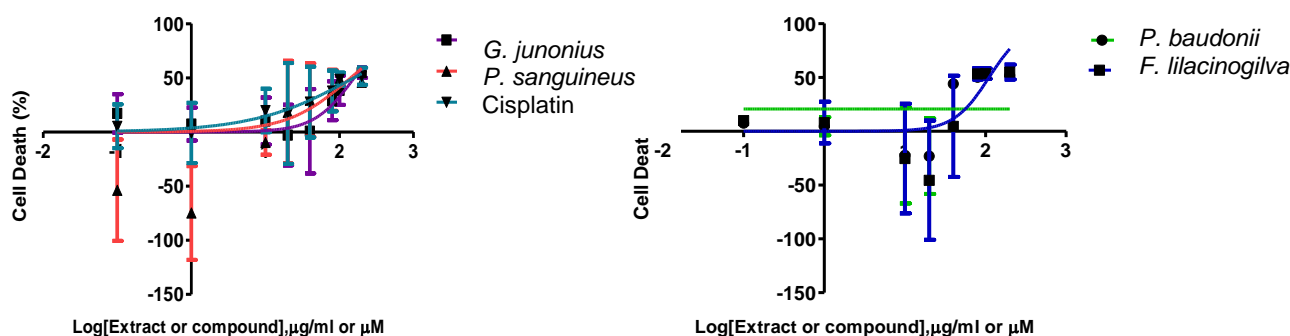


**Figure 3.7:** Dose-response curves of cytotoxicity of *G. junonius*, *P. sanguineus*, *P. baudonii*, *F. lilacinogilva* and cisplatin (positive control) against MRC5 cells. Cells were treated with varying concentrations of crude macrofungal extracts (0.1 – 200 µg/mL) for 48 h and MTT assay was performed to determine cell viability. Data presented as mean ± S.D of triplicate values of three independent experiments (n=3).

**Table 3.1:** IC<sub>50</sub> values (µg/mL) of 11 South African macrofungal species against normal lung fibroblast (MRC5) and lung cancer (A549) cell lines. Cell lines were treated for 48 h with crude ethanolic and aqueous macrofungal extracts at concentrations ranging between 0.1 – 200 µg/mL. Data presented is the mean ± S.D of triplicate values of three independent experiments (n=3).

Macrofungal spp.	Normal (MRC)		Cancerous cell line (A549)	
	Aqueous	Ethanolic	Aqueous	Ethanolic
<i>F. lilacinogilva</i>	N/A	110.4±1.3	>200	69.2±3.6 *
<i>G. junonius</i>	N/A	158.3±1.3	>200	57±5 *
<i>G. penetrans</i>	N/A	N/A	>200	>100
<i>P. sanguineus</i>	N/A	141.2±1.9	>200	7.4±1.1
<i>H. erinaceus</i>	N/A	N/A	>200	>200
<i>P. papilionaceus</i>	N/A	N/A	>200	>200
<i>L. sulphurous</i>	N/A	N/A	>200	>200
<i>P. ostreatus (grey)</i>	N/A	N/A	>200	>200
<i>A. campestris</i>	N/A	N/A	>200	>200
<i>P. baudonii</i>	>100	N/A	53.6±1.1	>200
<i>C. molybdites</i>	N/A	N/A	>200	>200
<b>Positive control</b>				
Cisplatin		156.2±1.7		14.1±1.1

\* Study by Dr. G.J. Boukes (unpublished data)

**Table 3.2:** Selectivity indices of the cytotoxicity of *G. junonius*, *P. sanguineus*, *P. baudonii* and *F. lilacinogilva* extracts against A549 cancer cells compared to MRC5 cells.

Treatment	Selectivity index (SI)
<i>F. lilacinogilva</i>	1.6
<i>P. baudonii</i>	1.9
<i>G. junonius</i>	2.8
<i>P. sanguineus</i>	19.1
Cisplatin	11.1

### 3.2.1 Cell cycle analysis

DNA cell cycle analysis was performed to determine if the selected macrofungal extracts induced cell cycle arrest in specific phases of the cell cycle. Figure 3.8 summarizes the effect of macrofungal extract treatments on the cell cycle phases (i.e. G0/G1, S, G2, early M and late M) of A549 cells. A549 cells were treated with ethanol extracts of *F. lilacinogilva*, *G. junonius*, and *P. sanguineus*, and an aqueous extract of *P. baudonii* at their IC<sub>25</sub>, IC<sub>50</sub> and IC<sub>75</sub> concentrations for 24 h and 48 h.

Cisplatin treated A549 cells showed more cells distributed in the G2 phase. After 24 h of treatment, the percentage doubled from 11.20% to 24.44% and 30.32% for untreated, cisplatin IC<sub>50</sub> (p<0.05) and cisplatin IC<sub>75</sub> (p<0.005), respectively. A significant increase (nearly 5-fold; p<0.005) was observed after 48 h of treatment (12.2% to 60.7% for IC<sub>50</sub>). The latter results therefore confirm G2 phase arrest in cisplatin treated cells. A decrease in the G2 phase of cisplatin IC<sub>75</sub> can be attributed to the high number of apoptotic cells ( $\pm 40\%$ ). Apoptotic cells degrade and detach, and the results cannot be used as a true representation to determine cell cycle arrest.

*F. lilacinogilva* (IC<sub>75</sub>) significantly increased (p<0.005) the percentage of A549 cells in the early M phase compared to untreated cells (10.94% to 30.31%; Figure 3.8A). This possibly indicates that *F. lilacinogilva* induced early M phase arrest, which was confirmed after 48 h for the IC<sub>75</sub> concentration. The high percentage of apoptotic cells observed after 24 and 48 h treatment with *F. lilacinogilva* (Figure 3.8 A and B) decreases the percentage viable cells that can be categorised into the specific growth phases. This therefore influences the results obtained. In order to confirm early M phase arrest, additional experiments can be performed.

A549 cells responded differently when treated with *G. junonius* and *P. sanguineus*. After 24 h, non-significant increases in the percentage of cells in the G2 and early M phases were observed compared to the untreated cells. Therefore, no definite conclusion can be drawn from the results after 24 h. After 48 h, significant ( $p < 0.05$ ;  $p < 0.005$ ) increases in both G2 and early M phase were observed for *G. junonius* treated cells ( $IC_{50}$ ), from 12.3% to 48.0% and from 3.1% to 26.7% for G2 and early M phase (UT and macrofungal treatment), respectively. An increase in the percentage G2 cells, from 12.3% to 28.9% and 42.0% phase were observed for untreated, *P. sanguineus*  $IC_{50}$  and *P. sanguineus*  $IC_{75}$  treated cells, respectively. This suggests that A549 cells potentially arrested in G2/M and G2 phases for *G. junonius* and *P. sanguineus*, respectively.

A549 cells treated with *P. baudonii* showed substantial dose-dependent increases in the percentage of apoptotic cells after 24 and 48 h of treatment. As mentioned, this may affect the results as a large portion of the cells have undergone apoptosis and can no longer be classified in a specific growth phase. Based on the results obtained after 24 h, the  $IC_{25}$  and  $IC_{50}$  concentrations showed significant ( $p < 0.05$ ) increases in G2 phase arrest. This increase was still evident after 48 h with the  $IC_{25}$  concentration, thus suggesting that *P. baudonii* induced G2 phase arrest. Consistently, the cells distributed in the G0/G1 and S phases were significantly reduced over time in a concentration-dependent manner with all macrofungal and cisplatin treatments. All the treatments resulted in a dose-dependent increase in apoptotic cells. *F. lilacinogilva* and *P. baudonii* were rapid inducers of apoptosis as significant increases were observed compared to the untreated and other macrofungal treatments after 24 h of exposure (Figure 3.8).

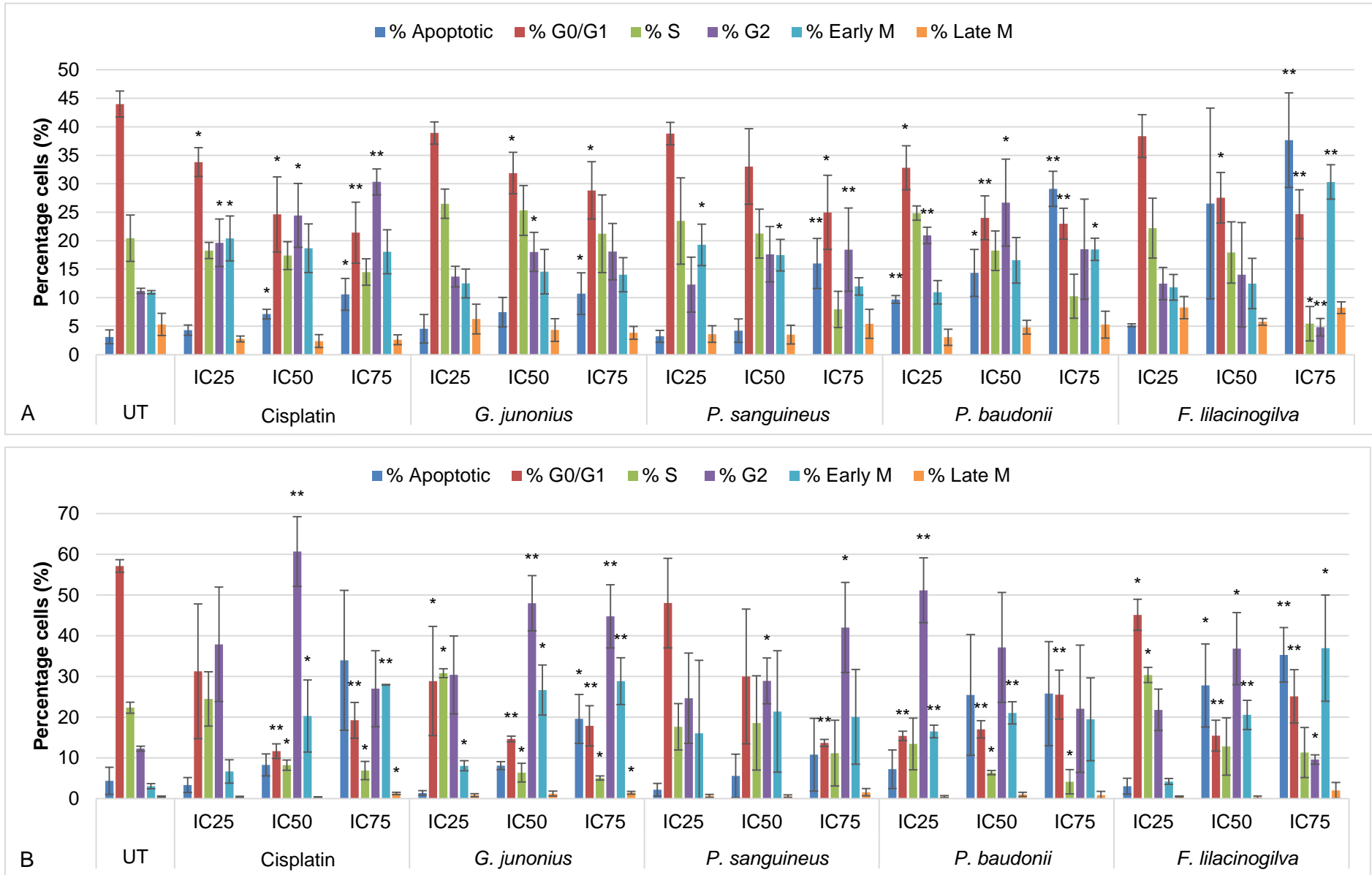


**Figure 3.8:** Cell cycle analysis of A549 cells treated with selected macrofungal extracts at IC<sub>25</sub>, IC<sub>50</sub> and IC<sub>75</sub> concentrations after (A) 24 h and (B) 48 h. Data presented as the average percentage (%) of cells in the various phases of the cell cycle. Each experiment was carried out in triplicate and repeated in three independent experiments (n=3). Significance was determined using the Student t-test: \*p<0.05 and \*\*p<0.005 compared to untreated control (UT).

### 3.3.2 Phosphatidylserine translocation

After 24 h, there was a dose-dependent increase in the percentage of apoptotic, necrotic and late apoptotic/necrotic cells following treatment with macrofungal extracts and cisplatin compared to untreated (UT) cells (Figure 3.9). After 24 h, the percentage of apoptotic cells was  $1.16 \pm 0.14\%$  for the UT cells. Exposure of A549 cells to macrofungal extracts at  $IC_{75}$  values for 24 h, significantly increased ( $p < 0.05$ ;  $p < 0.005$ ) the number of apoptotic cells (i.e. 14.98, 5.12, 4.71, and 6.94% for *F. lilacinogilva*, *G. junonius*, *P. sanguineus* and *P. baudonii*, respectively). After 48 h, the percentage of apoptotic cells increased to 25.98, 8.99, 22.91, and 7.25% for *F. lilacinogilva*, *G. junonius*, *P. sanguineus* and *P. baudonii*, respectively. *F. lilacinogilva* and *P. baudonii* were rapid inducers of apoptosis as significant increases were observed after 24 h. Cisplatin, *G. junonius* and *P. sanguineus* significantly increased apoptosis only after 48 h. This is consistent with the cell cycle analysis (Figure 3.8). *P. baudonii* treated A549 cells mainly underwent late apoptosis/necrosis at  $IC_{25}$ , and late apoptosis/necrosis and necrosis at  $IC_{50}$  and  $IC_{75}$  after 24 and 48 h of treatment. *P. baudonii* is a rapid inducer of apoptosis as  $\pm 40\%$  of cells were apoptotic in the cell cycle after 24 h. This therefore suggests that the large increases in late apoptosis/necrosis are rather an indication of apoptotic cells than necrotic cells. Cisplatin, *G. junonius*, *P. sanguineus* and *F. lilacinogilva* showed that the greatest percentage cells were apoptotic and late apoptotic/necrotic. These results suggest that apoptosis plays an important role in A549 cell death when exposed to macrofungal extracts and cisplatin (positive control).

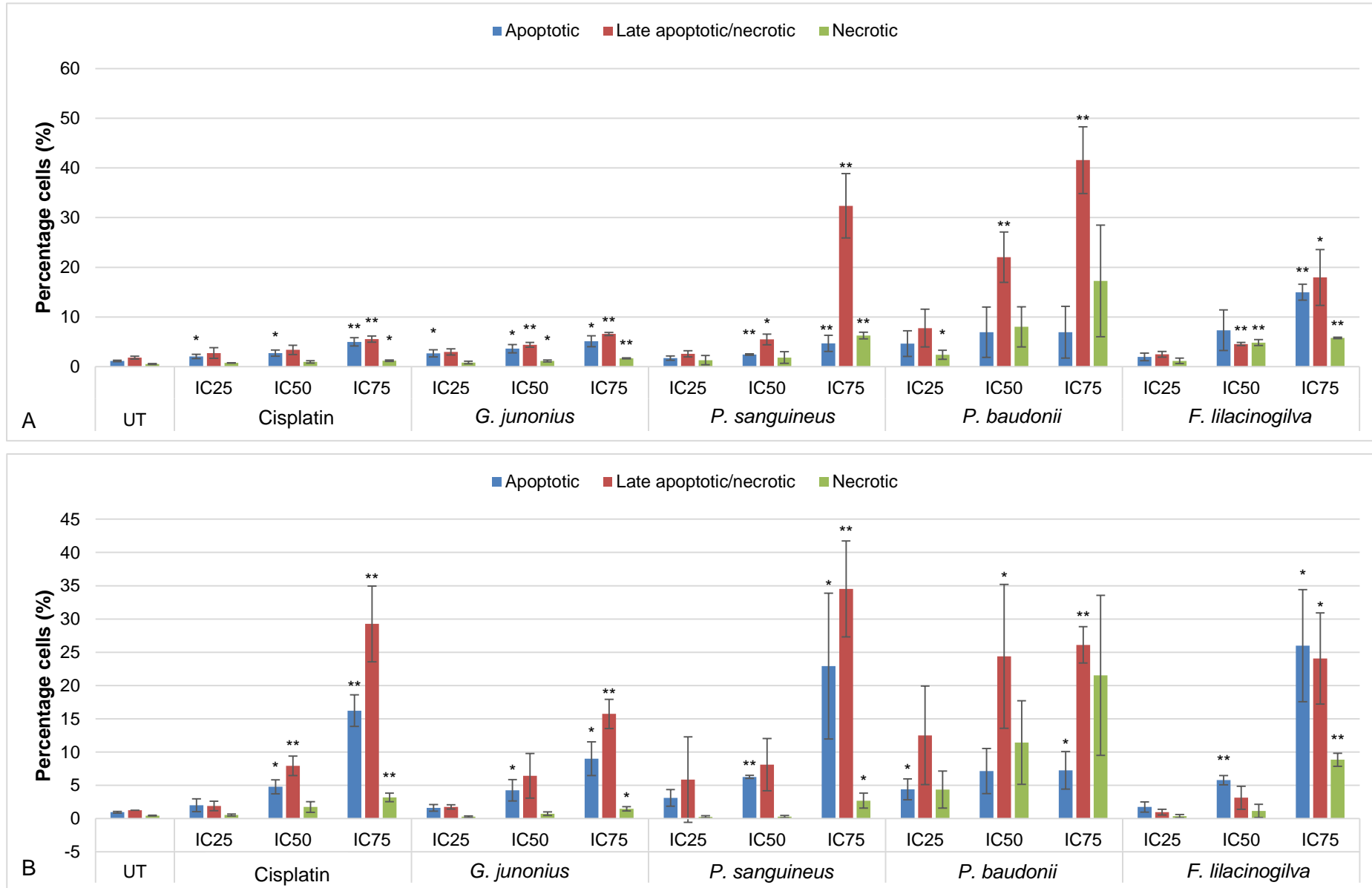


**Figure 3.9:** Analysis of PS translocation in A549 cells using Annexin V-FITC/PI dual staining following 24 h (A) and 48 h (B) of treatment with macrofungal extracts or cisplatin. Cells were treated with the ethanol extracts of *F. lilacinogilva*, *G. junonius* and *P. sanguineus*, and the aqueous extract of *P. baudonii*. Bar graphs represent the average of three independent experiments each performed in triplicate. SD is represented by error bars. Significance was determined using the two-tailed Student t-test: \* $p < 0.05$ ; \*\* $p < 0.005$  compared to the untreated (UT) control.

### 3.3.3 F-actin staining

The filamentous actin cytoskeleton of A549 cells was investigated to determine the preservation of cellular architecture after treatment with macrofungal extracts. Untreated cells exhibited well-organised actin filament bundles (stress fibers) in the cytoplasm (Figure 3.10). On the contrary, macrofungal treated cells (IC<sub>50</sub>) showed a reduction in phalloidin staining as well as several morphological changes. The morphological features observed, include chromatin condensation, loss of cytoskeletal arrangement and the rounding up of cells. These are all characteristic features of apoptosis. *G. junonius*, *P. sanguineus* and *F. lilacinogilva* induced micro- and multinucleation, whereas *P. baudonii* induced multinucleation only. The results therefore suggest that treatment with the macrofungal extracts led to the disruption of the cytoskeletal structure in A549 cells.

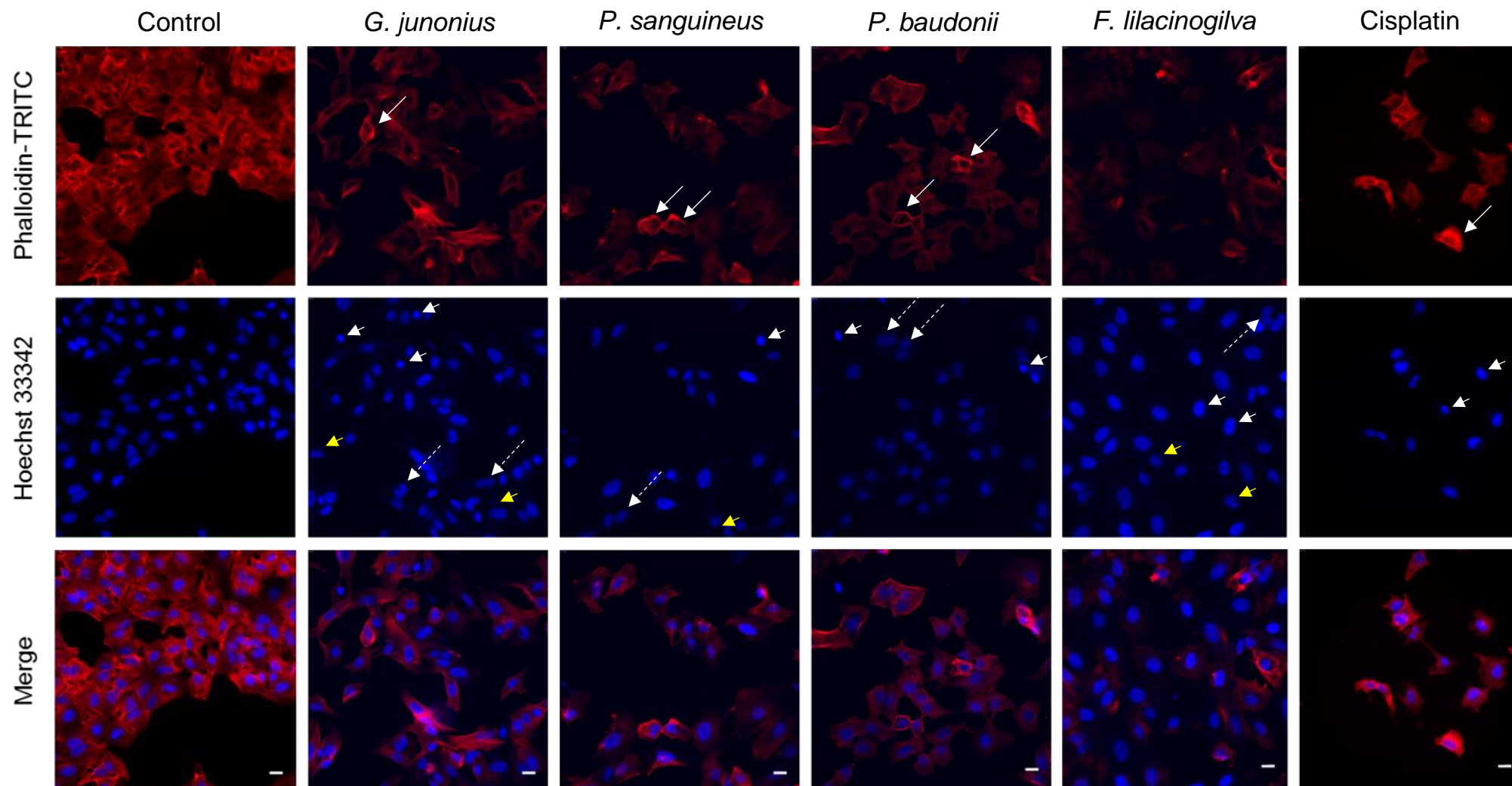


**Figure 3.10:** Morphological changes of A549 cells, associated with apoptosis, following 48 h exposure to *G. junonius*, *P. sanguineus*, *P. baudonii*, *F. lilacinogilva* and cisplatin. A549 cells were treated with the  $IC_{50}$  of macrofungal spp. or left untreated (control). Short white arrows = condensed chromatin. Long white arrows = loss of cytoskeletal arrangement and rounding up of cells. Dashed white arrows = multinuclei. Short yellow arrows = micronuclei. Scale bar = 23  $\mu$ M.



### 3.3.4 Caspase-8 and caspase-3 activation

Apoptosis is a highly organised mechanism of cell death and central to this is caspase activation. Activation of caspase-8 and -3 was determined by means of immunochemistry. Antibodies against activated/cleaved caspase-8 and -3 were used for their detection.

#### 3.3.4.1 Caspase-8

The levels of cleaved caspase-8 observed after 24 and 48 h exposure to macrofungal extracts are represented in Figure 3.11. The levels of caspase-8 increased in a concentration-dependent manner for the macrofungal extracts and the positive control, cisplatin. The percentages of cleaved caspase-8 for the untreated control were  $0.62\pm 0.05$  and  $0.58\pm 0.13\%$  for 24 and 48 h, respectively.

*P. sanguineus*, *P. baudonii*, *F. lilacinogilva* and cisplatin showed dose-dependent increases, with the highest percentage of active caspase-8 observed for the IC<sub>75</sub> after 24 and 48 h treatment. The percentages of cleaved caspase-8 were 2.31, 3.05, 1.86, and 2.52% after 24 h treatment, which further increased after 48 h to 3.52, 5.15, 18.36 and 11.88% for *P. sanguineus*, *P. baudonii*, *F. lilacinogilva* and cisplatin, respectively.

*G. junonius* only showed small increases or remained relatively constant compared to the untreated control over the time period tested, with the percentage cleaved caspase-8 ranging between 0.71-0.97% and 0.23-0.59% for 24 and 48 h, respectively. The results obtained therefore suggest that *P. sanguineus*, *P. baudonii*, *F. lilacinogilva* and cisplatin induced apoptosis through a caspase-dependent pathway involving caspase-8.

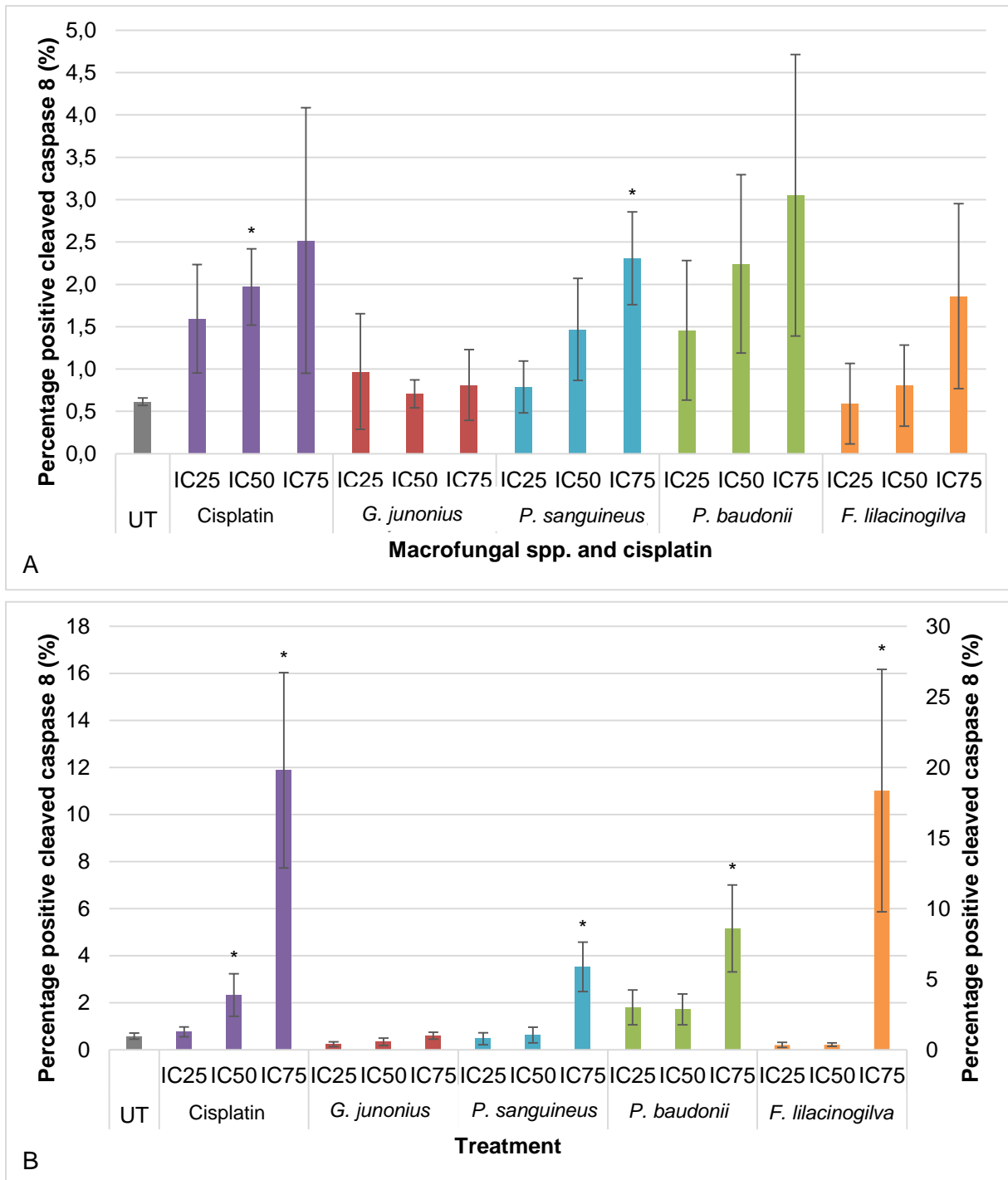


**Figure 3.11:** Detection of cleaved caspase-8 activity in A549 cells after 24 h (A) and 48 h (B) treatment with *G. junonius*, *P. sanguineus*, *P. baudonii* and *F. lilacinogilva*. *F. lilacinogilva* (48 h) data represented on the secondary axis. Positive control used was cisplatin. Data presented as mean  $\pm$  S.D of triplicate values of three independent experiments (n=3). Significance was determined using the two-tailed Student t-test: \*p<0.05; \*\*p<0.005 compared to the untreated (UT) control.

### 3.3.4.2 Caspase-3

Activation of caspase-3 was investigated as a general marker for the induction of apoptosis as it can be activated through the intrinsic and extrinsic pathways. Figure 3.12 shows the changes in percentage of activated caspase-3 after 24 (Figure 3.12A) and 48 h (Figure 3.12B) treatment with cisplatin and macrofungal extracts. Dose-dependent increases in the levels of cleaved caspase-3 were observed for cisplatin, *G. junonius*, *P. sanguineus* and *F. lilacinogilva*. After 24 and 48 h the percentages of cleaved caspase-3 in the untreated control were  $0.69 \pm 0.11\%$  and  $0.92 \pm 0.11\%$ , respectively.

Significant increases ( $p < 0.05$ ) in the levels of cleaved caspase-3 were observed after 24 h for cisplatin  $IC_{50}$  and  $IC_{75}$ , yielding  $1.51 \pm 0.28\%$  and  $2.50 \pm 0.95\%$ , respectively. A substantial increase ( $IC_{75}$ ;  $p < 0.05$ ) was observed after 48 h with  $8.97 \pm 2.79\%$ . A549 cells treated with the  $IC_{25}$  and  $IC_{50}$  concentration of *F. lilacinogilva* showed relatively low levels of caspase-3 (0.93 – 3.97%). A significant ( $p < 0.05$ ) increase was observed for the  $IC_{75}$  concentration after 24 and 48 h with  $22.03 \pm 9.27$  and  $35.41 \pm 4.77\%$ , respectively. From the latter results, it can be deduced that *F. lilacinogilva* and the positive control, cisplatin, activated caspase-3 in a concentration and time dependent manner ( $IC_{75}$  –  $p < 0.05$ ).

No significant ( $p > 0.05$ ) caspase-3 activity was seen for A549 cells treated with *G. junonius* (24 h) and *P. sanguineus* (24 and 48 h). After 48 h, small increases were observed for *G. junonius*  $IC_{25}$  ( $p < 0.005$ ) and  $IC_{50}$  ( $p < 0.05$ ). *P. baudonii* showed increases in caspase-3 levels that were relatively similar after 24 and 48 h, and the only statistically significant increase was observed after 24 h at the  $IC_{50}$  concentration. *G. junonius*, *P. sanguineus* and *P. baudonii* treatment indicated that apoptosis was slightly induced by the activation of caspase-3.

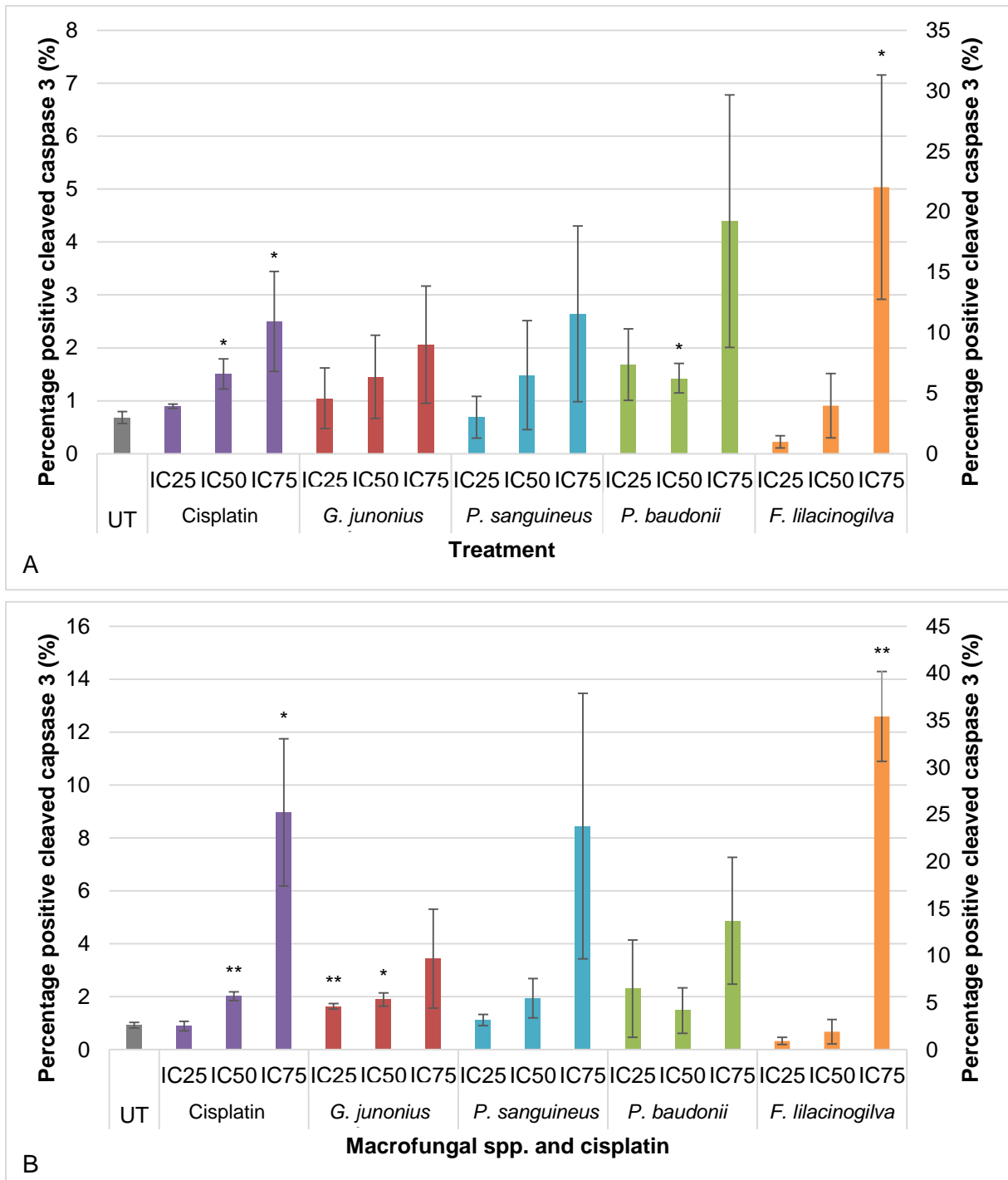


**Figure 3.12:** Detection of cleaved caspase-3 activity in A549 cells after 24 h (A) and 48 h (B) treatment with *G. junonius*, *P. sanguineus*, *P. baudonii* and *F. lilacinogilva*. *F. lilacinogilva* data represented on the secondary axis. Positive control used was cisplatin. Data presented as mean  $\pm$  S.D of three triplicate values of three independent experiments (n=3). Significance was determined using the two-tailed Student t-test: \*p<0.05; \*\*p<0.005 compared to the untreated (UT) control.

### 3.3.5 Acridine orange staining

Cells undergoing apoptosis have characteristic morphological features that can be used to distinguish them from other types of cell death such as necrosis. Fluorescent staining was performed using acridine orange to observe any changes in cell morphology and cell membrane integrity. Apoptotic cells exhibit chromatin condensation and cytoplasmic membrane blebbing, while necrotic cells show nuclear swelling, and nuclear and plasma membrane rupturing (Zhang et al., 2018). Morphological changes were observed after 48 h treatment with macrofungal extracts ( $IC_{50}$ ) and the positive control, cisplatin. The morphology of untreated A549 cells can be seen in Figure 4.13A, with round intact nuclei and cells that are uniformly stained green. By contrast, morphological examination of A549 cells treated with macrofungal extracts showed nuclear condensation (short white arrows), rounding up of cells (yellow short arrows) and membrane blebbing (yellow long arrows). The number of apoptotic cells increased in a concentration dependent manner (Figure 3.14).

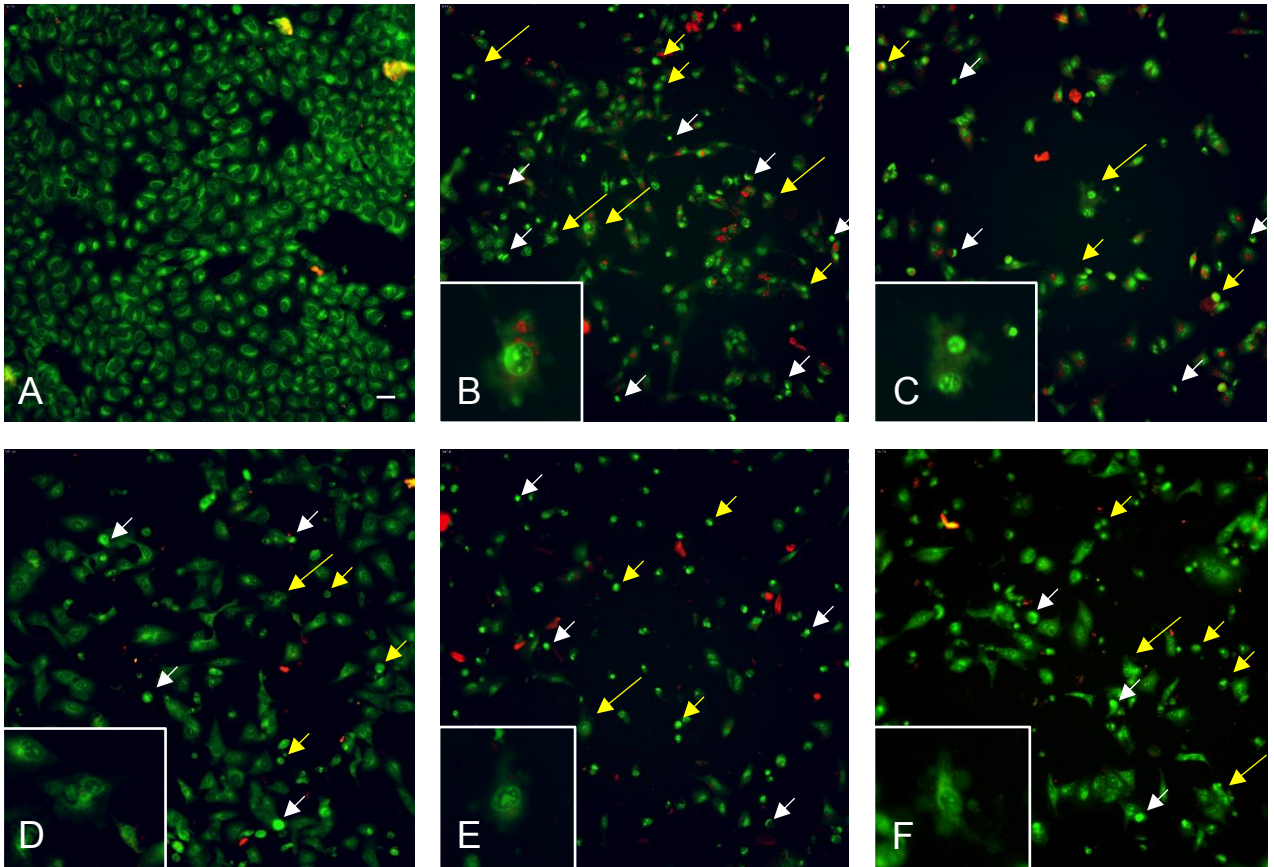


**Figure 3.13:** Morphological changes of A549 cells, associated with apoptosis, following 48 h exposure to *G. junonius* (B), *P. sanguineus* (C), *P. baudonii* (D), *F. lilacinogilva* (E) and cisplatin (F). A549 cells were treated with the IC<sub>50</sub> concentration or left untreated (control-A). Short white arrows = condensed chromatin. Short yellow arrows = rounding up of cells. Long yellow arrows = membrane blebbing. Scale bar = 37  $\mu$ M.

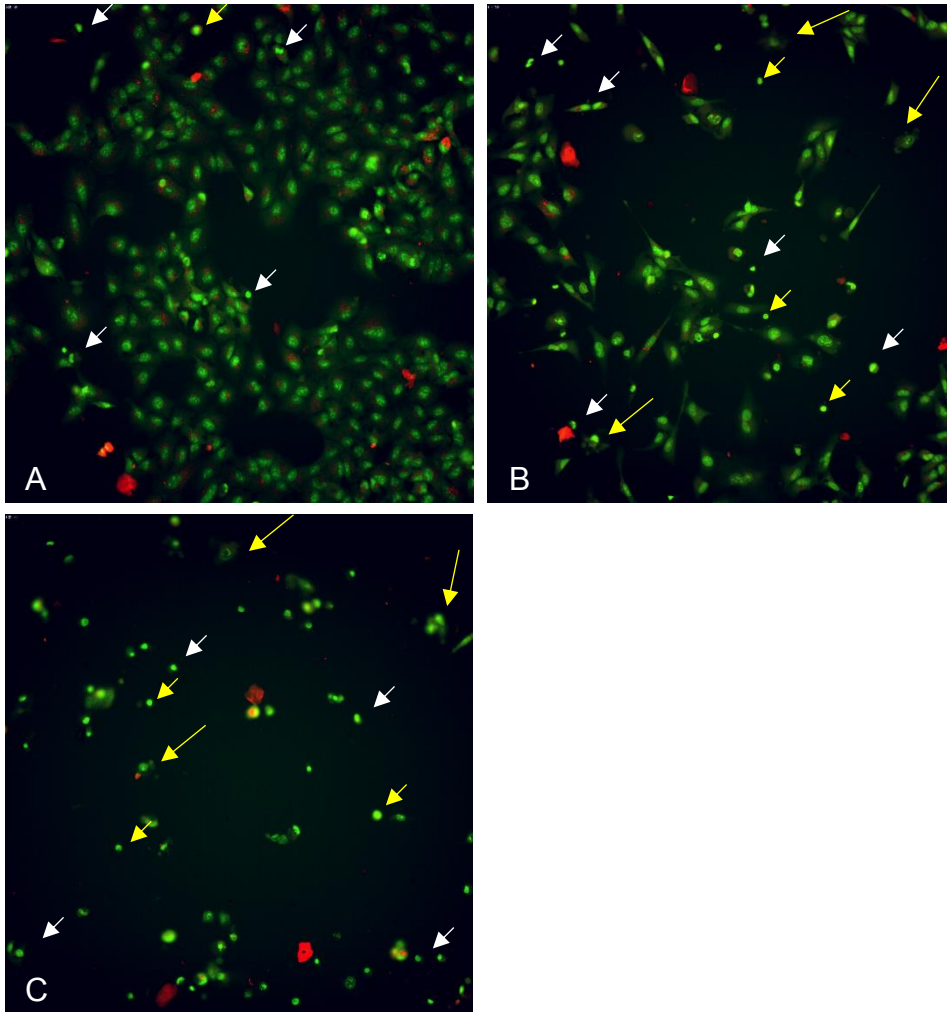


**Figure 3.14:** Morphological changes of A549 cells, associated with apoptosis, following 48 h exposure to IC<sub>25</sub> (A), IC<sub>50</sub> (B) and IC<sub>75</sub> concentrations of *P. sanguineus*. Short white arrows = condensed chromatin. Short yellow arrows = rounding up of cells. Long yellow arrows = membrane blebbing.

### 3.4 DISCUSSION

Macrofungal research has increased over the last decade due to scientists' ability to identify, isolate and synthesise various compounds with biological properties, which may serve as potential therapeutic drugs. Their anticancer- and immunomodulatory activities have been investigated and several papers have been published.

This chapter focussed on identifying South African macrofungal species with cytotoxic properties against the A549 lung cancer cell line and to determine the mechanism of action induced. Several modes of cell death exist, of which apoptosis is the most controlled mechanism of action. Cytotoxicity of several macrofungal species have been investigated against different cancer types, however studies on the mechanism of induced cytotoxicity are limited. This is the first study on the cytotoxicity of *P. baudonii*, and elucidation of mechanism of action of *P. baudonii*, *G. junonius*, *P. sanguineus* and *F. lilacinogilva* treated lung cancer cells. In this study, crude macrofungal extracts with IC<sub>50</sub> values of <100 µg/mL were considered significantly cytotoxic and IC<sub>50</sub> values between 100-200 µg/mL were considered moderately cytotoxic (Boukes et al., 2017).

Aqueous and ethanol extracts of South African macrofungal species were prepared and screened against A549 lung adenocarcinoma for potential cytotoxicity. Dose-response curves were plotted for the macrofungal species exhibiting cytotoxicity in order to determine the IC<sub>50</sub> value for each species (Figure 3.6). The aqueous extracts of the majority of macrofungal species did not exhibit any cytotoxicity at concentrations tested (0.1 – 200 µg/mL). *P. baudonii* was the only aqueous macrofungal extract with cytotoxicity against A549 cells, with an IC<sub>50</sub> value of 53.4±1.06 µg/mL. The ethanol extracts of *F. lilacinogilva*, *G. junonius* and *P. sanguineus* exhibited cytotoxicity with IC<sub>50</sub> values of 69.2±3.6, 57±5 and 7.42±1.12 µg/mL, respectively (Table 3.1). Ethanol extracts of *F. officinalis* and *F. pinicola* showed stronger inhibitory activities against human hepatoma (HepG2), lung (A549), colorectal (HCT-116) and breast (MDA-MB-231) cancer cell lines, and mouse sarcoma (S-180) compared to water extracts (Wu et al. 2014). This was also demonstrated by Choi et al. (2007) in which a methanol extract of *F. pinicola* showed greater inhibition than a hot water extract against HeLa (cervix carcinoma) and Hep3B (liver cancer) cells. The results obtained in this study,



in terms of enhanced cytotoxicity for ethanol extracts, are consistent with previous findings.

Cytotoxicity studies on the genus *Fomitopsis* have mainly focussed on three species, *F. pinicola*, *F. nigra* and *F. officinalis*. The ethanol extracts of *F. officinalis* and *F. pinicola* inhibited the growth of human breast (MDA-MB-231), colon (HCT-116), lung (A549), hepatoma (HepG2) cancer cell lines, and mouse sarcoma 180 cells (S-180) with IC<sub>50</sub> concentrations ranging between 15.7 – 62 µg/mL and 7.1 – 34.1 µg/mL, respectively (Wu et al., 2014). *F. officinalis* and *F. pinicola* inhibited lung cancer growth at IC<sub>50</sub> concentrations of 62.0 ± 4.4 µg/mL and 7.1 ± 3.2 µg/mL, respectively (Wu et al., 2014). Wang et al. (2014) showed that a chloroform extract of *F. pinicola* exhibited cytotoxicity against colorectal cancer cells, SW 480 and SW 320, at IC<sub>50</sub> concentrations of 190.28 µg/mL and 143.26 µg/mL, respectively (Wang et al., 2014b). An ethanol extract of *F. lilacinogilva* had IC<sub>50</sub> values of 52.2, 55.1, 63, 48.8 and 79.8 µg/mL against human HeLa (cervical adenocarcinoma), HT-29 (colorectal adenocarcinoma), MCF-7 (breast adenocarcinoma), MIA PaCa-2 (pancreatic ductal adenocarcinoma) and PC-3 (prostate adenocarcinoma) cancer cell lines, respectively (Boukes et al., 2017). The cytotoxicity observed for *F. lilacinogilva* (69.2±3.6 µg/mL) in this study is therefore similar to previous reports.

Research on the cytotoxicity of the genus *Gymnopilus* have been reported on two species, *G. spectabilis* and *G. penetrans*. The methanol extracts of *G. spectabilis* and *G. penetrans* were cytotoxic at IC<sub>50</sub> values <50 µg/mL and > 100 µg/mL, respectively, against the murine lymphocytic leukaemia (L1210) and Lewis lung carcinoma (3LL) cell lines (Tomasi et al., 2004). *G. junonius* showed moderate cytotoxic properties (>100 µg/mL) against PC-3, HT-29 and MCF-7 cells. High cytotoxicity was observed against HeLa and MIA PaCa-2 cancer cells at IC<sub>50</sub> values of 55.1 and 52.5 µg/mL, respectively (Boukes et al., 2017). Five compounds (gymnopilin K, gymnopilin A9, gymnopilin A10, gymnopilene and gymnoprenol A9) isolated from *G. spectabilis* showed inhibitory activities against A549 (lung), SK-OV-3 (ovarian), SKMEL-2 (melanoma), and HCT-15 (colon) with IC<sub>50</sub> values ranging between 3.26 – 26.30 µM (Kim et al., 2012). The results obtained in this study for the ethanol extract of *G. penetrans* are in agreement with previous studies on cytotoxicity at concentrations

>100 µg/mL. The IC<sub>50</sub> value obtained for *G. junonius* are also similar to previous studies (<60 µg/mL).

Doskocil et al. (2016) studied the cytotoxicity of 27 polypore species' ethanol extracts, including *P. cinnabarinus*. The *P. cinnabarinus* extract showed cytotoxicity against two colon epithelial cell lines, CaCo-2 and HT-29, at IC<sub>50</sub> values of 81 and 31 µg/mL, respectively (Doskocil et al., 2016). A study by Ren et al. (2006) investigated the petroleum ether, ethyl acetate and methanol extracts of *P. sanguineus* against human hepatoma and HeLa cell lines. All extracts had IC<sub>50</sub> values <60 µg/mL against human hepatoma and HeLa cell lines (Ren et al., 2006). The phytochemical screening of *P. sanguineus* showed the presence of fats, steroids, terpenoids and glycosides which were possibly responsible for the cytotoxic activity (Ren et al., 2006). *P. sanguineus* inhibited the growth of renal (TK-10), breast (MCF-7) and melanoma (UACC-62) cancer cell lines at 10 µg/mL (Rosa et al., 2009). An ethanol extract of *P. sanguineus* showed cytotoxicity against HeLa, HT-29, MCF-7, MIA PaCa-2 and PC-3 cells at IC<sub>50</sub> values of 24.2, 48.1, 32.7, <10, and 28.6 µg/mL, respectively (Boukes et al., 2017). The results obtained in this study for an ethanol extract of *P. sanguineus*, with an IC<sub>50</sub> value of 7.42 µg/mL, fall within ranges observed in previous studies.

Cisplatin was used as a positive control for all the experiments carried out in this chapter. Cisplatin is activated by hydrolysis once it enters the cell, forming an active electrophile that interacts with proteins, DNA and RNA. The toxic effects of cisplatin are primarily due to the formation of DNA intrastrand and interstrand crosslinks and other non-functional adducts. Cisplatin causes cell death by damaging DNA, inhibiting DNA synthesis and mitosis, and inducing apoptosis (Dasari and Tchounwou, 2014; Hassan et al., 2014). Cisplatin and carboplatin are platinum based treatments that are used for the treatment of lung cancer. Although cisplatin displays strong anti-tumour activity, its use can cause several damaging side effects such as vomiting, nausea and renal toxicity (Dasari and Tchounwou, 2014).

The macrofungal extracts were screened against MRC5 lung fibroblasts to determine if cytotoxicity was specific towards A549 lung cancer cells (Figure 3.7). The macrofungal extracts inhibited growth at IC<sub>50</sub> concentrations of 158.3, 141.2, >100,

110.4 and 156.2  $\mu\text{g/mL}$  for *G. junonius*, *P. sanguineus*, *P. baudonii*, *F. lilacinogilva* and cisplatin, respectively. Table 3.2 summarises the selectivity indices of the macrofungal extracts tested against the A549 cancer and MRC5 non-cancerous cell lines. Literature suggests that a selectivity index greater or equal to 2.0 is a good selectivity index (Suffness and Pezutto, 1990; Bézivin et al., 2003). The selectivity index is a value that relates to the preference of a compound to a specific target. For example, if the selectivity is 2.0, the compound is twice more cytotoxic to the cancerous cell line than the non-cancerous/normal cell line. Treatments with *G. junonius* and *P. sanguineus* had the highest selectivity indices of 2.8 and 19.1, respectively. These findings are encouraging as the macrofungal extracts show preferential cytotoxicity towards lung cancer cells, and may show promise for the development of anti-cancer drugs. *F. lilacinogilva* and *P. baudonii* had selectivity indices of 1.6 and 1.9, respectively. These macrofungal extracts show a higher possibility of causing cytotoxicity in normal cells.

The inhibition of cell proliferation may be caused by either DNA cell cycle arrest or the induction of apoptosis. Cell cycle arrest has been regarded as one of the most important targets for cancer treatment. This is due to the unrestrained proliferation of cancer cells due to gene mutations (Choi and Kim, 2008). Therefore, many studies are searching for compounds that are able to induce cell cycle arrest and apoptosis. To determine the effect of the macrofungal extracts on the distribution of cells in the cell cycle, DNA cell cycle analysis was performed. Cells were exposed to the extracts for 24 and 48 h (Figure 3.8). The results obtained suggest that after 48 h, *P. sanguineus*, *P. baudonii* and the positive control, cisplatin, blocked proliferation of A549 cells by arresting the cells in the G2 phase of the cell cycle. *G. junonius* and *F. lilacinogilva* showed arrest of cells in the G2/M phase and early M phase of the cell cycle, respectively. Bhattarai et al. (2012) showed that a lanostane triterpene glycoside (fomitocide-K), isolated from *F. nigra*, induced apoptosis in human oral squamous cell carcinoma (YD-10B), and caused cell cycle arrest in the G1 phase (Bhattarai et al., 2012). A chloroform extract of *F. pinicola* induced G1 phase arrest in colorectal cancer cells (Wang et al., 2014b). The crude extracts of macrofungi contain a diversity of compounds that have different interactions with cancer cells and may also induce effects at multiple sites.

It is known that cancer cells contain several mutations that disrupt cell cycle checkpoint systems. The G2 checkpoint is activated in response to DNA damage to prevent damaged cells from entering mitosis (Vermeulen et al., 2003). During the G2/M checkpoint cells can either repair the damage or permanently arrest growth if the damage is too severe. If cell cycle arrest is permanent, cell death pathways such as apoptosis and necrosis are induced (Mollah, et al., 2012). Cyclin B-dependent kinase activity (CDK1-cyclin B) is required for the progression of cells into the M phase of the cell cycle. If DNA damage is detected, CDK1 activation is inhibited. ATM-dependent activation of the protein kinases, Chk1 and Chk2, causes the phosphorylation of Cdc25. This in turn inhibits the activity of Cdc25 and promotes its binding to proteins. This leads to sequestering of Cdc25 outside the nucleus, preventing it from activating CDK1-cyclin B and cell cycle arrest in the G2/M phase. The G2/M checkpoint is also regulated by p53 (Vermeulen et al., 2003).

The checkpoint in mitosis is referred to as the spindle checkpoint and ensures that the chromosomes are correctly segregated. The signal is generated by the kinetochore, a multiprotein subunit found on the centromere that facilitate the correct attachment to the mitotic spindle. The cohesion protein, Scc1, holds the chromatids together and prevents their segregation. The cohesion protein is degraded by a separase protease (Esp1) which in turn is inactivated by a securin protein (Pds1). Chromosomal separation is initiated by the degradation of the securing protein by the APC-Cdc20 complex allowing progression to anaphase. The precise mechanism by which the checkpoint inhibits the activity of the APC-Cdc20 complex is still unclear. It is suggested that the Mitotic Checkpoint Complex prevent the activation of the APC-Cdc20 complex by competitive binding or phosphorylation (Doncic et al., 2005). The occurrence of spindle defects can activate the mitotic-damage checkpoint that can induce mitotic catastrophe. Mitotic catastrophe (MC) is a form of cell death with the characteristic feature of multinucleated cells. Studies suggest that MC may occur prior to apoptosis or necrosis (Vakifahmetoglu et al., 2008). Several studies also propose that G2/M arrest induced by anticancer drugs might be due to the disruption of microtubule dynamics causing mitotic arrest beyond the G2 checkpoint (Jiang et al., 2008).

*P. sanguineus*, *P. baudonii* and cisplatin caused DNA damage by inducing G2 phase arrest, possibly targeting the G2/M arrest pathway. *F. lilacinogilva* induced mainly M phase arrest, suggesting the extract influenced spindle formation and segregation of chromosomes. *G. junonius* significantly increased both G2 and M phase arrest; hence further investigation is required to determine if cell cycle arrest occurred in both these phases, or G2 or M phase alone. Further investigation is required to confirm cell cycle arrest of A549 cancer cells in their respective growth phases by determining regulatory proteins expressed in each phase. Fluorescence microscopy can also be conducted to determine if disruption occurred during spindle formation. The possibility of mitotic catastrophe must also be investigated. Pachymic acid, isolated from *F. pinicola*, inhibits cell growth and induces cell cycle arrest in the G1 phase. Pachymic acid also inhibits cell migration, invasion and downregulates the Akt/ERK signalling pathways in human gallbladder carcinoma cells (GBC-SD) (Chen et al., 2015)

To further elucidate the ability of macrofungal extracts to induce apoptosis, Annexin V-FITC/PI dual staining was performed. The translocation of PS from the inner to the outer leaflet is an indication of early apoptosis and detected using Annexin V; hence it is used as a biomarker for apoptosis. A cell population that is stained positively with annexin V-FITC and negatively with PI is considered early apoptotic, whereas a cell population that is stained positively with both annexin V-FITC and PI is considered late apoptotic/necrotic. The results obtained showed that constant exposure to the macrofungal extracts induced apoptosis in a concentration and time dependent manner. As depicted in Figure 3.9, *F. lilacinogilva*, *G. junonius*, *P. sanguineus* and the positive control, cisplatin, exhibited significant increases in apoptotic and late apoptotic/necrotic cell populations. Treatment of A549 cells with the aqueous extract of *P. baudonii* led to significant increases in late apoptotic/necrotic and necrotic cell populations. The substantial increase in late apoptotic/necrotic cells was interpreted to be apoptotic rather than necrotic. A significant increase in apoptosis was also observed during cell cycle arrest, when the Annexin V-FITC apoptotic marker was included. *P. baudonii* and *F. lilacinogilva* had the highest percentage of cells stained Annexin-V positive and PI negative (early apoptosis) after 24 h treatment. *G. junonius*, *P. sanguineus* and cisplatin induced apoptosis at a slower rate compared to *P. baudonii* and *F. lilacinogilva*. Increases in apoptotic cells were only evident after 48 h treatment. This implies that the crude extracts could induce apoptosis at different rates

due to varying concentrations of active compounds, or that the compounds function by different pathways. A similar trend was observed in the results obtained from the cell cycle (Figure 3.8) for the percentage apoptotic cells after 24 and 48 h treatment.

Targeting the actin cytoskeleton may provide an alternative chemotherapeutic option for cancer therapy as this could interfere with the proliferation, invasion and migration of cancer cells. Several attempts have been made to target the cytoskeleton, but it remains unsuccessful due to toxicity and the inability to discriminate between the actin filaments of cancerous and non-cancerous cells. This has changed the focus to identify agents targeting the actin regulatory proteins that are specifically expressed in cancerous cells (Stehn et al., 2017). Agents disrupting the actin cytoskeleton cause changes in the cellular structure and prevent the cells from dividing (cytokinesis). The cells are still able to initiate mitotic events leading to enlarged and multinucleated cells (Hermenean and Ardelean, 2017). A study by Lee and Song (2007) suggests the presence of an actin checkpoint pathway at the G2/M transition causing mitotic delay. The actin and proteins that function in the polymerization of actin can also be cleaved by caspases during the execution phase of apoptosis. However, evidence suggests that the disruption of the cytoskeletal structure and proteins can induce apoptosis (White et al., 2001; Park et al., 2007). The untreated A549 cells showed dense actin filaments with long fibres distributed in the cells. Treatment with the macrofungal extracts caused a decrease in polymerized actin filaments (Figure 2.10). Some of the cells became rounded, showing loss of cytoskeletal structure. *G. junonius*, *P. sanguineus* and *F. lilacinogilva* induced micro- and multinucleation, whereas *P. baudonii* induced multinucleation only. The presence of multinucleated A549 cells were seen after macrofungal treatment which could indicate the induction of mitotic catastrophe (Vakifahmetoglu et al., 2008). The results obtained support the occurrence of cytoskeletal disruption in A549 cells treated with macrofungal extracts.

The morphological features of apoptosis induced by macrofungal extracts were confirmed by AO staining (Figure 3.13 and 3.14). Cells treated for 48 h with the macrofungi's IC<sub>50</sub> concentrations showed chromatin condensation, shrinkage, rounding of cells and plasma membrane blebbing. These features confirm the apoptosis-inducing properties of *G. junonius*, *P. sanguineus*, *P. baudonii* and *F. lilacinogilva*.

The activation of caspases is a key biochemical feature that occurs in tumour cells undergoing apoptosis. Caspase signalling is initiated by either intracellular or extracellular signals that progress through proteolytic autocatalysis causing the activation of effector caspases that cleave various substrates. Apoptosis occurs through the mitochondrial- or death receptor pathways, however both these pathways converge and activates caspase-3. It is also known that the extrinsic pathway can influence the intrinsic pathway and amplify the signal. Caspase-3 activation has been identified to be partially or completely responsible for the cleavage of several proteins resulting in the morphological characteristic of apoptosis. The activation of caspase-3 has also been identified as a key point in apoptosis that is irreversible (Elmore, 2007; McIlwain et al., 2013).

To obtain further insight into the action of macrofungal extracts and their apoptotic-inducing activity on A549 cells, the activity of caspase-3 and -8 was investigated (Figure 3.11 and 3.12). Caspase-8 was used as a marker for the extrinsic pathway and caspase -3 as a general marker for the induction of apoptosis. Results showed that *P. sanguineus*, *P. baudonii* and *F. lilacinogilva* activated both caspase-3 and -8 after 24 and 48 h. The percentage activated caspase-3 was higher at 24 h for *P. baudonii* and *F. lilacinogilva* compared to caspase-8. As mentioned above, caspase-8 is an initiator caspase in the extrinsic pathway which would be activated early during apoptosis. Caspase-3 is an effector caspase for both the intrinsic and extrinsic pathways. The higher activity of caspase-3 at 24 h indicates that apoptosis is also activated by the intrinsic pathway. The activation of the intrinsic pathway would lead to the activation of caspase-3 by the effector caspase-9 and would explain the higher caspase-3 percentage. The results obtained suggest that both the intrinsic and extrinsic pathways were activated which will promote the activity of caspase-3, as seen after 48 h (Figure 3.12). This dual activation can be a result of different compounds found in the crude macrofungal extracts. *P. sanguineus* did not show a difference in the levels of caspase-3 and -8, and therefore require further investigation to determine if both pathways were activated. Fomitoid-K, isolated from *F. nigra*, is a lanostane triterpene glycoside (Lee et al., 2012). A study by Bhattarai et al. (2012) have shown that this triterpene induces apoptosis via the mitochondrial signalling pathway and causes accumulation of reactive oxygen species (ROS) in human oral squamous cell carcinoma cells (YD-10B; Bhattarai et al., 2012). Cinnabarinic acid (30  $\mu$ M) induces

apoptosis in mouse thymocytes by the loss of mitochondrial membrane potential, caspase-3 activation and the production of ROS (Hiramatsu et al., 2008). *G. junonius* showed a slight increase in caspase-3 after 48 h, while caspase-8 remained relatively constant compared to the untreated control. Further investigation is required to confirm whether the extract induced caspase-3 and therefore the intrinsic pathway of apoptosis.

In conclusion, the study demonstrated that several South African macrofungal extracts significantly inhibited A549 cancer cell proliferation by means of cell cycle arrest and the induction of apoptosis. The data obtained suggest that the macrofungal extracts induced apoptosis via caspase-3 dependent cell death. This would involve the activation of both the mitochondrial and death receptor pathways. The induction of apoptosis was confirmed by several morphological features such as chromatin condensation, nuclear fragmentation, cell shrinkage, membrane blebbing and loss of cytoskeletal arrangement. Therefore, the crude macrofungal extracts may contain promising compounds for cancer treatment. The induction of cell death is a complex and intricate network and therefore requires further investigation in order to determine the complete mechanism of action in which cell cycle arrest and the induction of apoptosis occur.



## CHAPTER FOUR

### CONCLUSIONS

#### 4.1. THE RESEARCH IN PERSPECTIVE

The present study screened 21 South African macrofungal species for their antimicrobial activity against selected Gram-positive and Gram-negative respiratory pathogens. Cytotoxic properties of the macrofungal spp. and the mechanism of action against lung cancer were also investigated.

Growth inhibition by macrofungal extracts (ethanol/ aqueous) was observed for *S. pneumoniae*, *S. pyogenes* and *S. aureus*, while there was no inhibition of *P. aeruginosa* and *K. pneumoniae*. The Gram-positive bacteria were more susceptible to the macrofungal extracts, which could be due to the lack of a cell envelope rendering the cells more permeable and susceptible to compounds and drugs. Production of biologically active compounds is influenced by multiple environmental factors, scientific method and the use of dissimilar bacterial strains with different susceptibility patterns, which may account for the contrasting reports on antimicrobial activities of macrofungi. The effect of extracts on structural changes of bacterial cells was also investigated using TEM. After 8 h of treatment, *S. aureus*, *S. pneumoniae* and *S. pyogenes* cells showed membrane damage and cellular leakage was observed in *S. aureus* treated cells. This suggests that the extracts act on the membrane by potentially forming pores, however no distinct conclusion can be drawn and the mechanism of action requires further investigation.

Minimal research has been performed on the antitubercular activity of macrofungal species, especially the species included in this study. Several macrofungal spp. inhibited *M. tuberculosis* growth, including *L. sulphureus*, *P. baudonii*, *G. penetrans*, *A. campestris* and *C. molybdites*. This should be further explored to isolate and identify active compounds that can be used as scaffolds for drug development.

Due to the co-infection of many HIV patients with TB and the numerous disadvantages of antiretroviral treatment, the macrofungal extracts were also screened for inhibitory

effects of certain HIV-1 enzymes. It is well documented that macrofungal spp. contain compounds that inhibit various viruses including the HIV-1 virus by affecting various stages of their life cycle. The macrofungal spp. did not show any significant effect on HIV-1 reverse transcriptase. *P. baudonii*, *P. papilionaceus* and *H. erinaceus* showed slight inhibitory activity of HIV-1 RT. *C. molybdites* showed significant inhibition of HIV-1 protease activity with an IC<sub>50</sub> value of 49.7 µg/mL. The ethanol extracts of *C. molybdites* require further investigation to determine its *in vivo* potential.

The investigation of the cytotoxic properties of macrofungi and their potential mechanism of action revealed that the ethanol extracts of *F. lilacinogilva*, *P. sanguineus* and *G. junonius* as well as the aqueous extract of *P. baudonii* were cytotoxic to A549 lung cancer cells. Dose-response analysis against the control cell line, MRC5, showed that the macrofungal extracts were not cytotoxic up to a concentration of 100 µg/mL and higher. The mechanism in which the macrofungal extracts induces cytotoxicity focussed on cell cycle arrest and the induction of apoptosis. Observations of cellular arrest in the G2 phase were noted after treatments with *P. sanguineus* and *P. baudonii*, whereas G2/M and early M phase arrest were observed for *G. junonius* and *F. lilacinogilva* treated cells, respectively.

The mode of cell death revealed signs of apoptosis, including phosphatidylserine translocation, chromatin condensation, membrane blebbing and loss of cytoskeletal structure. *P. sanguineus*, *P. baudonii* and *F. lilacinogilva* activated both the intrinsic and extrinsic apoptotic pathways and this was confirmed by the significant increase in both caspase-8 and -3 levels. *G. junonius* showed increased activation of caspase-3 only, and therefore may induce the intrinsic pathway. Further investigation is required in order to elucidate the complete pathway in which the macrofungal extracts induce apoptosis in A549 lung cancer cells.

Relating and comparing the cytotoxicity results to the antibacterial activity of the macrofungal spp. investigated, it was evident that the ethanolic extracts with cytotoxic activity also exhibited the highest antimicrobial activity against *S. pneumoniae* and *S. pyogenes* (MICs: 31.5 – 250 µg/mL). The aqueous extract of *P. baudonii* with cytotoxic activity against A549 cells showed weak antimicrobial activity against *S.*

*pneumoniae* and *S. pyogenes* (MICs: 2 000µg/mL). This might be of interest as the compounds conferring activity might differ and therefore requires further investigation.

Throughout this study, notable differences were observed between the ethanol and aqueous extracts of the macrofungal spp., with the former being more effective in inhibiting microbial growth and cytotoxic against lung cancer cells. Conclusions on the potential compound/s that confer these activities cannot be made as this is influenced by environmental conditions and extraction methods employed. Several active compounds have been documented in literature such as proteins, polysaccharides, lipids, terpenoids, polyphenols, sesquiterpenes, and several others, however this is only an indication and isolation and identification of compounds in active macrofungal spp. in this study are required.

#### **4.2. POTENTIAL FOR FUTURE DEVELOPMENT OF THE WORK**

There are various aspects of this study that can be reviewed and expanded on for future work. The antimicrobial potential of macrofungi against Gram-positive bacteria can be further investigated to determine their mechanism of action. There are a variety of techniques that can be used to assess the effects of extracts on cellular function and morphology. As membrane damage and cellular leakage were observed in treated cells, the leakage of intracellular potassium can be measured as it is considered to be an early indication of membrane disruption (Bouhdid et al., 2009). The loss of membrane potential and respiratory enzymes can be assessed using bis-oxonol dye and 5-cyano-2,3-ditoyl tetrazolium chloride (CTC), respectively (Bouhdid et al., 2009). Scanning electron microscopy can also be performed to determine if morphological changes occurred.

The extracts exhibiting anti-TB activity should be further investigated to determine their toxicity on human cells and to determine their *in vivo* potential. As the drugs administered by a patient will be detoxified by the liver and kidneys, it would be interesting to determine whether the extracts would have any toxic effects against liver and kidney cells (Chang/HepG cells and Vero cells). This would provide an indication at what concentration the extract could be administered without damaging the liver

and kidneys. It would also be interesting to investigate if the active extracts have any synergistic, antagonistic or additive effects as current TB treatment involves the use of multiple drugs. Further anti-TB research on the macrofungal extracts could include the isolation and identification of active compounds and to determine their mechanism of action, whether it might target specific enzymes or inhibit protein or DNA synthesis. The inhibitory effect on other *Mycobacterium* spp. could also be investigated as well as resistant strains.

For the detection of anti-HIV activity by macrofungal spp., the focus was on the enzymes reverse transcriptase and protease, as they are crucial for the replication of HIV-1. Testing of the macrofungal extracts on other enzymes in the HIV-1 life cycle would be valuable (i.e. HIV-1 integrase) to provide insight into possible novel HIV-1 agents. It would also be beneficial to determine the bioactive agent/s produced by macrofungi, which are responsible for the inhibitory activity against HIV-1 RT and protease.

The induction of cell death is a complex and multifaceted network and therefore requires further investigation in order to determine the complete mechanism of action. Future analysis can include DNA fragmentation, mitochondrial membrane potential analysis, cytochrome *c* release and reactive oxygen species (ROS) generation. The expression of genes involved in apoptosis can also be analysed by Western blotting (i.e. BAX, Bcl-2, PARP,  $\beta$  actin, Fas, TRAIL).

In conclusion, this study shows the biological activities of South African macrofungal spp. against human bacterial and viral pathogens as well as lung cancer and their potential mechanisms of action. Although the results obtained look promising, the human system is complex and the observations made *in vitro* may not be the same as *in vivo*. Therefore, in order to ascertain whether the macrofungal extracts have any physiological promise, *in vivo* studies must be conducted.

## REFERENCES

**Africa Check.** 2016. *FACTSHEET: The leading causes of death in Africa - Africa Check.* [online] Available at: <https://africacheck.org/factsheets/factsheet-the-leading-causes-of-death-in-africa/> [Accessed 14 Nov. 2016].

**Algiannis, N., Kalpotzakis, E., Mitaku, S., and Chinou, I.B.** 2001. Composition and Antimicrobial Activity of Essential Oils of Two *Origanum* Species. *Journal of Agricultural and Food Chemistry.* **49:** 4168-4170

**Alshatwi, A.A., Ramesh, E., Periasamy, V.S., and Subash-Babu, P.** 2012. The apoptotic effect of hesperetin on human cervical cancer cells is mediated through cell cycle arrest, death receptor, and mitochondrial pathways. *Fundamental & Clinical Pharmacology.* doi: 10.1111/j.1472-8206.2012.01061.x

**Altuner, E.M. and Akata, I.** 2010. Antimicrobial activity of some macrofungi extracts. *SAU. Fen Bilimleri Dergisi.* **14:** 45-49

**Alves, M.J., Ferreira, I.C.F.R., Dias, J., Teixeira, V., Martins, A., and Pintado, M.** 2012a. A Review on Antimicrobial Activity of Mushroom (Basidiomycetes) Extracts and Isolated Compounds. *Planta Medica.* **78:** 1707-1718

**Alves, M.J., Ferreira, I.C.F.R., Martins, A., and Pintado, M.** 2012b. Antimicrobial activity of wild mushroom extracts against clinical isolates resistant to different antibiotics. *Journal of Applied Microbiology.* **113:** 466-475

**Amaral, L., Martins, M., and Viveiros, M.** 2007. Enhanced killing of intracellular multidrug-resistant *Mycobacterium tuberculosis* by compounds that affect the activity of efflux pumps. *Journal of Antimicrobial Chemotherapy.* **59:** 1237-1246

**Ameri, A., Ghadge, C., Vaidya, J.G., and Deokule, S.S.** 2011. Anti-Staphylococcus aureus activity of *Pisolithus albus* from Pune, India. *Journal of Medicinal Plants Research.* **5:** 527-532

**Andrew, E.E., Kinge, T.R., Tabi, E.M., Thiobal, N., and Mih, A.M.** 2013. Diversity and distribution of macrofungi (mushrooms) in the Mount Cameroon Region. *Journal of Ecology and the Natural Environment.* **5:** 318-334

**Arora, S. and Tandon, S.,** 2014. DNA fragmentation and cell cycle arrest: a hallmark of apoptosis induced by *Ruta graveolens* in human colon cancer cells. *Homeopathy.* **104:** 36-47

**Badalyan, S.** 2012. Medicinal aspects of edible ectomycorrhizal mushrooms, *Edible Ectomycorrhizal Mushrooms*, Zambonelli, A. and Bonito, G.M. (Ed.), doi: 10.1007/978-3-642-33823-6\_18. Springer, Berlin, Germany pp. 317–34

**Badmus, J.A., Ekpo, O.E., Hussein, A.A., Meyer, M., and Hiss, D.C.** 2015. Antiproliferative and Apoptosis Induction Potential of the Methanolic Leaf Extract of *Holarrhena floribunda* (G. Don). *Evidence-Based Complementary and Alternative Medicine*. 2015:756482. doi:10.1155/2015/756482

**Bala, N., Aitken, E.A.B., Fechner, N., Cusack, A., and Steadman, K.J.** 2011. Evaluation of antibacterial activity of Australian basidiomycetous macrofungi using a high-throughput 96-well plate assay. *Pharmaceutical Biology*. **49**: 492-500.

**Bala, N., Aitken, E.A.B., Cusack, A., and Steadman, K.J.** 2012. Antimicrobial Potential of Australian Macrofungi Extracts Against Foodborne and Other Pathogens. *Phytotherapy Research* **26**: 465-469

**Bean, P.** 2005. New Drug Targets for HIV. *Clinical Infectious Diseases*. **41**: S96-100

**Beattie, K.D., Rouf, R., Gander, L., May, T.W., Ratkowsky, Donner, C.D., Gill, M., Grice, I.D., and Tiralongo, E.** 2010. Antimicrobial metabolites from Australian macrofungi from the genus *Cortinarius*. *Phytochemistry*. **71**: 948-955

**Bessong, P.O., Obi, C.L., Andréola, M., Rojas, L.B., Pouységu, L., Igumbor, E., Meyer, J.J.M., Quideau, S., and Litvak, S.** 2005. Evaluation of selected South African medicinal plants for inhibitory properties against human immunodeficiency virus type 1 reverse transcriptase and integrase. *Journal of Ethnopharmacology*. **99**: 83-91

**Bézivin, C., Tomasi, F., Lohézie-Le, D., and Boustie, J.,** 2003. Cytotoxic activity of some lichen extracts on murine and human cancer cell lines. *Phytomedicine*. **10**: 499–503.

**Bhattarai, C., Lee, Y., Lee, N., Yun, B., Hwang, P., and Yi, H.** 2012. Fomitoside-K from *Fomitopsis nigra* Induces Apoptosis of Human Oral Squamous Cell Carcinomas (YD-10B) via Mitochondrial Signaling Pathway. *Biological and Pharmaceutical Bulletin*. **35**: 1711-1719

**Bosch, A.A.T.M., Biesbroek, G., Trzcinski, K., Sanders, E.A.M., and Bogaert, D.** 2013. Viral and Bacterial Interactions in the Upper Respiratory Tract. *PLoS Pathogens*. **9**:e1003057. <https://doi.org/10.1371/journal.ppat.1003057>

**Bouhdid, S., Abrini, J., Zhiri, A., Espuny, M.J., and Manresa, A.** 2009. Investigation of functional and morphological changes in *Pseudomonas aeruginosa* and *Staphylococcus aureus* cells induced by *Origanum compactum* essential oils. *Journal of Applied Microbiology*. **106**: 1558-1568

- Boukes, G.J., Koekemoer, T.C., van de Venter, M., and Govender, S.** 2017. Cytotoxicity of thirteen South African macrofungal species against five cancer cell lines. *South African Journal of Botany*. **113**: 62-67
- Branch, M.** 2001. First Field Guide to Mushrooms of Southern Africa. Random House Struik (Pty) Ltd, Cape Town, South Africa 57 pp.
- Brink, A.J.** 2008. Updated guideline for the management of upper respiratory tract infections in South Africa: 2008. *Southern African Journal of Epidemiology and Infection*. **23**: 27-40
- Carrol, K.C.** 2002. Laboratory Diagnosis of Lower Respiratory Tract Infections: Controversy and Conundrums. *Journal of Clinical Microbiology*. **40**: 3155-3120
- Chaabane, W., User, S.D., El-Gazzah, M., Jaksik, R., Sajjadi, E., Rzeszowska-Wolny, J., and Los, M.J.** 2013. Autophagy, Apoptosis, Mitoptosis and Necrosis: Interdependence between Those Pathways and Effects on Cancer. *Archivum Immunologiae et Therapia Experimentalis*. **61**: 43-58
- Chazotte, B.** 2010. Labeling Cytoskeletal F-Actin with Rhodamine Phalloidin or Fluorescein Phalloidin for Imaging. *Cold Spring Harbor Protocols*. doi:10.1101/pdb.prot4947
- Chen, Y., Lian, P., Liu, Y., and Xu, K.** 2015. Pachymic acid inhibits tumorigenesis in gallbladder carcinoma cells. *International Journal of Clinical and Experimental Medicine*. **8**: 17781–17788
- Choi, D., Park, S., Ding, J., and Cha, W.** 2007. Effects of *Fomitopsis pinicola* Extracts on Antioxidant and Antitumor activities. *Biotechnology and Bioprocess Engineering*. **12**: 516-524
- Choi, E.U. and Kim, T.** 2008. Equol induced apoptosis via cell cycle arrest in human breast cancer MDA-MB-453 but not MCF-7 cells. *Molecular Medicine Reports*. **1**: 239-244
- Chowdhury, M.M.H., Kubra, K., and Ahmed, S.R.** 2015. Screening of antimicrobial, antioxidant properties and bioactive compounds of some edible mushrooms cultivated in Bangladesh. *Annals of Clinical Microbiology and Antimicrobials*. **14**: 1-6
- Collins, K., Jacks, T., Pavletich, N.P.** 1997. The cell cycle and cancer. *Proceedings of the National Academy of Sciences*. **94**: 2776-2778.
- Collins L.A. and S.G. Franzblau.** 1997. Microplate Alamar Blue Assay versus BACTEC 460 system for High-Throughput screening of Compounds against *Mycobacterium tuberculosis* and *Mycobacterium avium*. *Antimicrob Agents Ch.* **41**: 1004-1009

**Craig, A., Mai, J., Cai, S., and Jeyaseelan, S.** 2009. Neutrophil Recruitment to the Lungs during Bacterial Pneumonia. *Infection and Immunity*. **77**: 568-575

**Crothers, K., Thompson, B.W., Burkhardt, K., Morris, A., Flores, S.C., Diaz, P.T., Chaisson, R.E., Kirk, G.D., Rom, W.N., and Huang, L.** 2011. HIV-Associated Lung Infections and Complications in the Era of Combination Antiretroviral Therapy. *Proceedings of the American Thoracic Society*. **8**: 275-81

**Darzynkiewicz, Z.** 2010. Critical Aspects in Analysis of Cellular DNA Content. *Current Protocols in Cytometry*. doi:10.1002/0471142956.cy0702s52.

**Dasari, S. and Tchounwou, P.B.** 2014. Cisplatin in cancer therapy: molecular mechanisms of action. *European Journal of Pharmacology*. **5**: 364-378

**Demchenko, A.P.** 2013. Beyond annexin V: fluorescence response of cellular membranes to apoptosis. *Cytotechnology*. **65**: 157-172

**De Silva, D.D., Rapior, S., Fons, F., Bahkali, A.H., and Hyde, K.D.** 2012. Medicinal mushrooms in supportive cancer therapies: an approach to anti-cancer effects and putative mechanisms of action. *Fungal Diversity*. **55**: 1-35

**De Silva, D.D., Rapior, S., Sudarman, E., Stadler, M., Xu, J., Alias, S.A., Hyde, K.D.** 2013. Biological metabolites from macrofungi: ethnopharmacology, biological activities and chemistry. *Fungal Diversity*. **62**: 1-40

**Dias, D.A., Urban, S., and Roessner, U.** 2012. A Historical Overview of Natural Products in Drug Discovery. *Metabolites*. **2**: 303-306

**Dimitrijevic, M., Jovanovic, V.S., Cvetkovic, J., Mihajilov-krstev, T., Stojanovic, G., and Mitic, V.** 2015. Screening of antioxidant, antimicrobial and antiradical activities of twelve selected Serbian wild mushrooms. *Analytical methods*. DOI: 10.1039/c4ay03011g

**Doğan, H.H., Duman, R., Özkalp, B., and Aydin, S.** 2013. Antimicrobial activities of some mushrooms in Turkey. *Pharmaceutical Biology*. **51**:707-711

**Doncic, A., Ben-Jacob, E., and Barkai, N.** 2005. Evaluating putative mechanisms of the mitotic spindle checkpoint. *Proceedings of the National Academy of Sciences*. **102**: 6332-6337



- Doskocil, I., Havlik, J., Verlotta, R., Tauchen, J., Vesela, L., Macakova, K., Opletal, L., Kokoska, L., and Rada, V.** 2016. *In vitro* immunomodulatory activity, cytotoxicity and chemistry of some central European polypores. *Pharmaceutical Biology*. **54**: 2369-2376
- Duprez, L., Wirawan, E., Vanden Berghe, T., and Vandenabeele, P.** 2009. Major cell death pathways at a glance. *Microbes and Infection*. **11**: 1050-1062
- El Dine, R., El Halawany, A.M., Ma, C., and Hattori, M.** 2008. Anti-HIV-1 Protease Activity of Lanostane Triterpenes from the Vietnamese Mushroom *Ganoderma colossum*. *Journal of Natural Products*. **71**: 1022-1026.
- El-Mekawy, S., Meselhy, M.R., Nakamura, N., Tezuka, Y., Hattori, M., Kakiuchib, N., Shimotohno, K., Kawahata, T., and Otakec, T.** 1998. Anti-HIV-1 and anti-HIV-1-protease substances from *Ganoderma lucidum*. *Phytochemistry*. **49**: 1651-1657
- Elmore, S.** 2007. Apoptosis: A Review of Programmed Cell Death. *Toxicology Pathology*. **35**: 495–516.
- Eloff, J.N.** 1998. A Sensitive and Quick Microplate Method to Determine the Minimal Inhibitory Concentration of Plant Extracts for Bacteria. *Planta Medica*. **64**: 711-713
- Enshasy, H.E., Elsayed E.A., Aziz, R., and Wadaan, M.A.** 2013. Mushrooms and Truffles: Historical Biofactories for Complementary Medicine in Africa and in the Middle East. *Evidence-Based Complementary and Alternative Medicine*. 2013:620451. doi:10.1155/2013/620451
- Eroğlu, C., Seçme, M., Atmaca, P., Kaygusuz, O., Gezer, K., Bağcı, G., and Dodurga, Y.** 2016. Extract of *Calvatia gigantea* inhibits proliferation of A549 human lung cancer cells. *Cytotechnology*. **68**: 2075-2081
- Fan, L., Pan, H., Socol, A.T., Pandey, A., and Socol, C.R.** 2006. Advances in Mushroom Research in the Last Decade. *Food Technology and Biotechnology*. **44**: 303-311
- Fernando, D., Adhikari, A., Nanayakkara, C., de Silva, E.D., Wijesundera, R., and Soysa, P.** 2016. Cytotoxic effects of ergone, a compound isolated from *Fulviformes fastuosus*. *BMC Complementary & Alternative Medicine*. **16**: 1-11
- Ferreira, C.G., Epping, M., Kruyt, F.A.E., and Giaccone, G.** 2002. Apoptosis: Target of Cancer Therapy. *Clinical Cancer Research*. **8**: 2024-2034
- Francis, S.L. and Antonipillai, J.** 2017. Cytoskeletal Molecules Play a Major Role in Cancer Progression. *Insights in Bionedecine*. **2**: 1-3

**Franzblau, S.H., Witzig, R.S., McLaughlin, J.C., Torres, P., Madico, G., Hernandez, A., Degnan, M.T., Cook, M.B., Quenzer, V.K., Ferguson, R.M., and Gilman, R.H.** 1998. Rapid, Low-Technology MIC determination with Clinical Mycobacterium Tuberculosis Isolates by Using the Microplate Alamar Blue Assay. *Journal of Clinical Microbiology*. **36**: 362-366.

**Garrett, M.D.** 2001. Cell cycle control and cancer. *Current Science*. **81**: 515-522

**Gérard, C. and Goldbeter, A.** 2014. The balance between cell cycle arrest and cell proliferation: control by the extracellular matrix and by contact inhibition. *Interface Focus*. **4**: 1-13

**Gryzenhout, M.** 2010. Mushrooms of South Africa. Random House Struik (Pty) Ltd, Cape Town, South Africa 144 pp.

**Hanahan, D. and Weinberg, R.A.** 2011. Hallmarks of Cancer: The Next Generation. *Cell*. **144**: 646-674

**Hassan, M., Watari, H., AbuAlmaaty, A., Ohba, Y., and Sakuragi, N.** 2014. Apoptosis and Molecular Targeting Therapy in Cancer. *BioMed Research International*. doi:10.1155/2014/150845

**Hassanpour, S.H. and Dehghani, M.** 2017. Review of cancer from perspective of molecular. *Journal of Cancer Research and Practice*. **4**: 127-129

**Hermenean, A. and Ardelean, A.** 2017. Targeting the Cytoskeleton with Plant-Bioactive Compounds in Cancer Therapy. Structure, Dynamics, Function and Disease, Dr. Jose C. Jimenez-Lopez (Ed.), InTech, DOI: 10.5772/66911. [Online]. Available: <https://www.intechopen.com/books/cytoskeleton-structure-dynamics-function-and-disease/targeting-the-cytoskeleton-with-plant-bioactive-compounds-in-cancer-therapy>

**Hibbett, D.S.** 2006. A phylogenetic overview of the Agaricomycotina. *Mycologia*. **98**: 917-925

**Hibbett, D.S. and Matheny, P.B.** 2009. The relative ages of ectomycorrhizal mushrooms and their plant hosts estimated using Bayesian relaxed molecular clock analyses. *BMC Biology*. **7**: 1-13

**Hiramatsu, R., Hara, T., Akimoto, H., Takikawa, O., Kawabe, T., Isobe, K., and Nagase, F.** 2008. Cinnabarinic acid generated from 3-hydroxyanthranilic acid strongly induces apoptosis in thymocytes through the generation of reactive oxygen species and the induction of caspase. *Journal of Cellular Biochemistry*. **103**: 42-53

**Hirata, Y. and Nakanishi, K.** 1950. Grifolin, an antibiotic from a Basidiomycete. *The Journal of Biological Chemistry*. **184**: 135-144

**Holst-Hansen, C. and Brünner, N.**, 1998. MTT-cell proliferation assay, in: Celis, J. E., (Ed.), *Cell biology: A laboratory handbook*, 2nd ed., Academic Press, San Diego, CA, pp. 16–18.

**Hubregtse, J.** 2017. Fungi In Australia, Rev. 2.0, E-published by the Field Naturalists Club of Victoria Inc., Blackburn, Victoria, Australia. [Online]. Available: <http://www.fncv.org.au/fungi-in-australia/>

**Hwang, C.H., Jaki, B.U., Klein, L.L., Lankin, D.C., McAlpine, J.B., Napolitano, J.G., Fryling, N.A., Franzblau, S.G., Cho, S.H., Stamets, P.E., Wang, Y., and Pauli, G.F.** 2013. Chlorinated coumarins from the polypore mushroom *Fomitopsis officinalis* and their activity against *Mycobacterium tuberculosis*. *Journal of Natural Products*. **76**: 1916-1922.

**Indran, I.R., Tufo, G., Pervaiz, S., and Brenner, C.** 2011. Recent advances in apoptosis, mitochondria and drug resistance in cancer cells. *Biochimica et Biophysica Acta*. **1807**: 735-745

**Isaka, M., Chinthanom, P., Sappan, M., Supothina, S., Vichai, V., Danwisetkanjana, K., Boonpratuang, T., Hyde, K.D., and Choeyklin, R.** 2017. Antitubercular Activity of Mycelium-Associated Ganoderma Lanostanoids. *Journal of Natural Products*. **80**: 1361-1369

**Jang, K., Han, M., Lee, B., Kim, B., Kim, C., Yoon, H., and Choi, Y.** 2010. Induction of Apoptosis by Ethanol Extracts of *Ganoderma lucidum* in Human Gastric Carcinoma Cells. *Journal of Acupuncture & Meridian Studies*. **3**: 24-31

**Jayat, C. and Ratinaud, M.** 1993. Cell cycle analysis by flow cytometry: Principles and applications. *Biology of the Cell*. **78**: 15-25

**Jiang, P.D., Zhao, Y.L., Shi, W., Deng, X.Q., Xie, G., and Mao, Y.Q.** et al. 2008 Cell Growth Inhibition, G2/M Cell Cycle Arrest, and Apoptosis Induced by Chloroquine in Human Breast Cancer Cell Line Bcap-37. *Cellular Physiology and Biochemistry*. **22**: 431-440

**Johnston, L.** 2012. Rational use of antibiotics in respiratory tract infections. *South African Pharmaceutical Journal*. **79**: 34-39

**Kalsbeek, D. and Golsteyn, R.M.** 2017. G2/M-Phase Checkpoint Adaptation and Micronuclei Formation as Mechanism That Contribute to Genomic Instability in Human Cells. *International Journal of Molecular Sciences*. **18**: 1-16

**Kalyoncu, F. Oskay, M., Saglam, H., Erdogan, T.F., and Tamer, U.** 2010. Antimicrobial and Antioxidant Activities of Mycelia of 10 Wild Mushroom Species. *Journal of Medicinal Food*. **13**: 415-419

**Karaman, M., Matavulj M., and Janjic, L.** 2012. Antibacterial Agents from Lignicolous Macrofungi. Antimicrobial Agents. Dr. Varaprasad Bobbarala (Ed.). ISBN: 978-95351-0723-1. *InTech*, DOI: 10.5772/33919. Pp. 361-386

**Kasibhatla, S. and Tseng, B.** 2003. Why Target Apoptosis in Cancer Treatment?. *Molecular Cancer Therapeutics*. **2**: 573-580

**Kim, S.H., Jakhar, R., and Kang, S.C.** 2015. Apoptotic properties of polysaccharide isolated from fruiting bodies of medicinal mushroom *Fomes fomentarius* in human lung carcinoma cell line. *Saudi Journal of Biological Sciences*. **22**: 484-490

**Kim, K.H., Choi, S.U., and Lee, K.R.** 2012. Gymnopilin K: a new cytotoxic gymnopilin from *Gymnopilus spectabilis*. *The Journal of Antibiotics*. **65**: 135-137

**Kirk, P.M., Cannon, P.F., David, J.C., and Stalpers, J.A.** 2001. Ainsworth and Bisby's Dictionary of the Fungi. 9th ed. Cambridge, United Kingdom: CAB International University Press.

**Klos, M., van de Venter, M., Milne, P.J., Traore, H.N., Meyer, and D., Oosthuizen, V.** 2009. *In vitro* anti-HIV activity of five selected South African medicinal plant extracts. *Journal of Ethnopharmacology*. **124**: 182-188

**Kocyigit, A., Koyuncu, I., Dikilitas, M., Bahadori, F., and Turkkan, B.** 2016. Cytotoxic, genotoxic and apoptotic effects of naringenin-oxime relative to naringenin on normal and cancer cell lines. *Asian Pacific Journal of Tropical Biomedicine*. **6**: 872-880

**Koff, J.L., Ramachandiran, S., and Bernal-Mizrachi, L.** 2015. A Time to Kill: Targeting Apoptosis in Cancer. *International Journal of Molecular Sciences*. **16**: 2942-2955

**Kosanic, M., Rankovic, B., and Dasic, M.** 2013. Antioxidant and Antimicrobial Properties of Mushrooms. *Bulgarian Journal of Agricultural Science*. **19**: 1040-1046

**Krátký, M., Vinšová, J., Novotná, E., Mandiková, J., Trejtnar, F., and Stolaříková, J.** 2013. Antibacterial Activity of Salicylanilide 4-(Trifluoromethyl)benzoates. *Molecules*. **18**: 3674-3688

**Lee, K. and Song, K.** 2007. Actin Dysfunction Activates ERK1/2 and Delays Entry into Mitosis in Mammalian Cells. *Cell cycle* **6**: 1486-1494

**Lee, I., Jung, J., Yeom, J., Ki, D., Lee, M., Yeo, W., and Yun, B.** 2012. Fomitoside K, a New Lanostane Triterpene Glycoside from the Fruiting Body of *Fomitopsis nigra*. *Microbiology*. **40**: 76-78

**Lee, Y., Lee, D., Kim, Y.B., Lee, S., Cha, S., Park, H., Kim, G., Kwon, D., Lee, M., and Han, S.** 2015. The Mechanism Underlying the Antibacterial Activity of Shikonin against Methicillin-Resistant *Staphylococcus aureus*. *Evidence-Based Complementary and Alternative Medicine*. 2015:520578. <http://dx.doi.org/10.1155/2015/520578>

**Levin, H., Branch, M., Rappoport, S., and Mitchell, D.** 1987. 'n Veldgids tot die sampione van Suid-Afrika. C. Struik (Pty) Ltd, Cape Town, South Africa 180pp.

**Li, Y.R., Liu, Q.H., Wang, H.X., and Ng, T.B.** 2008. A novel lectin with potent antitumor, mitogenic and HIV-1 reverse transcriptase inhibitory activities from the edible mushroom *Pleurotus citrinopileatus*. *Biochimica et Biophysica Acta*. **1780**: 51-57

**Li, Y., Zhang, G., Ng, T.B., Wang, H.** 2010. A novel lectin with antiproliferative and HIV-1 reverse transcriptase inhibitory activities from dried fruiting bodies of the monkey head mushroom *Hericium erinaceum*. *Journal of Biomedicine and Biotechnology*. 2010:716515. doi:10.1155/2010/716515

**Lima, C.U.J.O., Gris, E.F., and Karnikowski, M.G.O.** 2016. Antimicrobial properties of the mushroom *Agaricus blazei* – integrative review. *Brazilian Journal of Pharmacognosy*. **26**: 780-786

**Lindequist, U., Niedermeyer, T.H.J., and Jülich, W.** 2005. The Parmaceutical Potential of Mushrooms. *Evidence-Based Complementary and Alternative Medicine*. **2**: 285-299

**Liu, F., Wang, Y., Zhang, K., Wang, Y., Zhou, R., Zeng, Y., Han, Y., and Ng, T.B.** 2017. A novel polysaccharide with antioxidant, HIV protease inhibiting and HIV integrase inhibiting activities from *Fomitiporia punctata* (P. karst.) murrill (Basidiomycota, hymenochaetales). *International Journal of Biological Macromolecules*. **97**: 339-347

**Liwa, A.C. and Jaka, H.** 2015. Antimicrobial resistance: Mechanisms of action of antimicrobial agents. *The Battle Against Microbial Pathogens: Basic Science, Technological Advances and Educational Programs*. A. Méndez-Vilas (Ed.). [Online]. Available: <https://www.researchgate.net/publication/275966839>

**Luo, Y., Cobb, R.E., and Zhao, H.** 2014. Recent advances in natural product discovery. *Current Opinion in Biotechnology*. **30**: 230-237

**Matijasevic, D., Pantic, M., Raskovic, B., Pavlovic, V., Duvnjak, D., Sknepnek, A., and Niksic, M.** 2016. The Antibacterial Activity of *Coriolus versicolor* Methanol Extract and Its Effect on Ultrastructural Changes of *Staphylococcus aureus* and *Salmonella Enteritidis*. *Frontiers in Microbiology*. **7**:1226. doi: 10.3389/fmicb.2016.01226

**Mesaros, N., Nordmann, P., Pleśiat, P., Roussel-Delvallez, M., Van Eldere, J., Glupczynski, Y., Van Laethem, Y., Jacobs, F., Lebecque, P., Malfroot, A., Tulkens, M.P., and Van Bambeke, F.** 2007. *Pseudomonas aeruginosa*: resistance and therapeutic options at the turn of the new millennium. *Clinical Microbiology and Infection*. **13**: 560–578

**McIlwain, D.R., Berger, T., and Mak, T.W.** 2013. Caspase Functions in Cell Death and Disease. *Cold Spring Harbor Perspectives in Biology*. **5**:a008656. doi: 10.1101/cshperspect.a008656

**McGee, M.M.** 2015. Targeting the Mitotic Catastrophe Signaling Pathway in Cancer. *Mediators of Inflammation*. **8**: 1-13

**Molinari, M.** 2000. Cell cycle checkpoints and their inactivation in human cancer. *Cell Proliferation*. **33**: 261-274

**Mollah, M.L., Park, D.K., and Park, H.** 2012. *Cordyceps militaris* Grown on Germinated Soybean Induces G2/M Cell Cycle Arrest through Downregulation of Cyclin B1 and Cdc25c in Human Colon Cancer HT-29 Cells. *Evidence-Based Complementary and Alternative Medicine*. 2012:249217. doi:10.1155/2012/249217

**Mourdjeva, M., Kyurkchiev, D., Mandinova, A., Altankova, I., Kehayov, I., and Kyurkchiev, S.** 2005. Dynamics of membrane translocation of phosphatidylserine during apoptosis detected by a monoclonal antibody. *Apoptosis*. **10**: 209-217

**Mushroomexpert.com.** 2017(a). *Herichium erinaceus* (MushroomExpert.Com). [online] Available at: [http://www.mushroomexpert.com/herichium\\_erinaceus.html](http://www.mushroomexpert.com/herichium_erinaceus.html) [Accessed 2 Dec. 2017].

**Mushroomexpert.com.** 2017(b). *Chlorophyllum molybdites* (MushroomExpert.Com). [online] Available at: [http://www.mushroomexpert.com/chlorophyllum\\_molybdites.html](http://www.mushroomexpert.com/chlorophyllum_molybdites.html) [Accessed 1 Dec. 2017].

**Mwita, L.N., Mshandete, A.M., and Lyantagaye, S.L.** 2010. Improved antimicrobial activity of the Tanzanian edible mushroom *Coprinus cinereus* (Schaeff) Gray by chicken manure supplemented solid sisal wastes substrates. *Journal of Yeast and Fungal Research*. **1**: 201-206

**Ngai, P.H.K. and Ng, T.B.** 2003. Lentin, a novel and potent antifungal protein from shitake mushroom with inhibitory effects on activity of human immunodeficiency virus-1 reverse transcriptase and proliferation of leukemia cells. *Life Science*. **73**: 3363-3374.

**Nguta, J.M., Appiah-Opong, R., Nyarko, A.K., Yeboah-Manu, D., and Addo, P.G.A.** 2015. Current perspectives in drug discovery against tuberculosis from natural products. *International Journal of Mycobacteriology*. **4**: 165-183

**Nojima, H.** 2004. G1 and S-phase checkpoints, chromosome instability, and cancer. *Methods in Molecular Biology*. **280**: 3-49

**Novak, B., Sible, J.C., and Tyson, J.J.** 2002. Checkpoints in the Cell Cycle. In: eLS. John Wiley & Sons Ltd, Chichester. <http://www.els.net> [doi: 10.1038/npg.els.0001355]

**Nowacka, N., Nowak, R., Drozd, M., Olech, M., Los, R., and Malm, A.** 2015. Antibacterial, Antiradical Potential and Phenolic Compounds of Thirty-One Polish Mushrooms. *PLOS ONE*. **10**:e0140355. doi:10.1371/journal.pone.0140355

**Nwachukwu, E. and Uzoeto, H.O.** 2010. Antimicrobial activity of some local mushrooms on pathogenic isolates. *Journal of Medicinal Plants Research*. **4**: 2460-2465

**Nyberg, K.A., Michelson, R.J., Putnam, C.W., and Weinert, T.A.** 2002. Toward Maintaining the Genome: DNA Damage and Replication Checkpoints. *Annual Review of Genetics*. **36**: 617-656

**Ogidi, O.C., Oyetayo, V.O., and Akinyele, B.J.** 2015. In Vitro Evaluation of Antimicrobial Efficacy of Extracts Obtained from Raw and Fermented Wild Macrofungus, *Lenzites quercina*. *International Journal of Microbiology*. 2015:106308. doi:10.1155/2015/106308 1-7

**Park, H., Teja, K., O'Shea, J.J., and Siegel, R.M.** 2007. The *Yersinia* Effector Protein YpkA Induces Apoptosis Independently of Actin Depolymerization. *The Journal of Immunology*. **178**: 6426-6434

**Patel, S. and Goyal, A.** 2012. Recent developments in mushrooms as anti-cancer therapeutics: a review. *3 Biotech*. **2**: 1-15

**Pietenpol, J.A. and Stewart, Z.A.** 2002. Cell cycle checkpoint signalling: Cell cycle arrest versus apoptosis. *Toxicology*. **181-182**: 475-481

**Poyraz, B., Gunes, H., Tul, B., and Sermenli, H.** 2015. Antibacterial and Antitumor Activity of Crude Extracts from Various Macrofungi Species. *Biyoloji Bilimleri Arastirma Dergisi*. **8**: 5-10

- Pratreep, A., Sumkhemthong, S., Suksomtip, M., Chanvorachote, P., and Chaotham, C.** 2017. Peptides extracted from edible mushroom: *Lentinus squarrosulus* induces apoptosis in human lung cancer cells. *Pharmaceutical Biology*. **55**: 1792-1799
- Pucci, B., Kasten, M., and Giordano, A.** 2000. Cell Cycle and Apoptosis. *Neoplasia*. **2**: 291-299
- Rahi, D.K. and Malik, M.** 2016. Diversity of Mushrooms and Their Metabolites of Nutraceutical and Therapeutic Significance. *Journal of Mycology*. 2016:7654123. doi:10.1155/2016/7654123
- Ramakrishna, S., Ramalingam, M., Kumar, T.S.S., and Soboyejo, W.O.** 2010. Biomaterials: A Nano Approach. Taylor and Francis Group, LLC, ISBN: 978-1-42004782-0, pg 72
- Ramya, R., Satish, K., Shubhashree, R., Manasa, D.A., Gaganashilpa, S., and Bhat, S.K.** 2013. Comparative evaluation of antimicrobial activity of fresh and dried samples of mushrooms. *International Journal of Recent Scientific Research*. **4**: 1946-1948
- Ranadive, K.R., Belsare, M.H., Deokule, S.S., Jagtap, N.V., Jadhav, H.K., and Vaidya, J.G.** 2013. Glimpses of antimicrobial activity of fungi from World. *Journal of New Biological Reports*. **2**: 142-162
- Rege, A., Dahake, R., Roy, S., and Chowdhary, A.** 2015. Screening of Natural Products for AntiHIV Potential: An In vitro Approach. *Journal of Immuno Virology*. **1**:JOJIV.MS.ID.555556
- Reid, T., Kashangura, C., Chidewe, C., Benhura, M.A., and Mduluza, T.** 2016. Antibacterial properties of wild edible and non-edible mushrooms found in Zimbabwe. *African Journal of Microbiology Research*. **10**: 977-984
- Ren, G., Liu, X.Y., Zhu, H.K., Yang, S.Z., and Fu, C.X.** 2006. Evaluation of cytotoxic activities of some medicinal polypore fungi from China. *Fitoterapia*. **77**: 408-410.
- Ren, L., Hemar, Y., Perera, C.O., Lewis, G., Krissansen, G.W., and Buchanan, P.K.** 2014. Antibacterial and antioxidant activities of aqueous extracts of eight edible mushrooms. *Bioactive Carbohydrates and Dietary Fibre*. **3**: 41-51
- Rezaeian, S. and Pourianfar, H.R.** 2016. Antimicrobial properties of the button mushroom, *Agaricus bisporus*: A mini-review. *International Journal of Advanced Research*. **4**: 426-429
- Ribble, D., Goldstein, N.B., Norris, D.A., and Shellman, Y.G.** 2005. A simple technique for quantifying apoptosis in 96-well plates. *BMC Biotechnology*. **5**: 1-7
- Robbins, W.J., Kavanagh, F., and Hervey, A.** 1947. Antibiotic substances from basidiomycetes *I. Pleurotus griseus*. *Botany*. **33**: 171-176



**Robles-Hernández, L., González-Franco, A.C., Soto-Parra, J.M., and Montes-Domínguez, F.** 2008. Review of agricultural and medicinal applications of basidiomycete mushrooms. *Technocienia Chihauhua*. **2**: 95-107.

**Rohilla, A., Sharma, V., and Sonu, S.K.** 2013. Upper Respiratory Tract Infections: An Overview. *International Journal of Current Pharmaceutical Research*. **3**: 1-3

**Rosa, L.H., Machado, K.M.G., Jacob, C.C., Capelari, M., Rosa, C.A., and Zani, C.L.** 2003. Screening of Brazilian Basidiomycetes for Antimicrobial Activity. *Memórias do Instituto Oswaldo Cruz*. **98**: 967-974

**Rosa, L.H., Machado, M.G.K., Rabello, A.L.T., Souza-Ragundes, E.M., Correa-Oliveira, R., Rosa, C.A., and Zani, C.L.** 2009. Cytotoxic, immunosuppressive, trypanocidal and antileishmanial activities of Basidiomycota fungi present in Atlantic Rainforest in Brazil. *Antonie van Leeuwenhoek*. **95**: 227-237

**Roupas, P., Keogh, J., Noakes, M., Margetts, C., and Taylor, P.** 2012. The role of edible mushrooms in health: Evaluation of the evidence. *Journal of functional foods*. **4**: 687-709

**Sandal, T.** 2002. Molecular Aspects of the Mammalian Cell Cycle and Cancer. *The Oncologist*. **7**: 73-81

**Saritha, K., Rajesh, A., Manjulatha, K., Setty, O.H., and Yenugu, S.** 2015. Mechanism of antibacterial action of the alcoholic extracts of *Hemidesmus indicus* (L.) R. Br. Ex Schult, *Leucas aspera* (Wild.), *Plumbago zeylanica* L., and *Tridax procumbens* (L.) R. Br. Ex Schult. *Frontiers in Microbiology*. **6**: 1-9

**Sathyan, A., Majeed, K.A., Majitha, V.K., and Rajeswary, K.R.** 2017. A Comparative Study of Antioxidant and Antimicrobial Activities of *Pleurotus Ostreatus*, *Pleurotus Eryngii* and *Pleurotus Djamor*. *International Journal of Agriculture Innovations and Research*. **5**: 907-912

**Schafer, K.A.** 1998. The cell cycle: A review. *Veterinary Pathology*. **35**: 46-478.

**Senese, S., Lo, Y.C., Huang, D., Zangle, T.A., Gholkar, A.A., Robert, L., Homet, B., Ribas, A., Summers, M.K., Teitell, M.A., Damoiseaux, R., and Torres, J.Z.** 2014. Chemical dissection of the cell cycle: probes for cell biology and anti-cancer drug development. *Cell Death and Disease*. **5**: e1462. doi:10.1038/cddis.2014.420

**Shen, H., Shao, S., Chen, J., and Zhou, T.** 2017. Antimicrobials from Mushrooms for Assuring Food Safety. *Comprehensive Reviews in Food Science and Food Safety*. **16**: 316-329

**Siddalingappa, C.M., Kalpana, L., Puli, S., Vasudha, T.K., and Acharya, A.** 2013. Sensitivity pattern of bacteria causing respiratory tract infections in a tertiary care centre. *International Journal of Basic & Clinical Pharmacology*. **2**: 590-595

**Simstein, R., Burow, M., Parker, A., Weldon, C., and Beckman, B.** 2003. Apoptosis, Chemoresistance, and Breast Cancer: Insights From the MCF-7 Cell Model System. *Experimental Biology and Medicine*. **228**: 995-1003

**Smânia, A., Monache, F.D., Smânia, E.F.A., Gil, M.L., Benchetrit, L.C., and Cruz, F.S.** 1995. Antibacterial activity of a substance produced by the fungus *Pycnoporus sanguineus* (Fr.) Murr. *Journal of Ethnopharmacology*. **45**: 177-181

**Smith, J.E., Rowan, N.J., and Sullivan, R.** 2002. Medicinal mushrooms: a rapidly developing area of biotechnology for cancer therapy and other bioactivities. *Biotechnology Letters*. **24**: 1839-1845

**Sreejaya, S.B. and Santhy, K.S.** 2013. Cytotoxic properties of *Acorus calamus* in MCR-7 breast cancer cells. *International Journal of Current Research and Academic Review*. **1**: 106-111

**Stanikunaite, R., Radwan, M.M., Trappe, J.M., Fronczek, F., and Ross, S.A.** 2008. Lanostane-Type Triterpenes from the Mushroom *Astraeus pteridis* with Antituberculosis Activity. *Journal of Natural Products*. **71**: 2077-2079

**Stehn, J.R., Haass, N.K., Bonello, T., Desouza, M., Kottyan, G., Treutlein, H., Zeng, J., Nascimento, P.R.B.B., Sequeira, V.B., Butler, T.L., Allanson, M., Fath, T., Hill, T.A., McCluskey, A., Schevzov, G., Palmer, S.J., Hardeman, E.C., Winlaw, D., Reeve, V.E., Dixon, I., Weninger, W., Cripe, T.P., and Gunning, P.W.** 2017. A Novel Class of Anticancer Compounds Targets the Actin Cytoskeleton in Tumor Cells. *Cancer Research*. **73**: 5169-5182

**Suffness, M. and Pezzuto, J.M.**, 1990. Assays related to cancer drug discovery. In: Hostettmann, K. (Ed.), *Methods in Plant Biochemistry: Assays for Bioactivity*. Academic Press, London, pp. 71–133.

**Tang, X., Mi, F., Zhang, Y., He, X., Cao, Y., Wang, P., Liu, C., Yang, D., Dong, J., Zhang, K., and Xu, J.** 2015. Diversity, population genetics, and evolution of macrofungi associated with animals. *Mycology*. **6**: 94-105

**Team, G. and Team, G.** 2017. Grey & White Oyster Mushroom - GANOFARM. [online] GANOFARM. Available at: <http://ganofarm.com/grey-white-oyster-mushroom/> [Accessed 2 Dec. 2017]

**Tepliyakova, T.V. and Kosogava, T.A.** 2016. Antiviral Effect of Agaricomycetes Mushrooms (Review). *International Journal of Medicinal Mushrooms*. **18**: 375-386

**Thatoi, H. and Singdevsachan, S.K.** 2014. Diversity, nutritional composition and medicinal potential of Indian mushrooms: A review. *African Journal of Biotechnology*. **13**: 523-545

**Tomasi, S., Dévéhat, F.L-L., Sauleau, P., Bézivin, C., and Boustie, J.** 2004. Cytotoxic activity of methanol extracts from Basidiomycete mushrooms on murine cancer cell lines. *Die Pharmazie*. **59**: 290-293.

**Udu-Ibiam, O.E., Ogbu, O., Nworie, O., Ibiam, U.A., Agah, M.V., Nnachi, A.U., Ogbu, K.I., and Chukwu, O.S.** 2014. Antimicrobial Activities of Some Selected Edible Mushrooms and Spices against Clinical Isolates from Federal University Teaching Hospital Abakaliki (FETHA), Ebonyi State, Nigeria. *International Journal of Scientific & Technology Research*. **3**: 251-255

**Ulukaya, E., Acilan, C., Ari, F. Ikitimur, E., and Yilmaz, Y.** 2011. A Glance at the methods for detection of apoptosis qualitatively and quantitatively. *Turkish Journal of Biochemistry*. **36**: 261-269

**Vakifahmetoglu, H., Olsson, M., and Zhivotovsky, Z.** 2008. Death through a tragedy: mitotic catastrophe. *Cell Death and Differentiation*. **15**: 1153–1162

**Valverde, M.E., Hernández-Pérez, T., and Paredes-López, O.** 2015. Edible Mushrooms: Improving Human Health and Promoting Quality Life. *International Journal of Microbiology*. 2015:376387. doi:10.1155/2015/376387

**Van der Westhuizen, G.C.A. and Eicker, A.** 1994. Field Guide: Mushrooms of Southern Africa. Struik Publishers (Pty) Ltd, Cape Town, South Africa, 270pp.

**Vejeslova, D. and Kutlu, H.M.** 2015. Inhibitory effects of salicylic acid on A549 human lung adenocarcinoma cell viability. *Turkish Journal of Biology*. **39**: 1-5

**Venables, J.H. and Coggeshall, R.** 1965. A simplified lead citrate stain for use in electron microscopy. *Journal of Cell Biology*. **25**: 407-408

**Vermeulen, K., Van Bockstaele, D.R., and Berneman, Z.N.** 2003. The cell cycle: a review of regulation, deregulation and therapeutic targets in cancer. *Cell Proliferation*. **36**: 131-149

**Visconti, R., Monica, R.S., and Grieco, D.** 2016. Cell cycle checkpoint in cancer: a therapeutically targetable double-edged sword. *Journal of Experimental and Clinical Cancer Research*. **35**: 1-8

**Wani, B.A., Bodha, R.H. and Wani, A.H.** 2010. Nutritional and medicinal importance of mushrooms. *Journal of Medicinal Plants Research*. **4**: 2598-2604

**Wang, H. and Ng, T.B.** 2001. Pleureryn, a novel protease from fresh fruiting bodies of the edible mushroom *Pleurotus eryngii*. *Biochemical and Biophysical Research Communications*. **289**: 750-755

**Wang H.X., and Ng, T.B.** 2004. Purification of a novel low-molecular-mass laccase with HIV-1 reverse transcriptase inhibitory activity from the mushroom *Tricholoma giganteum*. *Biochemical and Biophysical research Communications*. **315**: 450-454.

**Wang, H.X. and Ng, T.B.** 2006. Purification of a laccase from fruiting bodies of the mushroom *Pleurotus eryngii*. *Applied Microbiology and Biotechnology*. **69**: 521-525

**Wang, J., Wang, H.X., and Ng, T.B.** 2007. A peptide with HIV-1 reverse transcriptase inhibitory activity from the medicinal mushroom *Russula paludosa*. *Peptides*. **28**: 560-565

**Wang, S., Liu, Y., Zhang, G., Zhao, S., Xu, F., Geng, X., and Wang, H.** 2012. Cordysobin, a novel alkaline serine protease with HIV-1 reverse transcriptase inhibitory activity from the medicinal mushroom *Cordyceps sobolifera*. *Journal of Bioscience and Bioengineering* **113**:42-47

**Wang, C.R., Zhou, R., Ng, T.B., Wong, J.H., Qiao, W.T., and Liu, F.** 2014a. First report on the isolation of methyl gallate with antioxidant, anti-HIV-1 and HIV-1 enzyme inhibitory activities from a mushroom (*Pholiota adiposa*). *Environmental Toxicology and Pharmacology*. **37**: 626-637.

**Wang, Y., Cheng, X., Wang, P., Wang, L., Fan, J., Wang, X., and Liu, Q.** 2014b. Investigating migration inhibition and apoptotic effects of *Fomitopsis pinicola* chloroform extract on human colorectal cancer SW-480 cells. *PLoS One*. [Online]. Available: <http://dx.doi.org/10.1371/journal.pone.0101303>

**White, S.R., Williams, P., Wojcik, K.R., Sun, S., Hiemstra, P.S., Rabe, K.F., Dorscheid, D.R.** 2001. Initiation of Apoptosis by Actin Cytoskeletal Derangement in Human Airway Epithelial Cells. *American Journal of Respiratory Cell and Molecular Biology*. 282-294

**Wong, R.S.Y.** 2011. Apoptosis in cancer: from pathogenesis to treatment. *Journal of Experimental & Clinical Cancer Research*. **30**: 1-14

**World Health Organization.** 2017a. Cancer. [online] Available at: <http://www.who.int/mediacentre/factsheets/fs297/en/> [Accessed 2 Dec. 2017].

**World Health Organization.** 2017b. Tuberculosis (TB). [online] Available at: <http://www.who.int/mediacentre/factsheets/fs104/en/> [Accessed 25 November 2017].

**World Health Organization.** 2017c. HIV/AIDS. [online] Available at: <http://www.who.int/mediacentre/factsheets/fs360/en/> [Accessed 25 November 2017].

**World Health Organization.** 2017d. The top 10 causes of death. [online] Available at: <http://www.who.int/mediacentre/factsheets/fs310/en/> [Accessed 15 Apr. 2017].

**Wu, H., Lu, F., Su, Y., Ou, H., Hung, H., Wu, J., Yang, Y., and Chang, C.** 2014. *In vivo* and *in vitro* anti-tumor effects of fungal extracts. *Molecules*. **19**: 2546-2556.

**Xirogianni, A., Tsofia, M., Voyiatzi, A., Sioumala, M., Makri, A., Argyropoulou, A., Paniara, O., Markoulatos, P., Kourea-Kremastinou, J., and Tzanakaki, G.** 2013. Diagnosis of Upper and Lower Respiratory Tract Bacterial Infections with the Use of Multiplex PCR Assays. *Diagnostics*. **3**: 222-231

**Yahaya, A.A. and Fall, I.** 2016. Protocol for the investigation of acute respiratory illness outbreaks of unknown aetiology. WHO Regional Office for Africa, ISBN: 978-929023300-8

**Yaling, L., Pongnak, and W., Kasem, S.** 2014. Mushroom and macrofungi collection for screening bioactivity of some species to inhibit coffee anthracnose caused by *Colletotrichum coffeanum*. *Journal of Agricultural Technology*. **10**: 845-861

**Yamac, M. and Bilgili, F.** 2006. Antimicrobial Activities of Fruit Bodies and/or Mycelial Cultures of Some Mushroom Isolate. *Pharmaceutical Biology*. **44**: 660-667

**Younis, A., Stewart, J., Wu, F., Shikh, H.E., Hassan, F., and Elaasser, M.** 2014. Cytotoxic Activity of Edible Mushrooms extracts against Tumor Cell Lines. *International Journal of Science and Technology*. **3**: 736-749

**Zhang, Y., Chen, X., Gueydan, C., and Hand, M.** 2018. Plasma membrane changes during programmed cell deaths. *Cell Research*. **28**: 9-21

**Zhou, H., Zhao, L., Li, W., Yang, Y., Xu, L., and Ding, Z.** 2015. Anti-*Mycobacterium tuberculosis* Active Metabolites from an Endophytic *Streptomyces* sp. YIM65484. *Records of Natural Products*. **9**: 196-200

**Zong, A., Cao, H., and Wang, F.** 2012. Anticancer polysaccharides from natural resources: A review of recent research. *Carbohydrate Polymers*. **90**: 1395-141

**Websites:**

[www.cansa.org.za](http://www.cansa.org.za)

[www.cancerresearchuk.org](http://www.cancerresearchuk.org)

## APPENDIX

**Table A1:** Minimum inhibitory concentration (MIC) of eight ethanolic macrofungal extracts using MABA and their IC<sub>50</sub> concentrations.

	MIC	IC <sub>50</sub>
<i>A. campestris</i>	1.000 µg/mL	480.8± µg/mL
<i>C. molybdites</i>	500 µg/mL	361.8± µg/mL
<i>G. penetrans</i>	500 µg/mL	174.1± µg/mL
<i>H. erinaceus</i>	> 2.000 µg/mL	N/A
<i>L. sulphurous</i>	1.000 µg/mL	432.6± µg/mL
<i>P. papilionaceus</i>	> 2.000 µg/mL	N/A
<i>P. ostreatus</i>	> 2.000 µg/mL	N/A
<i>P. baudonii</i>	1.000 µg/mL	74.6± µg/mL
Rifampicin	< 0.0625 µg/mL	N/A
Ethambutol dihydrochloride	> 500 µg/mL	N/A

**Table A2:** IC<sub>25</sub>, IC<sub>50</sub> and IC<sub>75</sub> of *F. lilacinogilva*, *G. junonius*, *P. sanguineus* and *P. baudonii* used against A549 lung cancer experiments.

	Extract concentration (µg/mL)		
	IC <sub>25</sub>	IC <sub>50</sub>	IC <sub>75</sub>
<i>F. lilacinogilva</i>	49.6	69.2	96.5
<i>G. junonius</i>	28.5	57.0	85.5
<i>P. sanguineus</i>	2.1	7.4	26.2
<i>P. baudonii</i>	38.3	53.6	74.9
Cisplatin	7.6	14.1	26.0

## LIST OF CONFERENCE PRESENTATIONS

**J. Didloff**, G.J. Boukes, T.C. Koekemoer, M. van de Venter, S. Govender. 2018. Biological activity of South African macrofungi against respiratory and lung disease. 43rd FEBS Congress, Prague, 7 – 12 July. Registrant ID. 29454. Abstract ID. 30936.